MILL INTEGRATION-PULPING, STEAM REFORMING AND DIRECT CAUSTICIZATION FOR BLACK LIQUOR RECOVERY

FINAL REPORT

Reporting Period Start Date: 09/30/2002
Reporting Period End Date: 06/30/2007

Adriaan van Heiningen
University of Maine

Issue Date: August 2008

DOE Cooperative Agreement DE-FC26-02NT41493

Prime (submitting) Organization: University of Maine
5717 Corbett Hall
Orono, Maine 04469-5717

Project Subcontractors: North Carolina State University
Box 7514
Raleigh, NC 27695-7514

Manufacturing and Technology Conversion International, Inc.
6001 Chemical Road, Baltimore, MD 21226

EXECUTIVE SUMMARY

MTCI/StoneChem developed a steam reforming, fluidized bed gasification technology for biomass. DOE supported the demonstration of this technology for gasification of spent wood pulping liquor (or "black liquor") at Georgia- Pacific's Big Island, Virginia mill. The present pre-commercial R&D project addressed the opportunities as well as identified negative aspects when the MTCI/StoneChem gasification technology is integrated in a pulp mill production facility. The opportunities arise because black liquor gasification produces sulfur (as H_2S) and sodium (as Na_2CO_3) in separate streams which may be used beneficially for improved pulp yield and properties. The negative aspect of kraft black liquor gasification is that the amount of Na_2CO_3 which must be converted to NaOH (the so called causticizing requirement) is increased. This arises because sulfur is released as Na_2S during conventional kraft black liquor recovery, while during gasification the sodium associated Na_2S is partly or fully converted to Na_2CO_3. The causticizing requirement can be eliminated by including a TiO_2 based cyclic process called direct causticization. In this process black liquor is gasified in the presence of (low sodium content) titanates which convert Na_2CO_3 to (high sodium content) titanates. NaOH is formed when contacting the latter titanates with water, thereby eliminating the causticizing requirement entirely. The leached and low sodium titanates are returned to the gasification process.

The project team comprised the University of Maine (UM), North Carolina State University (NCSU) and MTCI/ThermoChem. NCSU and MTCI are subcontractors to UM. The principal organization for the contract is UM. NCSU investigated the techno-economics of using advanced pulping techniques which fully utilize the unique cooking liquors produced by steam reforming of black liquor (**Task 1**). UM studied the kinetics and agglomeration problems of the conversion of Na_2CO_3 to (high sodium) titanates during gasification of black liquor in the presence of (low sodium) titanates or TiO_2 (**Task 2**). MTCI/ThermoChem tested the performance and operability of the combined technology of steam reforming and direct causticization in their Process Development Unit (PDU) (**Task 3**).

The specific objectives were:

1. to investigate how split sulfidity and polysulfide (+ AQ) pulping can be used to increase pulp fiber yield and properties compared to conventional kraft pulping.
2. to determine the economics of black liquor gasification combined with these pulping technologies in comparison with conventional kraft pulping and black liquor recovery.
3. to determine the effect of operating conditions on the kinetics of the titanate-based direct causticization reaction during black liquor gasification at relatively low temperatures (≤ 750°C).
4. to determine the mechanism of particle agglomeration during gasification of black liquor in the presence of titanates at relatively low temperatures (≤ 750°C).
5. to verify performance and operability of the combined technology of steam reforming and direct causticization of black liquor in a pilot scale fluidized bed test facility.

Task 1 – Pulping Study

Three different pulping technologies were investigated using southern softwood chips relative to conventional Modified Continuous Cooking (MCC); green liquor (GL) pretreatment, split sulfidity (SS) cooking and polysulfide pulping with or without anthraquinone (PS or PSAQ).

SS pulp yields were 1-2% greater than corresponding MCC pulps at higher delignification rates. Initial high alkali SS cooks generated pulps of lower kappa number and higher yield compared to those of low initial alkali. The SS pulps also had 5 to 10 mPa.s higher viscosity and improved tensile and burst strength. SS pulps were slightly harder to refine relative to MCC pulps.

Compared to MCC cooking, PS pulping at 25% sulfidity and 1-2% sulfur charge produced pulps of 2% greater yield. PS pulping at 40% sulfidity and higher sulfur charge required more alkali charge to maintain delignification rate. Also the bleachability of the PS pulps was less than that of MCC pulps, with a degree of oxygen delignification of 40% compared to 60% for MCC pulps.

PSAQ pulping with an optimized alkali distribution procedure resulted in similar rate of delignification compared MCC. Total pulp yield improvements of approximately 1% per 1% PS charged on OD wood were obtained, in agreement with literature. PSAQ pulping at a high polysulfide charge of 3% (as PS) requires a high sulfidity (40%) white liquor for its generation. The bleachability of PSAQ pulps is similar to that of control MCC pulps, but the bleached PSAQ pulps have a significantly higher pulp viscosity. The PSAQ pulps were easier to refine than corresponding MCC pulps. The tear and bursting strength of PSAQ pulps produced at 25% sulfidity and 2% PS charge is lower than those of 25% sulfidity MCC pulps, while 40% S and 3% PS PSAQ pulps gave slightly higher strength properties than 40% sulfidity MCC pulps.

A WinGEMS module for black liquor gasifier (BLG) was developed. The module was utilized in simulation case studies exploring SS and PSAQ pulping using BLG for chemical recovery. The results show that the net process variable operating cost was driven by two major factors; lime kiln fuel and power sales price. At an assumed lime kiln fuel cost of $50/barrel and power sales price of $0.35/kWhr, the net variable operating costs for the simulated BLG cases showed a cost increase of about 3% compared to MCC kraft pulping. The pulp yield benefits of the studied modified pulping technologies plus the additional revenue generated from the generation and sale of green power (using BLG combined cycle (BLGCC)) were insufficient to compensate for this cost increase. However, if the lime kiln fuel cost is decreased or the power sale price increased, the BLGCC process with split sulfidity or PSAQ pulping becomes more economically favorable than the conventional MCC kraft process. If the sales price for power to the grid is increased from 3.5 to 6 ¢/KWh cost savings of about $40/ODT pulp could be realized.

Task 2 – Direct Causticization Study

The direct causticization (DC) of black liquor by TiO_2 or $Na_2O.3TiO_2$ is completed within 1 hour above 680°C in a pure nitrogen atmosphere. These kinetics are reasonably well modeled by the phase-boundary model. However, there is a strong decrease in DC final conversion and causticity (i.e. yield of NaOH from Na_2CO_3) at a $[CO_2]$ in the gas phase of about 10% or higher during gasification of black liquor – titanate mixtures at about 730 C. This suggest that implementation of the DC-gasification process requires a two-stage counter current process where carbon gasification takes place in a fluidized bed and the DC reaction in another reactor fed by steam to maintain a low $[CO_2]$ in the gas phase.

Softening/liquefaction of black liquor solids (BLS) during pyrolysis of the organics starting at around 300 °C followed by solidification to a char without swelling is the major mechanism responsible for agglomeration in the present BL-titanate system. The liquefied black liquor solids

pull the titanate particles together by capillary forces, and after resolidification the dense residual char forms strong bridges between the particles. Although most of the carbon is subsequently consumed, solid-phase sintering of Na_2CO_3 retains the strength of the agglomerates. These results suggest that agglomeration may be prevented or diminished by separately pre-pyrolysing the black liquor or by adding Al_2O_3 particles since Al_2O_3 does not sinter at the temperatures studied.

Task 3 – PDU testing

Initial tests in the fluid bed PDU by MTCI established that particle agglomeration resulted in bed defluidization and premature shut down when processing black liquor with TiO_2. UM determined that agglomeration was due to sintering of the organic matter in black liquor starting at ~300 °C. A contributing factor to the agglomeration is the absence of black liquor swelling during pyrolysis in the presence of TiO_2. Based on these results it was recommended by UM that the MTCI PDU be operated in the turbulent fluidization mode, preferably with larger particle sizes than 150 μm.

Subsequent PDU tests at 740 °C and a superficial velocity of about 2.0 ft/s (i.e. an increase by a factor of almost 2) with an initial bed of Al_2O_3 particles showed that the reformer could be operated without agglomeration problems for about 4 hours. The water-free product gas was approximately 62% H_2, 13% CO, 23% CO_2, 2 % H_2S and trace organics. Analysis of the bed solids showed a carbon gasification of about 90% and degrees of direct causticization varying from 25 to 80 %. However the test duration was still limited by the formation of a large amount of fine particles, leading to filter blinding. Therefore, additional tests in a properly configured larger test unit were needed to fully verify and characterize the process.

Because the PDU at MTCI was too small to fully verify and characterize the gasification and direct causticization process, the process was also tried in the 10 inch diameter fluidized bed steam reformer at the University of Utah under the direction of Kevin Whitty. The steam reformer was fed with a mixture of TiO_2 and kraft black liquor for 24 hours. The titanate causticization agent was TiPure R103 from DuPont, with >96% TiO_2 and <3.2% Al_2O_3. The KBL- TiO_2 slurry had a mass ratio of TiO_2 / KBL solids of 0.43 to make the molar ratio $[Na_2CO_3]$ / $[TiO_2]$ equal to 0.7. The following conclusions were made based on this test:

- Fluidized bed operation can be maintained for the TiO_2-KBL steam gasification process at a high temperature of about 715 °C as long as the fluidization velocity is maintained at about 1m/s. There are no agglomeration problems at these conditions with alumina as starting bed.
- Complete DC conversion is possible under steam gasification conditions at 715 C and in the presence of 5% or less CO_2 in the gas phase.
- Complete C conversion is obtained under the present conditions.
- Bed particle size needs to be much less than 3 mm to avoid poor sulfur release as H_2S due to mass transfer limitations.

TABLE OF CONTENTS

1. INTRODUCTION AND PREVIOUS WORK

1.1 Introduction

1.1.1 Kraft pulping process

In kraft pulping, an aqueous solution containing NaOH and Na_2S is used to liberate cellulose fibers from wood in a high pressure reactor called the digester. After reaction, the aqueous extract is collected and concentrated in a series of multiple effect evaporators to produce a unique fuel known as black liquor. The black liquor contains about 50% of the wood mostly in the form of degraded lignin and hemicelluloses and about 20% (based on original wood) spent pulping chemicals. To recover the chemicals and energy, the black liquor is burned in a so called Tomlinson recovery boiler. Na_2CO_3 and Na_2S are removed from the bottom of the boiler as a molten smelt. Because the combustion yields Na_2CO_3 rather NaOH as final product, Na_2CO_3 is converted to NaOH using slaked lime ($Ca(OH)_2$) by the causticizing reaction:

$$Ca(OH)_2(s) + Na_2CO_3(aq) \rightarrow 2NaOH(aq) + CaCO_3(s) \qquad (1.1)$$

The $CaCO_3$ is converted back into slaked lime using a lime kiln and a slaker. The process diagram of the kraft pulping and recovery process is shown in Figure 1.1.

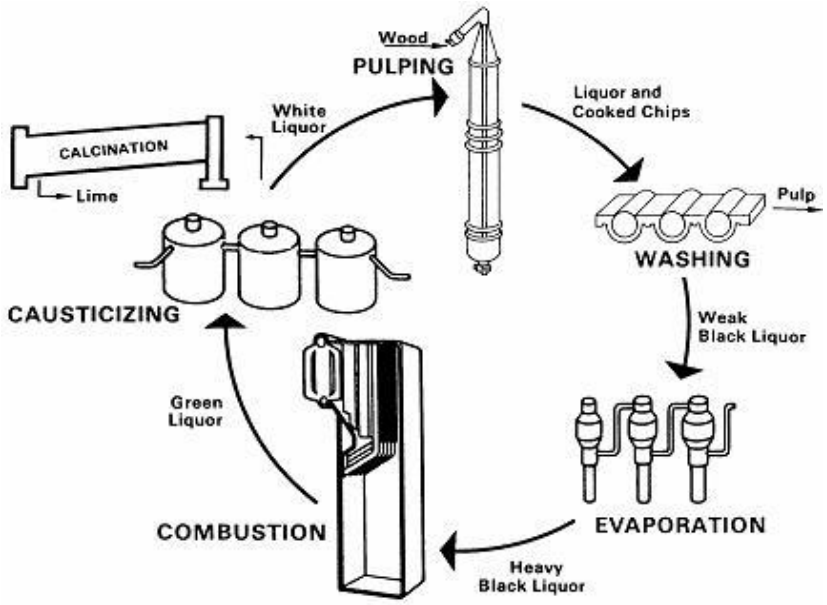

Figure 1.1 Process diagram of the kraft pulping and recovery process

The kraft or sulfate process is the dominant chemical pulping technology employed in the paper industry today. The competitive advantage that has led to its position is the capability to convert most wood species to high strength pulp combined with an efficient chemical recovery based around the Tomlinson recovery boiler. The annual US kraft pulp production is about 50 million tons. However the kraft process also has some important drawbacks. They are:

- High capital cost, high external energy cost and low energy efficiency
- Low pulp yield
- Complex causticizing process and risk of smelt-water explosion in the recovery boiler.

These drawbacks are the driving force for alternative pulping and recovery processes.

1.1.2 Black liquor gasification

There are approximately 280 Tomlinson recovery boilers in operation in North America, according to the Black Liquor Recovery Boiler Advisory Committee of the American Forest and Paper Association (AF&PA). Many of these boilers are nearing the end of their useful life, and will either need to be upgraded or replaced in the near future. Black liquor gasification (BLG) is a technology that could be implemented to replace the mature conventional recovery technology. Gasification is of interest because of its potential for higher energy efficiency, higher electricity/steam ratio, and higher pulp yield and quality because of the different cooking liquors which may be produced ([1]). In addition, gasification will lead to large environmental benefits in terms of NO_x, sulfurous species and CO_2 greenhouse gas emissions.

A drawback of black liquor gasification is that the causticizing requirement is increased. This occurs because the sodium associated with sulfur as Na_2S in the conventional process is partly or fully converted to Na_2CO_3 during gasification. Also, the recovery of H_2S leads to coabsorption of CO_2 and formation of $NaHCO_3$. Causticizing of $NaHCO_3$ requires twice the amount of lime as can be seen when comparing reaction (1.1) with reaction

$$2NaHCO_3 + 2Ca(OH)_2 \leftrightarrow 2CaCO_3 + 2NaOH + H_2O \quad (1.2)$$

1.1.3 Titanate direct causticization

The causticizing penalty of gasification may be eliminated through in-situ direct causticization of Na_2CO_3 by reaction with TiO_2 when the latter is present during the gasification process. This occurs because Na_2CO_3 in black liquor reacts with sodium tri-titanate ($Na_2O{\bullet}3TiO_2$) or titanium dioxide (TiO_2) to form sodium penta-titanate ($4Na_2O{\bullet}5TiO_2$) and carbon dioxide:

$$3TiO_2 + Na_2CO_3 \leftrightarrow Na_2O{\bullet}3TiO_2 + CO_2 \quad (1.3)$$

$$5(Na_2O{\bullet}3TiO_2) + 7Na_2CO_3 \leftrightarrow 3(4Na_2O{\bullet}5TiO_2) + 7CO_2 \quad (1.4)$$

NaOH and solid sodium tri-titanate is produced in a subsequent leaching operation with water:

$$3(4Na_2O{\bullet}5TiO_2) + 7H_2O \leftrightarrow 5(Na_2O{\bullet}3TiO_2) + 14NaOH \quad (1.5)$$

Sodium tri-titanate is recycled to the gasifier and NaOH is returned to the pulp mill for cooking. This so-called direct causticization process could in principle completely eliminate the lime cycle. It also allows a higher operating temperature in a fluid bed gasifier because the bed now consists mainly of high melting point titanates. The higher operating temperature introduces several advantages, e.g. higher carbon conversion, reduction of emission of tars, and increased black liquor throughput. In addition, the quality of energy generation in this process is also highest because the direct causticization reaction is endothermic and the heat required is provided by combustion of gasification gases, while in the lime cycle the heat for calcination of the lime is provided by fossil fuel combustion ([2]).

1.1.4. Modified pulping technologies

In addition to the increased energy efficiency, gasification of black liquor has the potential to improve the chemical pulping process because the separation of sodium and sulfur inherent to black liquor gasification enables the utilization of modified pulping technologies such as: green liquor pretreatment, split sulfidity pulping and polysulfide pulping

These pulping technologies will increase yield or reduce wood demand, improve product quality, decrease chemical usage and more importantly simplify the chemical recovery process. A simplification of the chemical recovery process will decrease the operating and capital costs for recovery. Besides power generation, the resulting syngas can be used to generate bio-derived liquid fuels and chemicals.

1.1.5. Economics

The fundamental question for implementation of any new technology is the impact it will have on overall process economics. Some deciding factors that will influence the implementation of BLG combined with modified pulping and chemical recovery involve the cost-benefits associated with power generation and other high-value products that can be derived from the syngas. The effect on wood, chemical and fuel demand from changes in the pulping process can have a significant effect on the variable operating cost, capital investment and maintenance costs.

The typical thermal efficiency of a recovery boiler is generally 65-70%, and the thermal efficiency of the Rankine cycle for the conversion of steam to electricity varies from 30-38%, depending on the temperature and pressures of the different streams in the cycle. These values result in an overall system thermal efficiency of about 23% ([3]). On the other hand, if black liquor is gasified, the syngas can after cleanup be combusted in a combined cycle for production of electricity. A conventional steam cycle produces about 120-180 kWh/ton of steam, but a gasifier along with combined cycle power generation has the potential to generate 600-1000 kWh/ton of steam ([4]). Such a production of power would turn a pulp mill into a net exporter of electricity, and this potential is the main motivation for the implementation of black liquor gasification.

1.2 Literature review

1.2.1 Review of black liquor gasification development

Figure 1.2 shows the typical process elements included in the gasification of black liquor. The black liquor is initially introduced into a process vessel, the black liquor gasifier, which can either be pressurized or operate under atmospheric pressure. In general terms, the process involves the conversion of hydrocarbons and oxygen to hydrogen and carbon monoxide while forming separate solid and gaseous product streams.

The inorganic material, including all sodium salts, leaves as a bed solid or smelt depending on the gasifier operating temperature. The bed solids or smelt is then slaked and causticized to form a caustic solution. The volatiles, including most of the reduced sulfur species, leave as a syngas of medium BTU value. The major components of the syngas are H_2S, CO_2, CO, H_2O, and H_2. To prepare the syngas for other applications and to regenerate the pulping liquor, all sulfur must be separated from the syngas, and dissolved into the caustic solution prepared from the bed solids or smelt. The clean product gas is burned in a gas turbine and the hot flue gases are combined and used to generate steam in heat recovery steam generators (HRSGs). This steam is then used in a steam turbine and other process applications.

Whitty and Verrill has reviewed the development of alternative recovery technologies to the Tomlinson recovery boiler ([5]). The following discussion will focus on the gasification processes currently in commercial operation. As suggested by Stigsson, black liquor gasification technologies can be classified by the operating temperature ([6]). High temperature gasifiers operate at about 1000°C and low temperature gasifiers operate at less than 700°C. In the high temperature gasifier, the inorganic material forms a smelt and leaves in the molten form, while in the low temperature system, they leave as solids. The fuel value of the syngas produced is also dependent on the gasifying technology. Typically, gasification produces a fuel gas with heating values of 3-4 MJ/Nm^3 using air and 89 MJ/Nm^3 using oxygen ([7]). In addition, a process operating at temperatures close to 700 °C has been under development by ABB. In this process a recirculating fluid bed was used to minimize agglomeration of the mixture of sodium salts ([8]).

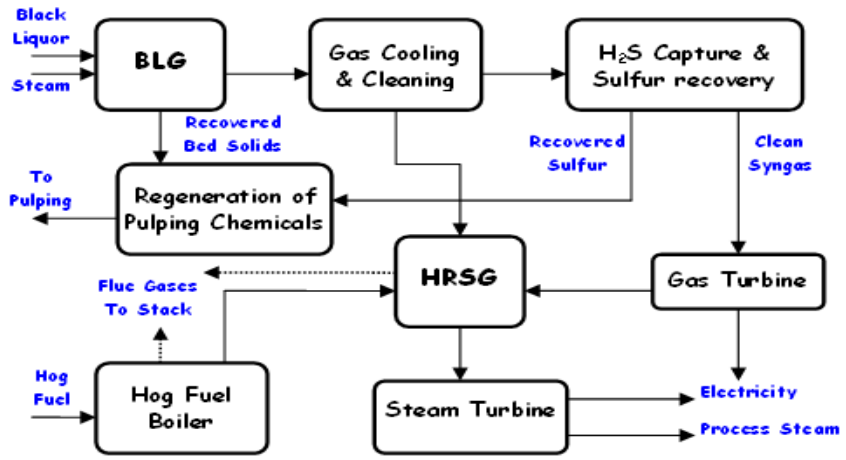

Figure 1.2 Simplified Representation of BLGCC Power/Recovery Systems

1.2.1.1 Low temperature gasifier/steam reformer

The development of low temperature fluidized bed gasifiers is being pursued by ThermoChem Recovery International (TRI) in the USA. The TRI system uses steam reforming to generate the product gases. Contrary to exothermic incineration or combustion technologies, steam reforming is an endothermic process. The steam reforming vessel operates at atmospheric pressure and at a temperature of about 600 °C when processing black liquor. The organics are exposed to steam in a fluidized bed in the absence of air or oxygen resulting in the steam reforming reaction:

$$H_2O + C + \text{Heat} \leftrightarrow H_2 + CO \qquad (1.6)$$

Carbon monoxide then reacts with steam to produce more hydrogen and carbon dioxide as:

$$CO + H_2O \leftrightarrow H_2 + CO_2 \qquad (1.7)$$

The result is a synthesis gas made up of about 65% hydrogen.

The TRI Steam Reformer technology, as shown in Figure 1.3, consists of a fluidized bed reactor that is indirectly heated by multiple resonance tubes arranged in one or more pulse combustion modules. Black liquor is directly fed to the reactor containing mostly sodium carbonate

particles, which are fluidized with superheated steam. The black liquor uniformly coats the bed particles, producing a char and volatile pyrolysis products which are steam cracked and reformed to produce a medium BTU gas. The residual char retained in the bed is more slowly gasified by reaction with steam. The sulfur and sodium are separated in that the sulfur becomes part of the gas stream and the sodium remains in the bed mostly as solid Na_2CO_3. Bed temperatures are about 600 ºC, thereby avoiding liquid smelt formation and associated agglomeration problems.

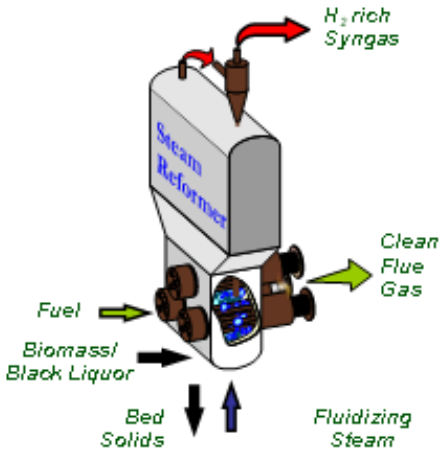

Figure 1.3 Schematic of MTCI Steam Reformer

Product gases are routed through a cyclone to remove the bulk of the entrained particulate matter and are subsequently quenched and scrubbed in a Venturi scrubber. A portion of the medium-Btu product gases can be supplied to the pulse combustion modules, and the combustion of these gases provides the heat necessary for the indirect gasification process. Low temperature gasification leads to complete separation of the sulfur and sodium in kraft black liquor to the gas and solid phases, respectively. Bed solids are continuously removed and mixed with water to form a sodium carbonate solution. The inorganic chemicals in the bed solids as well as the sulfur from the gas stream are recovered and used as cooking liquors for the mill. The product gas residence time in the fluid bed is about 15 seconds because of the deep bed (20 ft) used, while the solids residence time is about 50 hrs. These conditions promote tar cracking and carbon conversion; chemical processes which are very slow at the low temperature. In summary the steam reforming reactor vessel has three inputs; fluidizing steam, black liquor, and heat, and has three outputs; bed solids, hydrogen rich product gas, and flue gas ([9]).

1.2.1.2 High temperature gasifier

High temperature gasification stems from work initiated by SKF in the 1970s. The original patent for the technology was issued in 1987, and it has since been developed through a sequence of demonstration projects. The gasifier, as developed by Chemrec, is a refractory-lined entrained-flow reactor. In high temperature gasification (900-1000 ºC), concentrated black liquor is atomized, fed to the reactor and decomposed under reducing conditions using air or oxygen as the oxidant. The initial chemical reactions involve char gasification and combustion, and are influenced by physical factors like droplet size, heating rate, swelling, and the sodium

and sulfur release phenomena. The resulting products, smelt droplets and a combustible gas are then brought into direct contact with a cooling liquid in a quench dissolver. The two phases are separated as the smelt droplets dissolve in the cooling liquid, forming green liquor, an aqueous solution of mostly Na_2CO_3 and Na_2S. The exiting product gas is subsequently scrubbed and cooled for use in other unit operations. The split of sodium and sulfur between the smelt and gas phase is dependent on the process conditions. Typically, about eighty percent of the sulfur leaves with the product gas at atmospheric gasification or about half of the sulfur at pressurized (30 atm.) gasification, and essentially all of the sodium with the smelt ([10],[11],[12]).

1.2.1.3 Current status of BLG technologies

The TRI steam reformer has been installed in two locations in North America, at the Norampac Mill at Trenton, New Jersey and the Georgia Pacific Mill at Big Island, Virginia. The Trenton mill produces 500 tpd of corrugating medium using a sodium carbonate based pulping process. Prior to the start-up of the low-temperature black liquor gasifier in September 2003, the mill had no chemical recovery system. For over forty years the mill's spent liquor was sold to local counties for use as a binder and dust suppressant on gravel roads. This practice was discontinued in 2002. The capacity of the spent liquor gasification system is 115 tpd of black liquor solids, and the syngas is burned in an auxiliary boiler ([9]).

Georgia-Pacific's mill at Big Island produces 900 tpd of linerboard from OCC and 600 tpd of corrugating medium from mixed hardwoods semi-chemical pulp. Like the Trenton mill, the Big Island mill uses a sodium carbonate process. In the past, the semi-chemical liquor was burned in two smelters providing chemical recovery but no energy recovery. Instead of replacing the smelters with a traditional recovery boiler Georgia-Pacific decided to install a low temperature black liquor gasification process. One difference between the two systems is that unlike Trenton, Big Island burns the generated product syngas in the pulsed combustors, so the product gas exiting the reformer vessel is cleaned prior to combustion. The Big Island BLG project was terminated in the fall of 2006.

The evolution of the high temperature gasifier has taken the technology from an air-blown process near atmospheric pressure to a high pressure (near 30 atm.) oxygen-blown process. Benefits realized through high pressure oxygen-blown operation are higher efficiencies, higher black liquor throughput and improved compatibility with down-stream unit operations such as combined cycle power generation.

An air-blown pilot plant at Hofors, Sweden, was developed to verify the possibility of gasifying black liquor using an entrained-flow reactor operating at 900-1000 ºC. The project showed that green liquor of acceptable quality could be generated; and the plant was dismantled in 1990. The Frövi, Sweden plant was designed as a capacity booster for the AssiDomän facility and was operated from 1991 to 1996, demonstrating the potential for black liquor gasification at a commercial scale. During its operation several technical problems were encountered and addressed. The identification of a suitable material for the refractory lining remained a problem. A subsequent commercial project was initiated in 1996 at the Weyerhauser plant in New Bern, North Carolina. The black liquor gasifier was more or less a scale-up of the Frövi plant, designed for a capacity of 300 tons of dissolved solids/day. In 1999 the process maintained greater than 85% availability. However, over the course of the project the plant experienced several technical problems, mainly related to the refractory lining, and it was shut down after

cracks in the reactor vessel were discovered in 2000. After detailed studies and re-engineering, the gasifier operation at New Bern was resumed in the summer of 2003. During the rebuild, it was retrofitted with spinel refractory materials developed at Oakridge National Labs in cooperation with other partners. The refractory material is in its second year of operation. The gasifier can burn up to 730,000 lb/day of solids or about 20% of the mill production ([13]). The syngas generated in the gasifier is currently burned in a boiler.

A pressurized air-blown demonstration project was established at the Stora Enso plant at Skoghall, Sweden, in 1994. The project showed the capability of a pressurized system to generate acceptable quality green liquor while maintaining high carbon conversion ratios. The process was converted to an oxygen-blown operation in 1997 resulting in a capacity increase of more than 60%. A second pressurized demonstration plant was completed in Piteå, Sweden, in 2005. The purpose of the project is to demonstrate high pressure operation (near 30 atm.) with associated gas cooling and sulfur handling unit operations required for a full-scale BLG process. The next step is scaling up the Piteå design to a commercial facility. This plant will have a capacity of 275-550 tDS/day and encompasses all the required unit operations, including the power island, for a BLG process with combined-cycle power generation.

1.2.2 Review of kraft pulping chemistry

To liberate the cellulose fiber contained in wood, lignin, the "glue" which holds the wood together, must be degraded for it to be dissolved in the pulping liquor. In kraft pulping, this is achieved by heating the wood in the presence of an alkaline pulping liquor containing nucleophiles that attack the lignin polymer. The active chemical agents in kraft pulping chemistry are the hydroxide (OH^-) and hydrosulfide (HS^-) anions. While these chemicals act to degrade wood lignin, the alkaline conditions and elevated temperatures also degrade the wood carbohydrates, cellulose and hemicelluloses, resulting in overall pulp yield losses. The presence of HS^- also causes partial demethylation of lignin methoxyl groups. The resulting methyl mercaptan reacts further as nucleophiles combining with an additional methoxyl group to form dimethyl sulfide, which is extremely volatile and together with the mercaptans produces the odor typically associated with kraft mills.

Several reviews of kraft pulping chemistry and its effects on wood component degradation and pulp yields have been given ([14,15,16]). Delignification in kraft pulping has three distinct phases: a rapid initial phase followed by the bulk phase where most of the lignin is degraded and dissolved, and the final residual phase ([17]). In the initial phase a substantial amount of hemicelluloses undergo deacetylation and dissolution resulting in significant yield losses ([18]). Phenolic lignin structures also undergo some degradation while the effect on cellulose is minor. In the bulk phase about 70% of the lignin is degraded, while the carbohydrates undergo further degradation through peeling and alkaline hydrolysis reactions. Methanol and hexenuronic acid are formed during this phase. The carbohydrate degradation reactions that occur during heat-up and the early stages of the cook liberate or produce a substantial amount of uronic, acetic and sugar acids. As a consequence, by the time the cook reaches cooking temperature and the bulk delignification phase starts, a substantial amount of the available alkali has already been consumed to neutralize the acids formed. This means that a much smaller amount of alkali is available for lignin degradation than what was initially charged. Delignification reaches the residual phase when about 90% of the lignin has been removed. At this point, delignification reactions slow down as reactive lignin moieties have been depleted, and the remaining alkali

generates rapid carbohydrate degradation ([19]). Thus, there is a state of diminishing returns for lignin removal from wood in kraft pulping relative to overall yield losses from carbohydrate degradation. Therefore in practice kraft pulping operations are typically interrupted during the bulk phase of delignification to prevent excessive degradation of carbohydrates, which would result in overall yield loss and poor pulp quality. The residual lignin, typically about 4-5% for softwood and 3% for hardwood, can be removed during subsequent oxygen delignification, or addressed during bleaching operations ([16]).

1.2.3 Review of modified kraft pulping processes

Process modifications that work within the pre-existing process unit operations and equipment can significantly improve process economics or be devised to meet new environmental regulations without need for additional capital expenditure. These processes are reviewed below.

1.2.3.1 Modified continuous cooking

Modified kraft pulping processes have gained widespread acceptance, because they can be used either to extend delignification or to enhance the yield and pulp properties. The basic principles of modified extended delignification consist of a level alkali concentration throughout the cook, a high initial sulfide concentration, low concentrations of lignin and Na^+ in the final stage of the cook, and lower temperature in the initial and final stages of the cook ([20]). This process approach has been developed by Kamyr around their continuous digester. Using conventional kraft recovery operations the generated white liquor is split into different feed streams applied during feed, transfer circulation and a countercurrent cooking zone. The process modifications have resulted in higher pulp yield or improved delignification with increased Degree of Polymerization (DP) of cellulose (measured as pulp viscosity) and bleachability properties.

1.2.3.2 Green liquor pretreatment

One alternative to avoid the increase in causticization requirements which occur as a result of black liquor gasification (BLG) would be to pre-treat wood with green liquor. Previous work has demonstrated the feasibility of using green liquor in the impregnation stage, without increasing overall chemical usage ([21,22]). It has also been shown that the amount of sulfur adsorbed during the pretreatment decreases with higher $[OH^-]$ ([23]). By impregnating chips with high sulfidity, low pH liquor, a mill may enhance yield and further decrease the causticizing load. Figure 1.4 outlines the unit operations for a green liquor pretreatment process in conjunction with BLG.

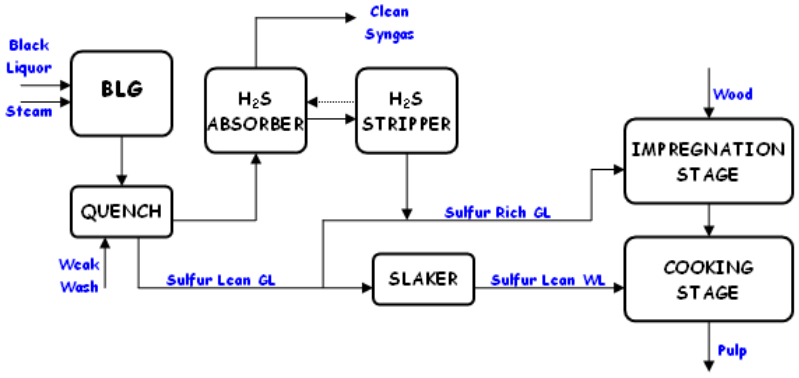

Figure 1.4 Outline of Process Using Green Liquor Pretreatment

Comparing conventional kraft pulping with the green liquor pretreatment described above, the greatest relative cost-benefit from a decrease in causticization using green liquor pretreatment would be achieved in a situation where the level of Total Titratable Alkali (TTA; i.e. the sum of Na_2CO_3, Na_2S and NaOH) was the same in both processes. This requires that similar pulp kappa numbers must be attainable through both processes at the same TTA charge.

1.2.3.3 Split sulfidity pulping

BLG would enable a mill to generate high sulfidity liquor which can be used to provide a high sulfide concentration during the initial phase of the cook. In split sulfidity pulping, it would be necessary to generate two streams of white liquor – one that is sulfide-rich and another that is sulfide-lean. Sulfur profiling would be the lowest capital cost process to implement a modified pulping process especially for mills with a modified continuous or batch pulping process. Figure 1.5 shows the basic concept design for generating liquors of different sulfide concentrations.

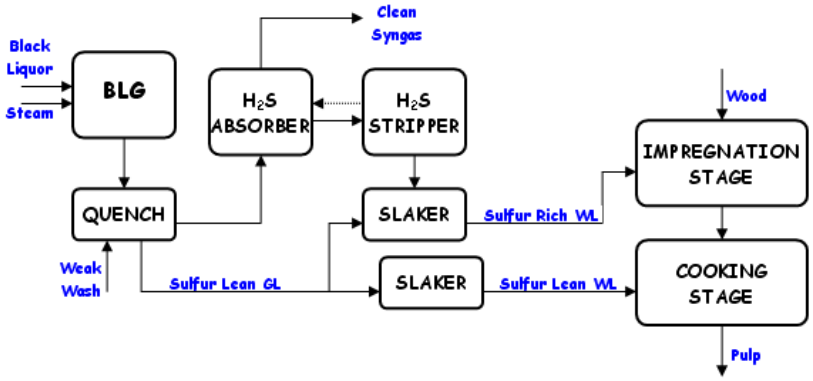

Figure 1.5 Schematic of Unit Operations in Split Sulfidity Pulping

The concept of sulfur profiling, or split sulfidity pulping, employing a sulfur-rich stream in the rapid initial phase, followed by a sulfur-lean stream in the bulk and residual phase, has been investigated as a method for extending delignification or increasing yield ([24,25,26,27]). Compared to conventional kraft cooks of similar H-factor, split sulfidity pulping has been shown to enhance selectivity of the pulping reactions, resulting in increases in both lignin removal and pulp viscosity. Moreover, split sulfidity pulping has been shown to increase pulp yield and strength properties ([28,29]).

The effects of multiple stage cooking using sulfur profiling, has also been studied. The process showed a significant improvement in selectivity ([30,31]). Increased sulfide sorption resulted in both higher lignin-free yields and increased viscosities. At 30% overall sulfidity, the lignin-free yield was 0.6 to 0.9% higher and viscosity about 10 mPa.s higher than conventional kraft. At increasing overall sulfidities, the yield advantage was reduced. Screened yield increased only slightly with higher sulfidity levels during impregnation. Similar findings were reported in subsequent work ([32]). Pulping work conducted at STFI found that sorption of sulfide increases

with increasing hydrosulfide concentration, time, temperature and concentration of positive ions, but decreases with an increasing concentration of hydroxide ions ([33]). The potential for modifying softwood kraft pulping by sulfur profiling was also investigated. When all of the sulfide was added to the beginning of the cook, a high hydrosulfide concentration could be maintained both in the initial phase and near the transition point from the initial to the bulk delignification phase ([34]).

The work described above is difficult to implement in a mill that utilizes conventional recovery technologies. However, BLG generates separate streams of sulfur and sodium, which will allow for independent sulfur and alkali profiling. Thus, the alkali profile can be adjusted independent of the sulfur concentration at any point in the cook. These opportunities were investigated at NC State University, exploring split sulfidity pulping of southern pine with different initial alkali concentrations. Based on a modified continuous cooking (MCC) laboratory procedure, different approaches were devised to explore split sulfidity and different initial alkali profiles ([35,36]). Two levels of initial alkali were investigated where a fraction of the available hydroxide was charged in the initial stage. The low initial alkali procedure used 11% of the alkali; the corresponding value for the high initial alkali procedure was 33%.

1.2.3.4 Kraft polysulfide pulping with anthraquinone

The effect on pulping chemistry of polysulfide (PS), often in conjunction with anthraquinone (AQ) as additives to the Kraft process, has been explored for some time ([37,38,39,40,41,42]). Its effectiveness has been established, and it is typically reported that each percent of PS added increases the pulp yield by one percent ([43, 44]). However, efficiently generating high concentrations of PS within the Kraft chemical recovery cycle is difficult. There are currently three primary competing processes available for PS generation: Chiyoda, MOXY™ and Paprilox® ([45]). These processes produce pulping liquors with PS concentrations of five to eight grams per liter and PS selectivities ranging from 60 to 90 percent ([46,47,48,49]). This results in a PS limit of about 1% PS charge on oven dry wood for a mill operating at 25% sulfidity. However, a chemical recovery system based around BLG would allow for different pathways to generate PS liquors which would enable higher charges of polysulfide. In addition, the separation of sodium and sulfur would allow for alkali profiling in conjunction with PS utilization. Figure 1.6 shows a schematic of PS process unit operations with BLG.

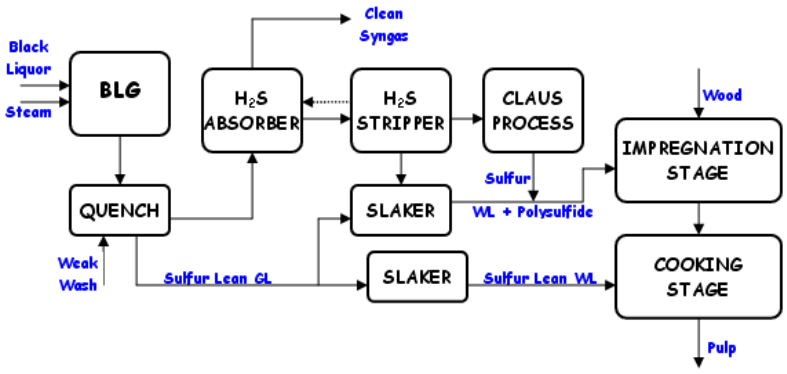

Figure 1.6 Outline of Process Using Polysulfide

Research efforts in the area of PS have generally been in one of two major areas; work on PS pulping associated with PS utilization in Kraft process operations and/or associated PS generation technologies ([46,47,48,49,50,51,52,53]) and work investigating optimum parameters for PS pulping ([54,55,56]). A smaller area of work has been based around the potential implementation of BLG and the opportunities created by the unrestricted management of sulfur and sodium as separate entities. The splitting of sulfur and sodium enables the application of polysulfide, sodium sulfide and sodium hydroxide independently of each other. Two processes have been described based on this concept. The ZAP process (Zero effective alkali in pretreatment), entails a two-stage pulping procedure, where the sulfur-containing cooking chemicals (Na_2S and PS) are charged along with AQ to the wood in the pretreatment stage ([57]). In the subsequent cooking stage, NaOH is added and the temperature increased. The obtained results using PS without AQ indicate a potential yield benefit of 1% relative to conventional PS pulping at kappa 30. With the addition of AQ, the yield benefit was increased to 1.5-2%. Additional results indicate even greater yield benefits at kappa 90. The other process is called hyperalkaline polysulfide pulping ([58]). The process utilizes two pretreatment stages followed by a cooking stage. In the first stage, alkali is charged to the wood at elevated concentrations, neutralizing the acids formed during the temperature elevation. PS is then charged in the second stage, followed by the cooking stage. The process resulted in a higher delignification rate, increased pulp viscosities and yield improvements of 1.5% as compared to modified pulping without PS. The bleachability and tear strength of the hyperalkaline PS pulps were similar to those of the Kraft reference pulp.

In addition to the capability for independent profiling of NaOH and PS, the implementation of BLG would allow for the conversion of all the sulfur in the cooking liquor to PS. This would enable higher PS charges than available through conventional technologies. The total amount of sulfur that is available is dependent on the sulfidity of the pulping liquor. Table 1.1 illustrates this balance displaying two examples of the partitioning of the total sulfur available in the system at 25 and 40% sulfidity. As seen in the table, PS charges slightly exceeding 2 % on wood are possible at 19.5% AA with 25% sulfidity. To enable higher PS charges the sulfidity must be increased and the PS value at 40% sulfidity is between 3 and 4% PS on wood.

Table 1.1 Sulfur Availability as Na_2S (Kraft) or Na_2S/PS (Kraft-PS)

	25% Sulfidity			**40% Sulfidity**		
Cook Procedure	***Tot. avail. Sulfur (S) (kg/ton)***	***S req. for PS (kg/ton)***	***S avail. as Na_2S (kg/ton)***	***Tot. avail. Sulfur (S) (kg/ton)***	***S req. for PS (kg/ton)***	***S avail. as Na_2S (kg/ton)***
MCC	25.2	0	25.2	40.3	0	40.3
1% PS	25.2	10.0	15.2	40.3	10.0	30.3
2% PS	25.2	20.0	5.2	40.3	20.0	20.26
3% PS	25.2	30.0	*- 4.8*	40.3	30.0	10.3
4% PS	25.2	40.0	*- 14.8*	40.3	40.0	*0.3*

1.2.4 Direct causticization of black liquor

Causticization of black liquor during combustion or gasification of black liquor using amphoteric oxides is a promising alternative chemical recovery technique. It involves the elimination of CO_2 from Na_2CO_3 as a result of the reaction between Na_2CO_3 and the amphoteric oxides at high temperature. Thus it has the potential to minimize or even eliminate the conventional lime causticizing process of the kraft recovery process. Depending on the solubility of the amphoteric oxide formed from the causticization reactions, these alternative causticization processes can be divided into two types: 1. autocausticization when the metal oxide can be dissolved in water; for example with B_2O_3, and 2. direct causticization when the product is insoluble in alkali solution. The oxides proposed to be used for direct causticization are TiO_2, Fe_2O_3 and Mn_2O_3 ([59,60]). The products formed from these oxides are insoluble in an alkali solution, and thus can be separated from the caustic solution before they are recycled. Therefore the direct causticization agents added to the black liquor recovery process will not affect the pulp quality because they do not participate in pulping process. Borate auto causticization is not discussed in the present review.

The main advantage of direct causticization is the reduction or elimination of lime causticizing and its associated external heating oil requirements. Other advantages are an energy improvement for overall chemical recovery process, improvements in the white liquor concentration and composition (less dead load of Na_2CO_3) and the possibility of creating a caustic solution mostly free of Na_2S. However there are also several disadvantages associated with this process: (i) a higher amount of solids are recirculating in the recovery system; (ii) the make-up cost of the causticizing agent; (iii) removal of non-process elements from the direct causticizing solids must be accomplished as a separate process step, and (iv) less energy generated from the gasification process because of the heat required for the endothermic direct causticization reaction.

Although the basic principles for the three direct causticization agents are very similar, the kinetics and reaction conditions are quite different for each of them. The focus of the present review is on titanium with some information also provided on iron because the latter has been applied commercially for the soda pulping process.

1.2.4.1 Titanates

Titanium dioxide (TiO_2) and sodium trititanate ($Na_2O{\cdot}3TiO_2$) are the only known direct causticization agents suitable for kraft black liquor recovery because they do not form sulfides and are not reduced to elemental titanium at the required process temperatures . Both iron oxide and manganese oxide cannot be used for kraft recovery because of the formation of iron and manganese sulfide. Research on direct causticization with titanates has been carried out by Kiiskilä ([61,62]), Zou ([63]), Zeng ([64]), Richards ([65]) and Nohlgren ([66]). The general reaction between Na_2CO_3 and TiO_2 can be described as follows:

$$bTiO_2 + aNa_2CO_3 \leftrightarrow aNa_2O{\cdot}bTiO_2 + aCO_2 \qquad (1.8)$$

Although quite a few chemical species of the form of $aNa_2O{\cdot}bTiO_2$ can be formed during the decarbonization reaction, only a few of them are stable at temperature between 700 and 1000°C. They are sodium hexatitanate, $Na_2O{\cdot}6TiO_2$, sodium tri-titanate, $Na_2O{\cdot}3TiO_2$, sodium penta-titanate, $4Na_2O{\cdot}5TiO_2$, and sodium meta-titanate, $Na_2O{\cdot}TiO_2$ ([67]). With this information,

reaction (1.8) can be simplified into two major reactions and three less important reactions. The two major reactions are:

$$Na_2CO_3(s) + 3TiO_2(s) \rightarrow Na_2O{\cdot}3TiO_2(s) + CO_2(g) \quad (1.3)$$

$$7Na_2CO_3(s) + 5(Na_2O{\cdot}3TiO_2)(s) \rightarrow 3(4Na_2O{\cdot}5TiO_2)(s) + 7CO_2(g) \quad (1.4)$$

The other reactions are:

$$6TiO_2(s) + Na_2CO_3(s) \rightarrow Na_2O{\cdot}6TiO_2(s) + CO_2(g) \quad (1.9)$$

$$Na_2O{\cdot}6TiO_2(s) + Na_2CO_3(s) \rightarrow 2(Na_2O{\cdot}3TiO_2)(s) + CO_2(g) \quad (1.10)$$

$$4Na_2O{\cdot}5TiO_2(s) + Na_2CO_3(s) \rightarrow 5(Na_2O{\cdot}TiO_2)(s) + CO_2(g) \quad (1.11)$$

It has to be pointed out that reaction (1.11) only takes place in a CO_2 free atmosphere ([63,62,68]), while the combination of reactions (1.9) and (1.10) leads to reaction (1.3) although no obvious evidence of reaction (1.9) has been found ([69]). Thus the main reactions in the gasification reactor are considered to be reaction (1.3) and reaction (1.4). Both reactions have been found to be strongly influenced by temperature, and are hindered by the presence of CO_2. Reaction rate and activation energy at temperature above 800°C have been determined by Zou ([63]) and Nohlgren et al. ([68,70]).

After sodium penta-titanate is formed, the hydrolysis of the product is accomplished in the leacher. The contact with water decomposes sodium penta-titanate to form sodium hydroxide and sodium tri-titanate shown below.

$$3(4Na_2O{\bullet}5TiO_2)(s) + 7H_2O \leftrightarrow 5(Na_2O{\bullet}3TiO_2)(s) + 14NaOH\ (aq) \quad (1.5)$$

Sodium trititanate is insoluble in the alkali solution. It is filtered off and recycled to the gasifier. The aqueous solution of sodium hydroxide is recycled for making new white liquor either for pulping or oxygen delignification purposes. The hydrolysis reaction rate is affected by the bulk concentration of NaOH and temperature ([71]).

Both of the decarbonisation reactions (1.3) and (1.4) and hydrolysis reaction (1.5) are endothermic (see Table 1.2). In the conventional causticization process, a large amount of the external energy is needed for the burning the lime at high temperature (850~900°C), while the energy is released as heat at low temperature (100°C) in the slaking and causticization process. In comparison, the direct causticization process requires only half of the energy delivered at high temperature and a small amount of energy during low temperature hydrolysis. Thus the direct causticization process has much better energy efficiency than conventional causticization ([66]).

Table 1.2 The Heat of Reaction and Temperatures of the Key Causticizing Reactions ([65])

Process/Reaction	Temperature(°C)	Heat of reaction (kJ/mol NaOH)
Lime		
Calcination	850	85
Slaking	100	-32.5
Causticizing	100	-2.1
Borate		
Causticizing	800	127.6
Dissolving	100	-125.3
Titanate		
Causticizing	850	30.5
Leaching	100	7.6

Thermodynamic analysis shows that sulphur will not combine with titanate ([72,63,73,74]) but will be released into the gas phase rather than retained as solid Na_2S. Thus white liquor with different sulfidities can be obtained after recovering the sulphur. This capability can be used to increase pulp yield in modified cooking processes. However, in practice Na_2CO_3 does not react instantaneously with titanate so that the volatilization of sulphur is determined by the following reaction equilibrium:

$$Na_2S(s) + H_2O(g) + CO_2(g) \leftrightarrow Na_2CO_3(s) + H_2S(g) \quad (1.12)$$

Based on the equilibrium of the reactant and the gas composition on the MTCI reactor it was estimated by Le Zeng and van Heiningen ([73]) that at atmospheric conditions the temperature needs to be lower than 725°C for complete release as H_2S.

Because the melting point of the eutectic titanate mixture produced by reaction (5) is 985°C, direct causticization would be suitable for combination with the fluidized bed gasification technology. The principle of this combined technology is shown in Figure 1.7.

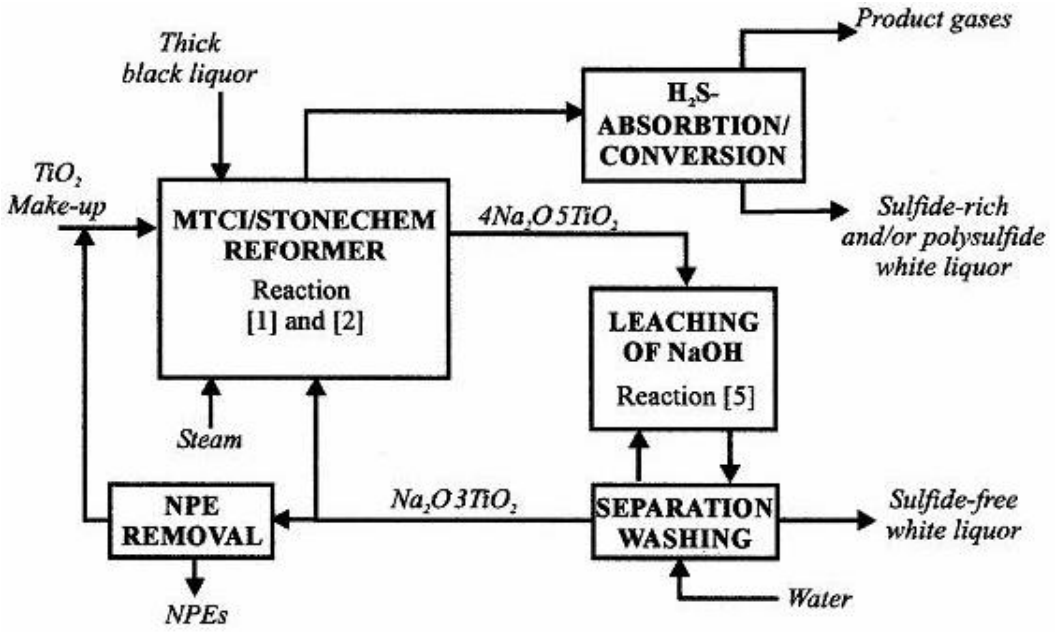

Figure 1.7. Schematic diagram of the MTCI Steam Reformer technology combined with titanate direct causticization

1.2.4.2 Previous research on titanate direct causticization

The research carried out by Kiiskilä in 1979 ([61,62]) showed that sodium trititanate ($Na_2O{\cdot}3TiO_2$) is the main product at low temperatures for the sodium carbonate (Na_2CO_3)-titanium dioxide (TiO_2) system. He also showed that the main products at high temperatures and low partial pressures of carbon dioxide are sodium meta-titanate ($Na_2O{\cdot}TiO_2$) and sodium penta-titanate ($4Na_2O{\cdot}5TiO_2$). At temperatures above 1000°C, the amount of CO_2 released is more than can be expected based on the formation of sodium meta-titanate. This is probably due to the decomposition of sodium carbonate. His work was continued by Zou ([63]) who used thermo gravimetric and differential thermal analysis (TG and DTA) to determine the weight loss at different temperature (655°C, 750°C and 985°C) for a mixture of sodium carbonate and titanium dioxide with a molar ratio of 1.0 in an atmosphere of air. The observed weight loss was in agreement with the formation of sodium trititanate, sodium pentatitanate and sodium metatitanate respectively. The products from the reactions were confirmed by X-ray diffraction (XRD) analysis. He also studied the kinetics of an equimolar mixture of Na_2CO_3 and TiO_2 below the melting point of sodium carbonate (858°C) (see Figure 1.8). Additionally he determined that a mixture of sodium carbonate and titanium dioxide of molar ratio 1.25 leads to a faster reaction rate and complete conversion of Na_2CO_3 at 825°C. In comparison, mixtures with a molar ratio below 1.25 never reached 100% conversion. Finally it was found that the conversion-time data are well described by Jander model when X>0.4 with an activation of 216 kJ/mol (Figure 1.9).

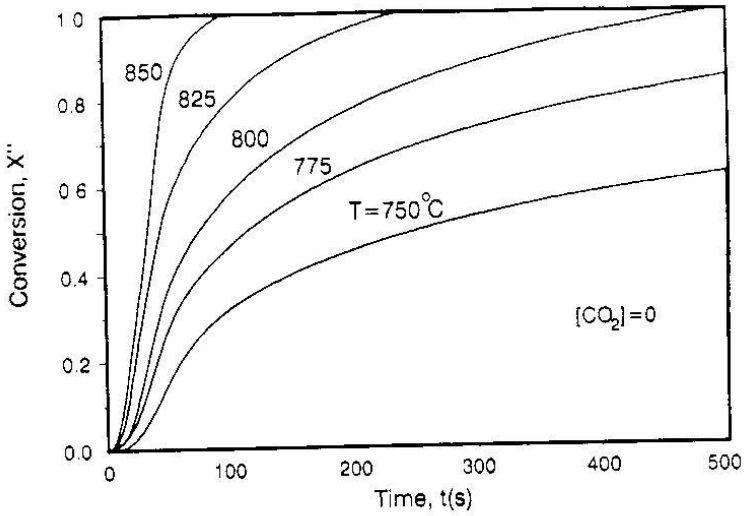

Figure 1.8. Kinetic data with recycled $Na_2O{\cdot}3TiO_2$ (TiO_2/Na_2O=1.0 mol/mol) in pure nitrogen ([63]). X is defined as conversion of $Na_2O{\cdot}3TiO_2$ to $4Na_2O{\cdot}5TiO_2$

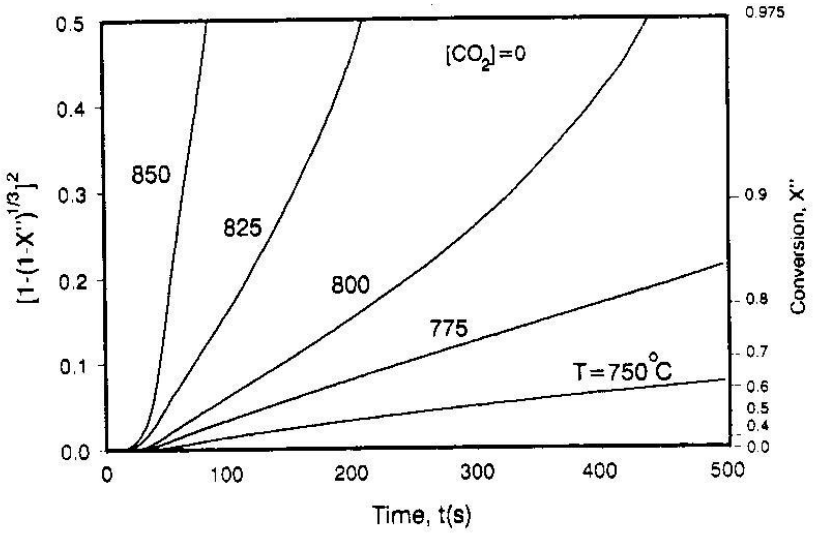

Figure 1.9. Jander kinetic model of $(1-(1-x)^{\frac{1}{3}})^2$ versus t. (TiO_2/Na_2O=1.0 mol/mol. X is defined as conversion of $Na_2O{\cdot}3TiO_2$ to $4Na_2O{\cdot}5TiO_2$)

More recent work was done by Nohlgren ([66]). She focused on the kinetics of the direct causticization reactions between sodium carbonate and sodium tri-titanate. The results are similar to that of titanium dioxide. In addition she used three different kinetic models to simulate her experiment data: a diffusion controlled model (Valensi-Carter model), a chemical reaction rate controlled model (phase boundary model) and a diffusion plus chemical reaction rate controlled model (shrinking core model). An example of the data simulation results can be seen in Figure 1.10. The results indicate that at 800°C the reactions are mostly diffusion controlled, while above 850°C the reactions are probably more controlled by chemical kinetics. Experiments in a pilot-

scale fluidized bed reactor using EDX (Energy Dispersive X-ray) analysis along cross-sections of reacted TiO_2 particles showed that the diffusion of Na_2CO_3 controls the rate of the direct causticization reaction between TiO_2 and Na_2CO_3. The results suggested that the mixing conditions are very important to obtain high conversion in a fluid bed reactor.

The melting point of the eutectic mixture of $4Na_2O{\cdot}5TiO_2$ and $Na_2O{\cdot}3TiO_2$ is 985°C ([75]). However, the temperature at which the surface of the bed particles becomes sticky will be much lower if the titanate particles are coated with significant amounts of Na_2CO_3, Na_2S and potassium and chloride- containing salts. Therefore, the direct causticizing reaction kinetics should be fast enough to minimize the amount of Na_2CO_3 in the bed, and the temperature should be low enough to allow complete conversion of Na_2S to Na_2CO_3 and H_2S by reaction (1.10). Based on the equilibrium of this reaction ([76]), it is estimated that the bed temperature should be kept below about 725 °C at atmospheric conditions to shift the reaction fully to the right.

Richards ([65]) calculated that compared to conventional causticization and borate auto causticization the titanate direct causticization process has the lowest energy demand (Table 1).

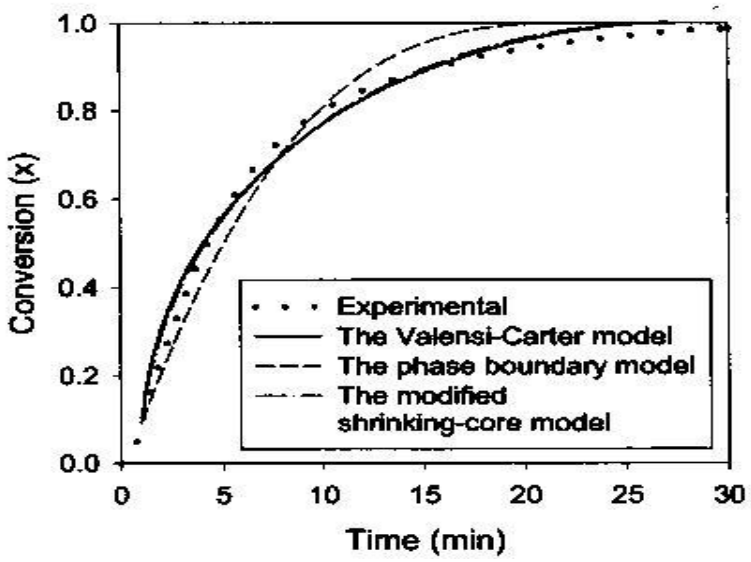

Figure 1.10. Degree of conversion versus time for the models and the experimental data at 840°C and 0.5% CO_2 ([66])

This process completely eliminates the lime cycle. It also allows a higher fluid bed operating temperature because the bed now consists mainly of high melting point titanates. The higher operating temperature also introduces several advantages, e.g. higher carbon conversion, reduction of emission of tars, and increased black liquor throughput. In addition, the quality of energy generation in this process is also highest because the direct causticization reaction is endothermic and the heat required is provided by combustion of gasification gases, while in the lime cycle the heat for calcination of the lime is provided by fossil fuel combustion.

1.2.4.3 Iron (III) oxide

The direct causticization of soda black liquor using iron (III) oxide (Fe_2O_3) is known as direct alkali recovery system (DARS) which was developed in the late seventies ([77]). Because iron oxide will react with Na_2S to form insoluble iron sulfides, this system is only applicable to the soda-process, which is a sulfur-free system, and not applicable to the kraft pulping process. Also the DARS process can only operate under oxidizing conditions, because gasification conditions lead to reduction of Fe_2O_3 to Fe at the operating temperature.

Similar to the titanates, the decarbonization reaction with iron oxide is quite complicated because sodium ferrite and ferric oxide have a number of crystal forms and the actual reaction mechanism depends on temperature and the crystal forms involved. ([78]). For temperatures above 850°C when carbon dioxide pressure has a minor influence on the decarbonization reaction rate, the main direct causticization reaction is:

$$Fe_2O_3 + Na_2CO_3 \rightarrow 2NaFeO_2 + CO_2 \qquad (1.13)$$

In the separated leacher the following hydrolysis reaction takes place:

$$2NaFeO_2 + H_2O \rightarrow 2NaOH + Fe_2O_3 \qquad (1.14)$$

A commercial plant in Burnie, Tasmania was the first mill in the world using Iron(III) oxide as the decarbonization agent from 1986 until 1998 when the mill was shut down ([79]). This mill was an integrated pulp and paper mill producing 300 tons of pulp per day. Only hardwood was used in this soda-AQ pulping process. It is reported that the initial installation cost (approximately $20 million AUD in 1985) was about half the cost for a conventional recovery boiler installation. The capacity of the DARS plant increased from below 25% of its original design in 1990 to 70% in 1995. For successful operation the following is recommended:

1. Fluidized bed operation requires a good control of bed particle size, furnace temperature (°C), black liquor quality, flue gas oxygen level and excess iron level.
2. Effective leaching and washing of the ferrite product
3. Pelletizing the disintegrated leached product to the desired particle size

1.2.5 Kinetic models for solid-solid reactions

Because the direct causticization involves the reaction between two solids, Na_2CO_3-TiO_2/$Na_2O.3TiO_2$, the solid-solid reaction models which are used to describe the kinetics of this reaction are summarized in Table 1.3 below. The Jander model is the simplest diffusion controlled model because it neglects a change in reactant radius and is only applicable when the ratio of the inner and outer surface of the product shell is small. The Valensi-Carter model is a similar diffusion controlled model, which takes the change of volume due to reaction into account. Both are a called “shrinking-core” model because they assume a reactant particle is surrounded by a continuous product layer where the unreacted core shrinks during the reaction. A phase-boundary model is a chemical reaction controlled model. It assumes that the mass transport of the reactant through the product layer is rapid enough compared to the chemical reaction. In the modified shrinking core model, the reaction rate is controlled by both diffusion and chemical reaction ([80]).

Table 1.3. General Description of Solid-Solid Reaction Models

(X is the degree of conversion (0≤X≤1), k the rate constant, t the time, z the volume of product formed per volume of reactant consumed, r the spherical particle radius at time t, and r_0 the initial radius of the sphere.)

Model	Rate Controlling Step	Equation integrated	Source
Jander	Diffusion	$\frac{2k}{r_0^2}t = (1-(1-X)^{\frac{1}{3}})^2$	Jander ([81])
Valensi-Carter	Diffusion	$\frac{2(1-z)k_1}{r_0^2}t + z = (1+(z-1)X)^{\frac{2}{3}} + (z-1)(1-X)^{\frac{2}{3}}$	Carter ([82])
Phase-boundary	First order chemical kinetics	$\frac{k_2}{r_0}t = 1-(1-X)^{\frac{1}{3}}$	Tamhankar and Doraiswamy ([83])
Modified shrinking core model	Diffusion and chemical kinetics	$t = -\frac{r-r_0}{k_3} - \frac{(\frac{r^2-r_0^2}{2} - \frac{1}{2(1-z)}((r^3(1-z)+zr_0^3)^{\frac{2}{3}} - r_0^2))}{k_4}$	Nohlgren ([66])

The above listed models assume 100% at sufficient long reaction times, while it is known that direct causticization does not reach complete conversion at certain operating conditions. Therefore a model developed by Lee ([84]) which accounts for incomplete conversion was also considered. If Xu is the ultimate conversion of sodium carbonate, then for a second order chemical reaction or diffusion controlled reaction it follows that:

$$\frac{dX}{dt} = k(1-\frac{X}{Xu})^2 \qquad (1.15)$$

Initially a thin product layer is formed during which Eq. (1.15) describes a second order chemically controlled reaction. Then the reaction slows down dramatically because the overall reaction rate is now controlled by diffusion. Integration of equation (1.15) gives:

$$X = \frac{Xu \cdot t}{(Xu/k)+t} \qquad (1.16)$$

If a constant *b* is used to represent the time to achieve half of the ultimate conversion (X=Xu/2 at t=b), it follows that:

$$Xu = kb \qquad (1.17)$$

By substituting equation (1.17) into equation (1,16), the final conversion as a function of time can be expressed as:

$$X = \frac{kbt}{b+t} \qquad (1.18)$$

This equation can also be written in a linear form for data fitting ([84]):

$$\frac{1}{X} = \frac{1}{k}\left(\frac{1}{t}\right) + \frac{1}{kb} \qquad (1.19)$$

which is applicable both when the reaction is controlled by surface chemical reaction during the initial phase, and by diffusion in the final phase; each phase described by a different set of constants k and b.

2. TASK 1 – PULPING STUDIES

The pulping studies explored in this project focused on the effects which implementation of black liquor gasification might have on conventional pulping operations. A two pronged approach was pursued: to investigate modified pulping technologies that BLG implementation would enable, and to explore potential process modifications to a kraft mill through process simulation. The first approach entailed laboratory pulping experiments exploring different modified or advanced pulping technologies based on the separation of sodium and sulfur in chemical recovery. The second entailed the generation of a BLG model, its integration into the WinGEMS software package, and process simulation exploring the combined effects of BLG integrated with the different pulping technologies outlined above on process economics.

2.1 Objectives

2.1.1 Objectives for laboratory pulping work

Different opportunities arise in the application of pulping chemicals to wood during pretreatment and digestion when sulfur and sodium are separated during chemical recovery operations. The capability to independently charge sulfur and sodium was explored through laboratory pulping using green liquor pretreatment, split sulfidity pulping, and polysulfide pulping with and without anthraquinone addition. The objective for the pulping work was to establish the potential benefits with regard to total pulp yield, delignification, pulp viscosity and physical properties as compared to pulps generated using conventional kraft pulping methods.

2.1.2 Objectives for process simulation work

When considering the implementation of new technologies, it is of great benefit to use process simulation as a tool to predict the potential effects of process modifications on overall process operation and economics. In order to simulate BLG and BLG enabled modified kraft pulping operations, it was necessary to develop a BLG WinGEMS model. This model was then to be integrated into the WinGEMS software package, and used to explore the effects of retrofitting BLG into kraft pulping on process operation and economics.

2.2 Results and discussion of laboratory pulping work

2.2.1 Pulping procedures

Wood

Screened mixed southern softwood chips were used throughout the laboratory cooking. For each cook, 800 oven dry grams of chips were soaked in water over night. The chips were drained for 30 minutes and placed in the M&K batch digester prior to chemical addition.

Development of Modified Continuous Cooking as baseline pulping procedure

A laboratory cooking procedure was developed to simulate modified continuous cooking, MCC™. The results obtained with this procedure were taken as the baseline against which the other modified cooking methods; green liquor pre-treatment, split sulfidity and PS-AQ, were compared. The MCC™ cooking protocol was divided into three stages with addition of active chemical at the end of the first and second stage. The total cooking time from "time 0" (time = 0 at T = 100 ºC) was fixed at 240 minutes, while the cooking temperature was varied to produce the desired h factor (153-166 ºC). The active alkali, AA was set to 19.5 % on OD pulp and the

sulfidity to 25 %. In addition, Na_2CO_3 was added as 15 % of the total chemical on wood, simulating a system dead load. The resulting total titratable alkali, TTA was divided for addition between the three stages. In the first stage, the chips were placed in the digester with 65 % of the TTA and water, to bring the liquor to wood ratio, L/W, to 3.5. The cook was then brought to 120 ºC and held at temperature for 15 minutes. For the second stage white liquor heated to 125 ºC was added being equal to 20 % of the TTA, bringing the cumulative added TTA to 85 %. The cook was then brought to the desired temperature and held there until 105 minutes had elapsed from "time 0". For the third stage, white liquor heated to 125 ºC being equal to the final 15 % of the TTA was added, bringing the L/W to about 4.5. The cook was then held at temperature until complete. The M&K batch digester system used in the experimental work was fitted with valves to enable liquor addition and extraction. An American LEWA Inc. type EK2 pump was used to feed heated liquor under pressure into the lab digester. The parameters for the MCC procedure are outlined in Table 2.1**.**

Table 2.1 Parameters for MCC protocol

	Cumulative %	L/W	Temperature (ºC)	Minutes at T
Stage I	65	3.5	120	15
Stage II	85	4.1	153-166	~ 70
Stage III	100	4.5	153-166	120

Development of Split Sulfidity and Green Liquor Pretreatment procedur*e*

The split sulfidity cooking protocols, displayed in Table 2.2, closely resembled that of the MCC baseline. The main difference is the liquor profile used. The total titratable alkali was kept constant throughout both the MCC baseline and split sulfidity cooks, but the addition scheme of the Na_2S and NaOH was altered. To maximize the sulfidity effect on the pulp, the total amount of Na_2S used was added in Stage 1. The NaOH was then split between the three different stages using two different approaches: Split Sulfidity – High Initial Alkali and Split Sulfidity – Low Initial Alkali (SS_HIA and SS_LIA). The Na_2CO_3 was evenly added to each stage to simulate system dead load. In the first approach (SS_HIA) the NaOH was added evenly, one third to each stage, resulting in a high initial alkali concentration followed by uniform increases in alkali through the liquor additions. In the second approach (SS_LIA), the amount of NaOH added to stage I was limited to a small amount (about 11 % of the total NaOH added), resulting in a low initial alkali concentration, but a sufficiently high level of pH during the first stage.

The green liquor pretreatment protocol is analogous to the one described for split sulfidity. To generate a high concentration Na_2CO_3 green liquor, simulating a decreased level of causticization in the recovery loop, 25 % of the NaOH used previously was replaced by 25 % Na_2CO_3 maintaining a constant system TTA. The concept of high and low initial alkali was again employed and the resulting parameters for the green liquor pretreatment cooks are shown in Table 2.3. In order to produce pulps of lower kappa a series of cooks was additionally performed where the system TTA was increased by 10 %, using the same TTA component breakdown as the high initial alkali protocol. The modified green liquor pretreatment procedure was labeled "High TTA".

Table 2.2 Parameters for Split Sulfidity protocols, high initial and low initial alkali (SS_HIA/SS_LIA)

SS_HIA	% of chemical added						
	Cum. %	Na_2S	NaOH	Na_2CO_3	L/W	Temp. (ºC)	Min. at T
Stage I	47.6	100	33.3	33.3	3.5	120	15
Stage II	73.9	0	33.3	33.3	4.1	153-166	~70
Stage III	100	0	33.3	33.3	4.5	153-166	120
SS_LIA	% of chemical added						
	Cum. %	Na_2S	NaOH	Na_2CO_3	L/W	Temp. (ºC)	Min. at T
Stage I	33.28	100	10.9	33.3	3.5	120	15
Stage II	66.76	0	44.5	33.3	4.1	153-166	~70
Stage III	100	0	44.5	33.3	4.5	153-166	120

Table 2.3 Parameters for Green Liquor Pretreatment protocols, high initial and low initial alkali (GLPT_HIA/GLPT_LIA)

GLPT_HIA	% of chemical added						
	Cum. %	Na_2S	NaOH	Na_2CO_3	L/W	Temp. (ºC)	Min. at T
Stage I	57.33	100	33.3	65.0	3.5	120	15
Stage II	78.7	0	33.3	17.5	4.1	153-166	~70
Stage III	100	0	33.3	17.5	4.5	153-166	120
GLPT_LIA	% of chemical added						
	Cum. %	Na_2S	NaOH	Na_2CO_3	L/W	Temp. (ºC)	Min. at T
Stage I	46.6	100	10.9	65.0	3.5	120	15
Stage II	73.3	0	44.5	17.5	4.1	153-166	~70
Stage III	100	0	44.5	17.5	4.5	153-166	120

Development of polysulfide-anthraquinone pulping procedure

Polysulfide liquor was generated by dissolving elemental sulfur in Na_2S. The mixture was heated at 60 ºC under an N_2 atmosphere until completely dissolved. Cooks employing PS were performed according to the earlier described MCC procedure with some modifications. The main differences were the utilization of sulfur added as a combination of PS and Na_2S, the profile of NaOH and Na_2CO_3 addition, and the addition of anthraquinone, AQ. AQ was added to each PS cook at a charge of 0.1% on oven dry wood to enhance the delignification rate. Furthermore, to maximize the effect of PS and system sulfidity, according to the principles of extended delignification, the total amount of Na_2S used was added in Stage 1. Table 1.1 shows the charges of sulfur as elemental sulfur and as Na_2S for 19.5% AA and 25% or 40% sulfidity.

To offset the loss of TTA added to Stage 2 and 3 resulting from the addition of the entire amount of sulfur species in Stage 1, the profile for alkali addition was altered accordingly. The lost balance of TTA in Stage 2 and 3 was made up by decreasing the addition of NaOH and Na_2CO_3 to Stage 1 in amounts equal to that of the added sulfur species, and charging the alkali to Stage 2 and 3 maintaining the 65/20/15 ratio employed in the MCC baseline cooks. The values for the

40% sulfidity system are given in parenthesis. The resulting splits for chemical addition in the PSAQ cooks are shown in Table 2.4.

Table 2.4 Parameters for Polysulfide-Anthraquinone (PSAQ) cooks

PSAQ		% of chemical added					
	Cum. %	Na_2S	NaOH	Na_2CO_3	L/W	Temp. (ºC)	Min. at T
Stage I	65	100	56	56 (47)	3.5	120	15
Stage II	85	0	25	25 (30)	4.1	164	~70
Stage III	100	0	19	19 (23)	4.5	164	120

In addition to the PSAQ liquor parameters outlined in Table 2.4, two more cooking protocols were investigated at 3% PS charge, where the alkali charge in Stage 1 was increased. These conditions were aimed at exploring the effect of higher initial alkali charge on the effectiveness of PS relative the delignification rate and pulp properties. The initial PSAQ protocol employed at 3% PS charged was labeled low initial alkali (LIA), which was then followed by a medium initial alkali charge (MIA) and a high initial alkali charge (HIA). The liquor parameters for the PSAQ-MIA and HIA protocols are displayed in Table 2.5.

Table 2.5 Parameters for medium (MIA) and high (HIA) initial alkali PSAQ cooks

PSAQ-MIA		% of each chemical added					
	Cum. %	Na_2S	NaOH	Na_2CO_3	L/W	Temp. (ºC)	Min. at T
Stage I	77	100	65	65	3.5	120	15
Stage II	90	0	20	20	4.1	164	~70
Stage III	100	0	15	15	4.5	164	120
PSAQ-HIA		% of each chemical added					
	Cum. %	Na_2S	NaOH	Na_2CO_3	L/W	Temp. (ºC)	Min. at T
Stage I	84	100	75	75	3.5	120	15
Stage II	94	0	15	15	4.1	164	~70
Stage III	100	0	10	10	4.5	164	120

All obtained pulps were thoroughly washed with water, disintegrated using an impeller mixer and screened. The screen accepts were fluffed prior to yield determination and refrigerated for storage. The total yield is given as the sum of the oven dry accepts and rejects. Pulp kappa numbers and viscosities were determined for all screened accept samples. Samples with kappa number exceeding 50 were treated with standard chlorite delignification before pulp viscosity determination. A total of six screened pulp samples, representing each procedure in the low and high kappa range, were refined using a PFI mill according to CPPA Standard C.7. Handsheets were made according to TAPPI T 205, and tested following T 220. The resulting sheet caliper, tear, tensile and burst, were determined according to TAPPI T 411, T 414, T 494, and T 403 respectively.

2.2.2 Pulping results

The following sections discuss the laboratory pulping results exploring green liquor pretreatment, split sulfidity pulping and polysulfide pulping with anthraquinone.

2.2.2.1 Green liquor pretreatment

The green liquor pretreatment pulping experiments show that pulps of higher kappa than those of the MCC base line pulps were produced at the same level of total titratable alkali (see Figure 2.1). However, as shown in the figure it would be possible to achieve a similar kappa number at the same level of system TTA by pulping to a higher H factor. Another option for decreasing the kappa number would be to increase the system TTA. Experiments performed with a 10% increase in TTA, labeled Hi-TTA, also resulted in a higher kappa number than the MCC baseline. In this study, if the TTA is increased by 20% the active alkali is the same in both processes, and the no causticizing benefits exist. The resulting pulp yield did not show any improvement with green liquor pretreatment. Thus these results did not show the yield benefit reported elsewhere for green liquor pretreatment, and may be the result from differences in pulping procedures ([22]). Figure 2.2 displays the obtained viscosity values as a function of kappa. As seen in the figure, the modified green liquor pretreatment procedure produced pulps of similar viscosity to those of the MCC procedure.

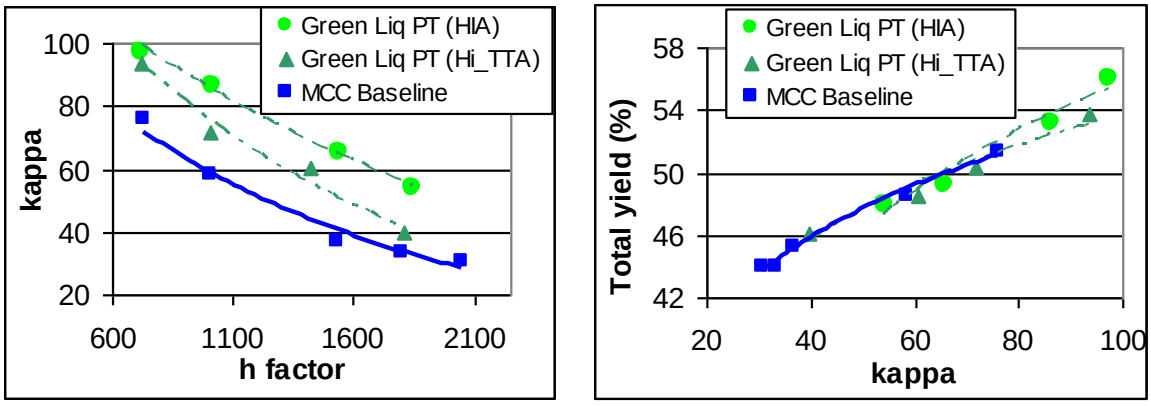

Figure 2.1 Comparison of green liquor pretreatment and MCC™ pulping results

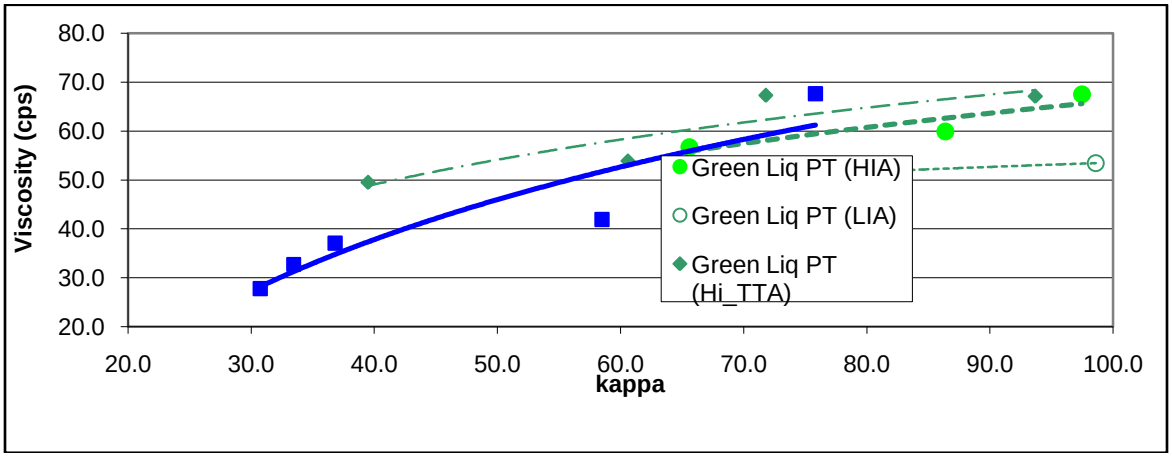

Figure 2.2 Viscosity versus kappa for MCC baseline and green liquor pretreatment cooks

2.2.2.2 Split sulfidity pulping

The effects of split sulfidity and different levels of initial alkali on delignification and total pulp yield are presented in Figure 2.3. As shown, split sulfidity pulping produced lower kappa pulps at similar H factors relative to the MCC procedure. The high initial alkali cooks generated pulps of lower kappa number compared to those of low initial alkali. The split sulfidity procedures produced pulp yields 1-2% greater than the MCC procedure, and the difference is more pronounced at higher kappa. Since the high initial alkali approach produced higher yields and lower kappa numbers than the low initial alkali approach, this would be the preferred option. At similar kappa numbers the split sulfidity pulps had viscosities 5 to 10 mPA.s (or cP) greater than those of the MCC pulps as can be seen in Figure 2.4. The 1800 h-factor, high initial alkali pulps produced higher tensile and burst index values relative the 1800 h-factor MCC pulps at a similar tear index as shown in respectively Figures 2.5 and 2.6. The MCC pulps were slightly easier to refine relative to the split sulfidity pulps.

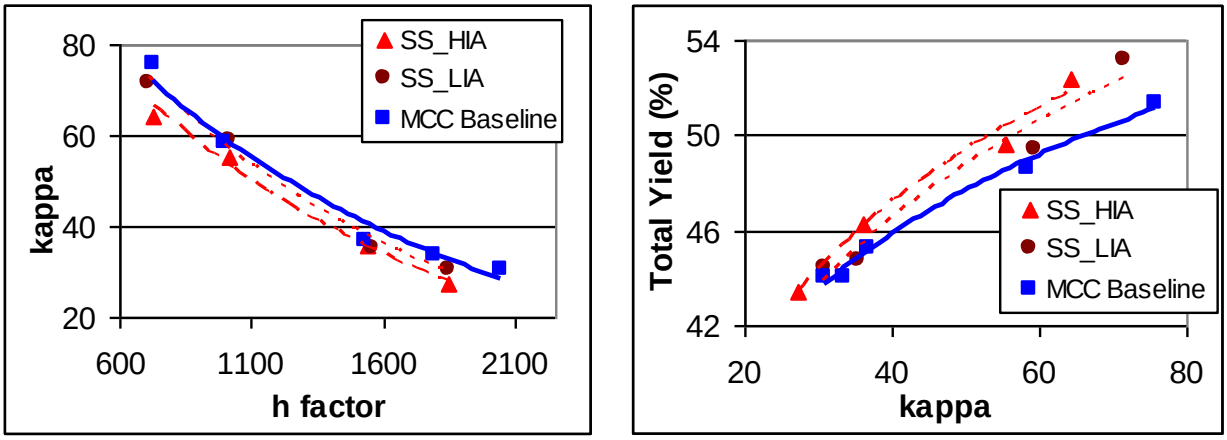

Figure 2.3 Delignification and yield results for split sulfidity pulping

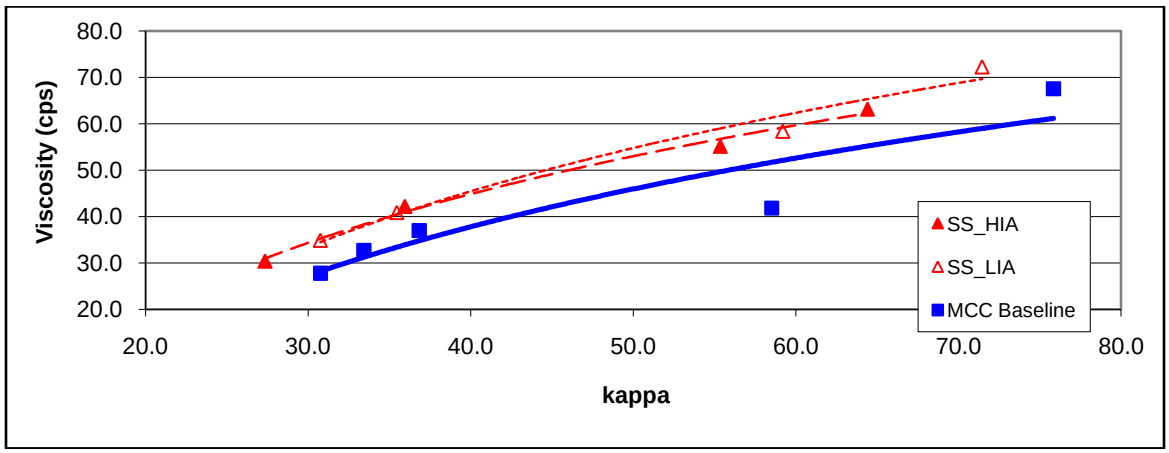

Figure 2.4 Viscosity versus kappa for the MCC baseline, SS_HIA and SS_LIA cooks

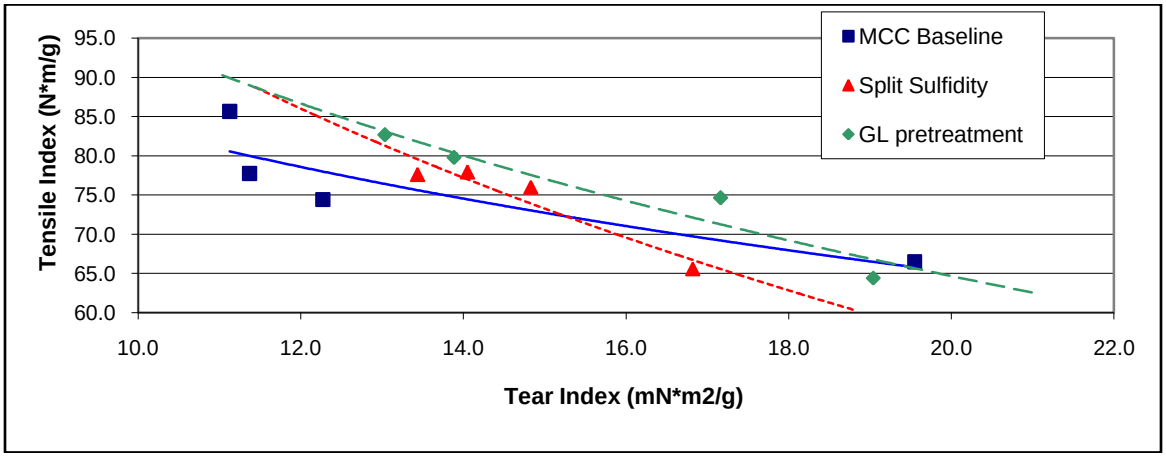

Figure 2.5 Tensile index versus tear index for low kappa pulps (h-factor of 1800 hrs.)

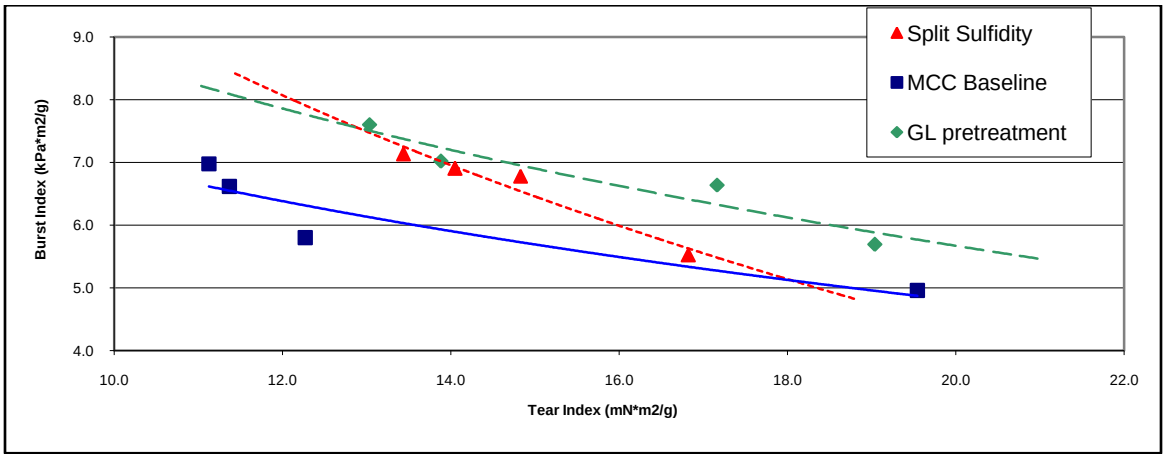

Figure 2.6 Burst index versus tear index for low kappa pulps (h-factor of 1800 hrs.)

2.2.2.3 Polysulfide (PS) and polysulfide-anthraquinone (PSAQ) pulping

Figure 2.7 shows how the 1 and 2% PS procedures compare with the MCC procedure at 25% sulfidity, in terms of lignin removal as a function of AA charge. As shown, the 1% PS procedure produced lower kappa pulps at similar AA charge relative the MCC procedure, whereas the 2% PS procedure produced pulps of somewhat higher kappa. This can be explained by the polysulfide chemistry which results in an alkali consumption which is different from MCC. During the preparation of the polysulfide solution, alkali is consumed when sulfur reacts with Na_2S to form polysulfide according to Dorris and Uloth ([85]):

$$HS^- + nS^0 + OH^- \rightarrow S_nS^{2-} + H_2O \qquad \text{where n=2-3} \qquad (2.1)$$

Thus for n=2, i.e. the formation of Na_2S_3, the consumption of effective alkali (EA, i.e. NaOH) expressed as Na_2O is 31/64 gram per gram of polysulfide (as Sulfur). In terms of AA this is equal to 1/(1-0.5S)x31/64 gram of Na_2O per gram of polysulfide (as Sulfur), where S is sulfidity as fraction. For 25 and 40 % sulfidity (S=0.25 and 0.40), the AA consumption is 0.55 and 0.61

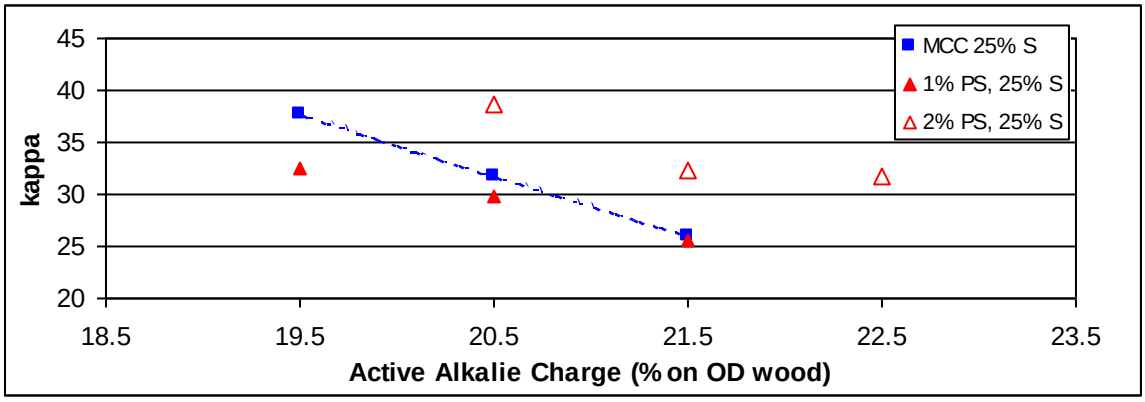

Figure 2.7 Kappa number versus AA charge for MCC and PS cooks at 25% sulfidity

times the polysulfide charge as % sulfur on wood respectively. In addition during stages 2 and 3 more alkali is consumed due to the reaction ([85]):

$$2Na_2S_3 + 2NaOH + H_2O \xrightarrow{>130^oC} 4NaHS + Na_2S_2O_3 \qquad (2.2)$$

However, polysulfide leads to oxidation of reducing end groups of the carbohydrates, and thus to a reduction in the peeling reaction which consumes alkali. Thus the explanation for the slightly increased delignification at 1% PS at 25% sulfidity is that the reduction in alkali consumption due to oxidation of the carbohydrate reducing ends is larger than the alkali consumption due to reactions (2.1 and 2.2). The opposite occurs at 2% PS because the available reducing ends is limited. Another aspect is that the amount of sulfur in the form of Na_2S should be at least about half of that of the sulfur as polysulfide in order to form Na_2S_3. This requirement is not satisfied at 2% PS and 25% sulfidity (see Table 1.1), resulting in less active polysulfide at this condition. At 40% sulfidity this situation occurs at a PS charge of slightly less than 3%. (see Table 1.1)

The total pulp yield as a function of kappa for the 1 and 2% PS and MCC procedures are compared in Figure 2.8. The results show that the PS procedures produced pulp yields about two percent greater than the MCC procedure irrespective of whether 1 or 2% PS was used.

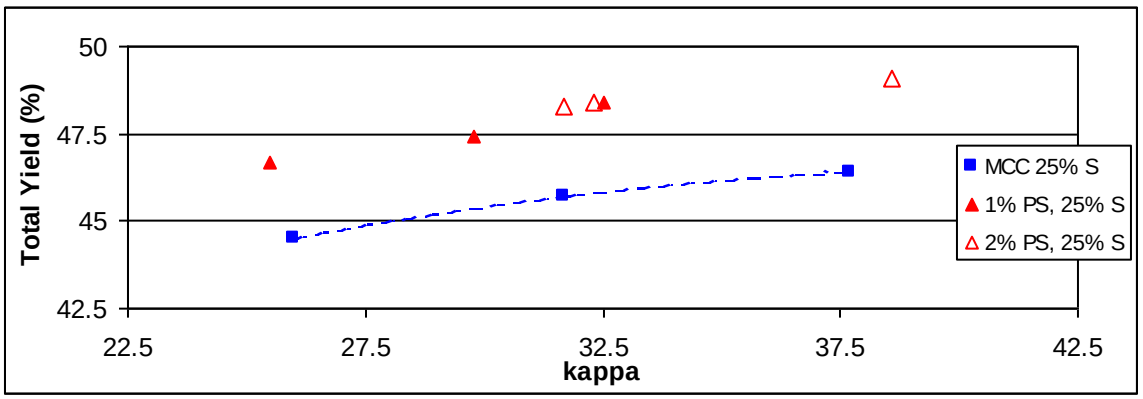

Figure 2.8 Total yield versus kappa for the MCC baseline and PS cooks at 25% sulfidity

The explanation for the similar yield increases for the 1 and 2% PS cooks might be that a less effective form of polysulfide is formed at 2% PS (n < 2), while also less alkali is consumed in a thiosulfate formation reaction similar to that of equation 2.2. The higher effective hydroxide concentration during would further reduce the retention of carbohydrates.

The pulp viscosity as a function of kappa was similarly compared for the different procedures. The resulting graph is shown in Figure 2.9. As shown in the figure, the 1% PS procedure produced pulps of slightly greater viscosities than the MCC reference, whereas the 2 % PS procedure resulted in slightly lower viscosities at similar kappa. Again the higher hydroxide concentration during the 2% PS cook may explain the reduced reduction in pulp viscosity compared to the 1% PS and MCC reference.

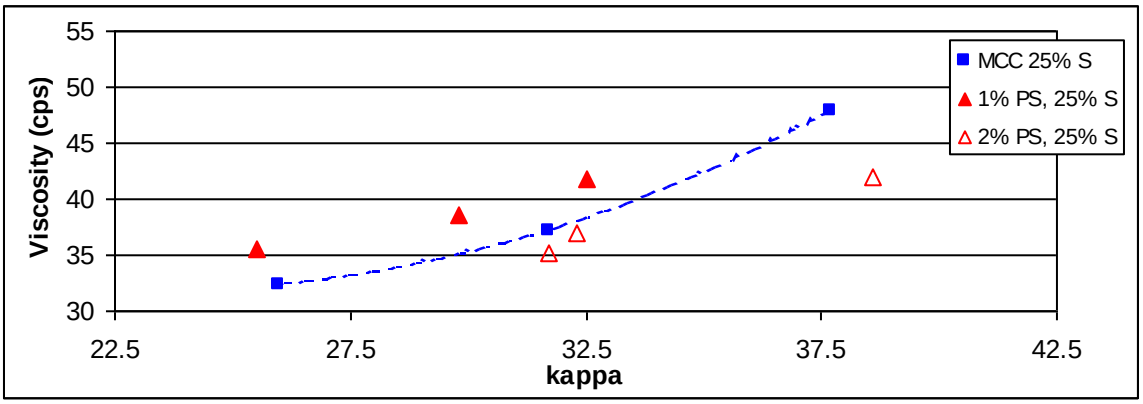

Figure 2.9 Viscosity versus kappa for the MCC baseline and PS cooks at 25% sulfidity

Similar experiments were performed at 40% sulfidity and 1 and 2% PS. These cooks produced a similar yield as the PS pulps generated at 25% sulfidity, but required a significant increase in AA charge relative to the MCC reference cooks to obtain a 30 kappa number pulp (21.5 and 23.5 respectively versus 19.5%). No clear explanation for this decrease in delignification efficiency at 40% sulfidity can be provided, except perhaps that the liquor composition is not right for the stoichiometry of reaction 2.1. For more information see Lindstrom ([90])

When pulping at 40% sulfidity and 3% PS it was also found that more initial alkali is required to maintain delignification rates. Another finding for these high PS cooks was that the delignification rate and pulp yield are significantly affected by the distribution of the alkali charges over the three stages ([90]). Therefore a new series of experiments were performed which aimed to optimize the alkali distribution over the three stages of the PS cooks.

Cooks were completed using 20.5% AA at sulfidity levels of 25% and 40%. 0.1% AQ was added to both the MCC and PS cooks. The total AA available was split between the three stages. Table 2.6 outlines the performed cooks and the alkali profiles. The PSAQ cooks at 25% sulfidity had a PS charge of 2% on OD wood; the 40% sulfidity cooks had a 3% PS charge. As shown in Table 2.6, the three levels of alkali charged in stage 1 of the MCC procedure match the middle three levels of initial alkali for the PSAQ procedure.

Table 2.6 Outline of cooks performed using 25% and 40% sulfidity

COOK	% AA on OD wood	Sulfidity (%)	% PS on OD wood	% AQ on OD wood	Alkali Profile
MCC1	20.5	25 / 40	0 / 0	0.1	(20/46/34)
MCC2	20.5	25 / 40	0 / 0	0.1	(45/31/24)
MCC3	20.5	25 / 40	0 / 0	0.1	(65/20/15)
PSAQ1	20.5	25 / 40	2 / 3	0.1	(0/54/46)
PSAQ2	20.5	25 / 40	2 / 3	0.1	(20/46/34)
PSAQ3	20.5	25 / 40	2 / 3	0.1	(45/31/24)
PSAQ4	20.5	25 / 40	2 / 3	0.1	(65/20/15)
PSAQ5	20.5	25 / 40	2 / 3	0.1	(80/11/9)

The obtained results from the cooks outlined in Table 2.6 are displayed in Figures 2.10 through 2.13. The first two figures show the data generated from the cooks performed at 25% S, the following two figures the data from the 40% S.

Figure 2.10 describes the pulp kappa numbers generated at 25% S using different alkali profiles. The obtained pulp kappa numbers for the MCC pulps using different alkali profiles were very similar, ranging from 27.8 to 29.3. The effect from alkali profiling was much more pronounced for the 25% S PSAQ pulps, where the zero initial alkali cook resulted in a pulp kappa of 39.0. As the alkali charge in the initial stage was increased, the pulp kappa decreased significantly. At a charge of 45% of the initial alkali the resulting kappa from PSAQ is similar to the MCC and at higher initial alkali charge PSAQ resulted in lower kappa values. Thus, these results show that at 25% sulfidity it is possible to achieve similar to lower kappa numbers using PSAQ relative to that of the MCC reference.

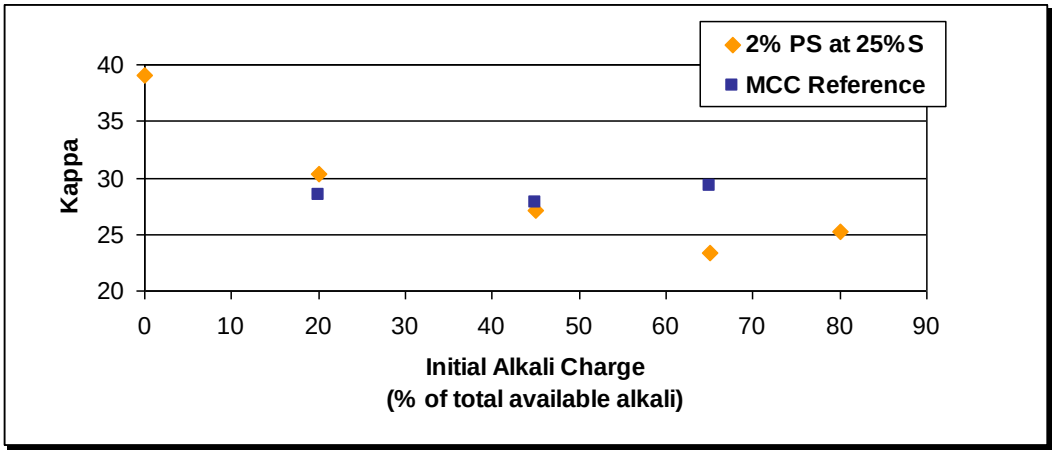

Figure 2.10 Kappa number versus initial alkali charge for 25% sulfidity pulps (PSAQ and MCC)

The obtained total pulp yields were normalized to kappa 30 using the relationship ± 0.15 % pts. total pulp yield / kappa unit different from 30. Figure 2.11 displays the normalized total pulp yields obtained from 25% S cooks using different levels of initial alkali. As shown the PSAQ procedure resulted in higher pulp yields than the MCC reference pulp.

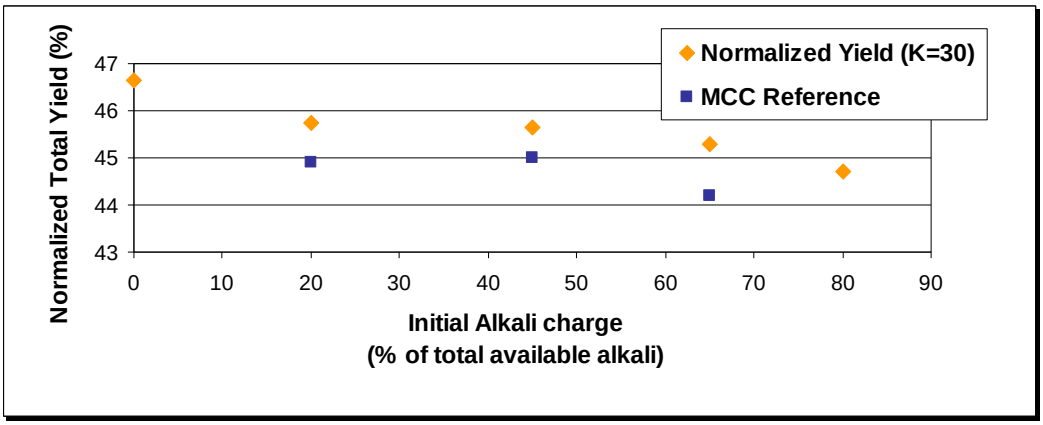

Figure 2.11 Normalized total yield versus initial alkali charge for 25% sulfidity pulps (PSAQ and MCC)

At zero initial alkali charge the PSAQ normalized yield was 46.7% compared to 44.3% for the conventional MCC pulp using 65% of the initial alkali in the first stage, indicating a potential yield benefit of 2.4% pts. As the amount of initial alkali charged in the PSAQ procedure was increased from 0% to 80%, the obtained yield decreased by about 2% pts. while the kappa decreased by about 15.

The pulps prepared at 40% sulfidity followed similar trends, but the differences in PSAQ delignification rates and pulp yields were more pronounced. Figure 2.12 shows that as the initial alkali charge was increased from zero to 80% of the total available alkali, the obtained kappa values for the PSAQ procedure decreased from 50.4 to 26.1. Meanwhile the total yield at a kappa number normalized to 30 decreased from 48.5 to 47.7 as can be seen in Figure 2.13. Thus the yield benefit from PSAQ pulping at 40% sulfidity was more pronounced across the investigated range of initial alkali than that at 25% sulfidity. When comparing zero initial alkali PSAQ to the standard MCC reference using 65% of the available alkali in the first stage, the yield benefit is about 3%.

The 40% sulfidity PSAQ results show that compared to the 25% sulfidity MCC pulps, the greatest benefits with regard to both kappa and total pulp yield were obtained for the PSAQ pulps using 20 and 45% initial alkali. For these pulps the obtained kappa was similar to that of the MCC pulp while maintaining a yield benefit of about 1%. When comparing PSAQ pulping at 40% sulfidity to the MCC reference, a significant improvement in yield is possible while maintaining a similar delignification rate. The yield benefit from PSAQ pulping at 40% sulfidity using a PS charge of 3% on wood and a (45/31/24) alkali profile was 3-3.5%. These optimum conditions resulted in a relatively uniform alkali concentration throughout the three stages of PSAQ pulping.

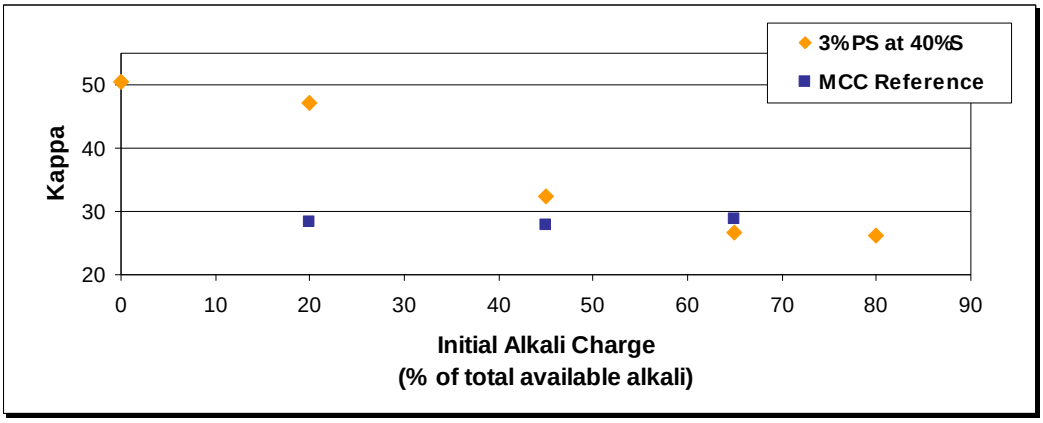

Figure 2.12 Kappa number versus initial alkali charge for 40% sulfidity pulps (PSAQ and MCC)

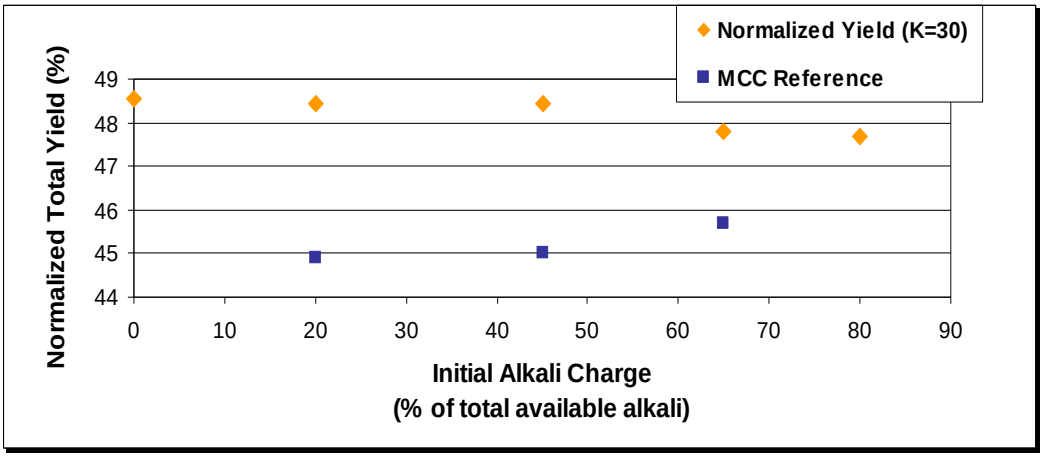

Figure 2.13 Normalized total yield versus initial alkali charge for 40% sulfidity pulps (PSAQ and MCC)

In conclusion, based on the pulping procedures used in this research, a greater benefit from PSAQ pulping can be realized at higher levels of sulfidity, where it is possible to charge a higher concentration of PS, and the effects of alkali profiling can be used to optimize both delignification rate and resulting pulp yield.

2.2.3. Pulp bleachability of PS and PSAQ relative to MCC pulps

The bleachability of the PS and MCC pulps were also determined. The change in pulp kappa and final obtained ISO brightness are shown in Table 2.7. The kappa reduction during the O-stage was about 40% for the PS pulps. These values are somewhat smaller than 50%, a value expected for typical kraft pulps. However, the corresponding kappa reduction for the MCC pulps was significantly greater, around 60 - 65%.

Table 2.7 Bleachability for MCC and PS pulps using ODEopD sequence

Pulp Sample	Initial Pulp	Kappa after O-	Final ISO Brightness
MCC (65/20/15) at 25%	29.3	11.0	86.02
PS (45/31/24) at 25% S	27.1	16.2	86.00
MCC (65/20/15) at 40%	28.8	11.8	86.58
PS (45/31/24) at 40% S	32.4	20.4	85.84

A series of PSAQ cooks was also performed with the aim of determining the bleachability of these pulps. Four MCC and PSAQ pulps were obtained at 20.5% AA charge and an h factor of 1800 hours. The pulping conditions and pulp properties before and after $OD_0(EoP)D_1$ bleaching are listed in Table 2.8. The bleaching conditions are given in Table 2.9. It should be noted that the PSAQ pulps are produced at zero alkali charge in the first stage rather than the optimum alkali profile (45/31/24) which was earlier shown to produce a similar kappa number as that obtained with the reference MCC procedure. No bleaching experiments were performed on the optimal PSAQ pulps due to time limitations.

Table 2.8 MCC and PSAQ pulping and unbleached and bleached pulp properties

Cook ID	Liquor TTA Profile	Kappa	Unbleached Pulp Viscosity (cP)	Pulp Yield (%)	Pulp Yield at ~30 Kappa (%)	Bleached Pulp Brightness (ISO)	Bleached Pulp Viscosity (cP)
BMCC-H1800-20.5%AA-25%S (45-31-24)	45-31-24	27.8	30.8	45	45.2	86.0	12.3
BMCC-H1800-20.5%AA-40%S (45-31-24)	45-31-24	27.7	22.1	44.9	45.3	86.6	16.7
PSAQ-H1800-20.5%AA-25%S-2%PS (0-65-35)	0-65-35	37.3	36.4	47	45.9	86.0	25.0
PSAQ-H1800-20.5%AA-40%S-3%PS (0-65-35)	0-65-35	42.3	52.7	51.5	49.7	85.8	30.8

Table 2.9 Bleaching conditions for the PSAQ and MCC pulps

Conditions	Oxygen stage (O)	Chlorine dioxide stage (D_0)	Extraction stage (EoP)	Chlorine dioxide stage (D_1)
Chemical charge	2.5% alkali			
Temperature (C)	100	70	70	70
Time (min)	60	60	60	180
Consistency (%)	10	10	10	10
Oxygen pressure (psig)	100			
$MgSO_4$ (%)	0.1			

The results in Table 2.8 show that the bleachability of the PSAQ pulps is the same as that of the control MCC pulps, but that the PSAQ pulps have a significant larger pulp viscosity. The present PSAQ procedure at 25%S and 2%PS produces a pulp with a 1 % yield benefit relative to the MCC reference, while a 4% yield benefit is obtained for PSAQ at 3% PS and 40%S.

2.2.4 Strength properties of PS and PSAQ relative to MCC pulps

The strength properties of fully bleached beaten PS and MCC pulps were determined. The four bleached pulps listed in Table 2.8 were refined in a PFI refiner. As expected the PSAQ pulps refined faster than the MCC pulps. Shown in Figure 2.14 is the apparent density of the handsheets versus the number of PFI revolutions. It can be observed that the apparent density for the PSAQ pulps is higher than that of the MCC pulps.

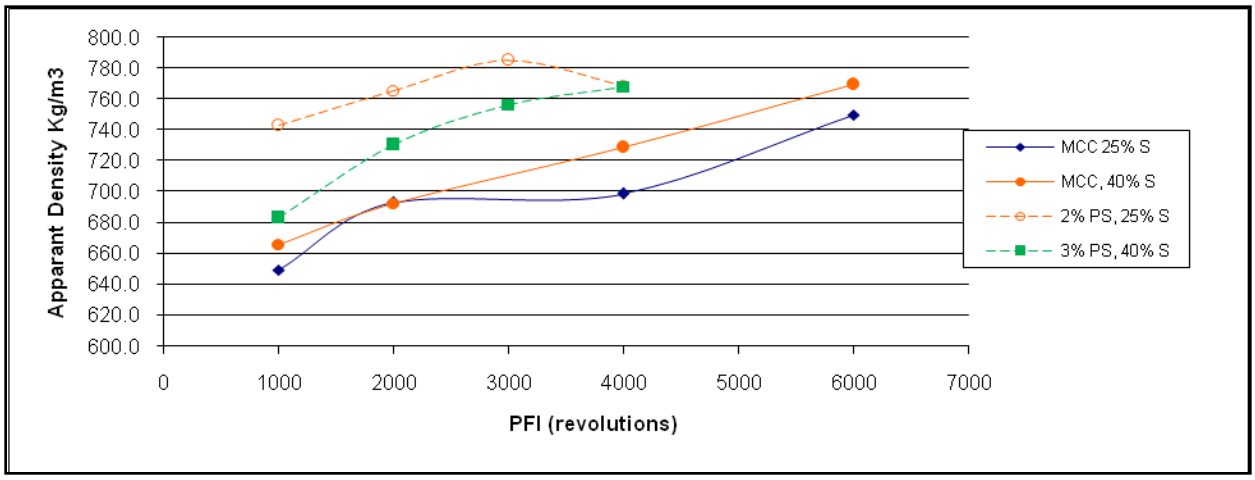

Figure 2.14 Variation of Apparent Density with PFI revolutions for the MCC and PSAQ pulps at 25%S and 40%S

The pulp strength comparisons are seen in Figures 2.15 and 2.16.

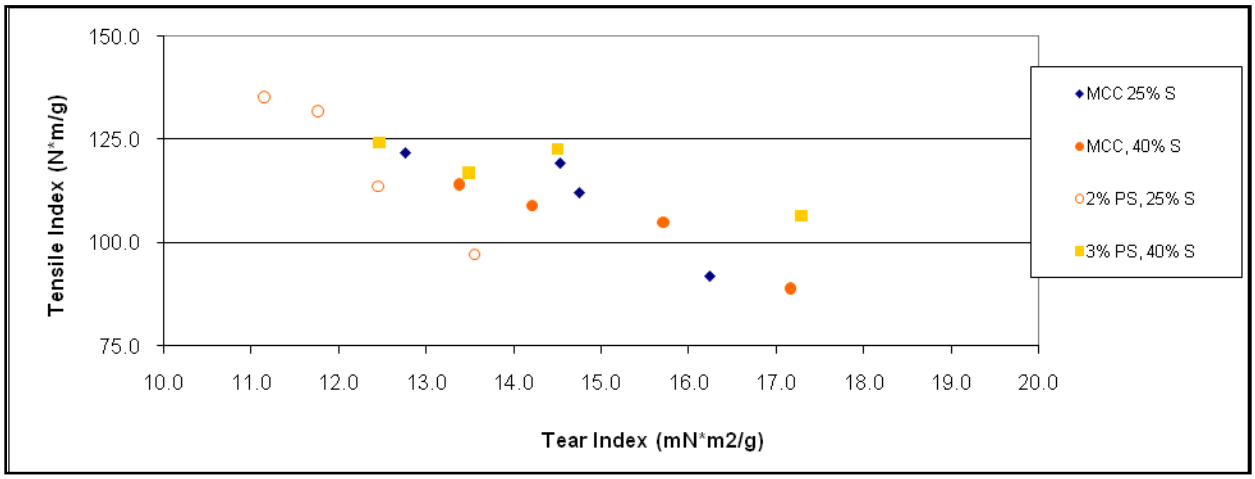

Figure 2.15 Variation of Tensile index with Tear index for the MCC and PSAQ pulps at 25%S and 40%S

Figure 2.15 shows that the Tear index for the 25% S and 2% PS PSAQ pulp is lower than the corresponding MCC pulp. However the PSAQ pulp at 40% S and 3% PS charge produced a slightly higher tear value at the same tensile as the 40% S MCC pulp. The same trends are seen for the burst index versus tear index in Figure 2.16.

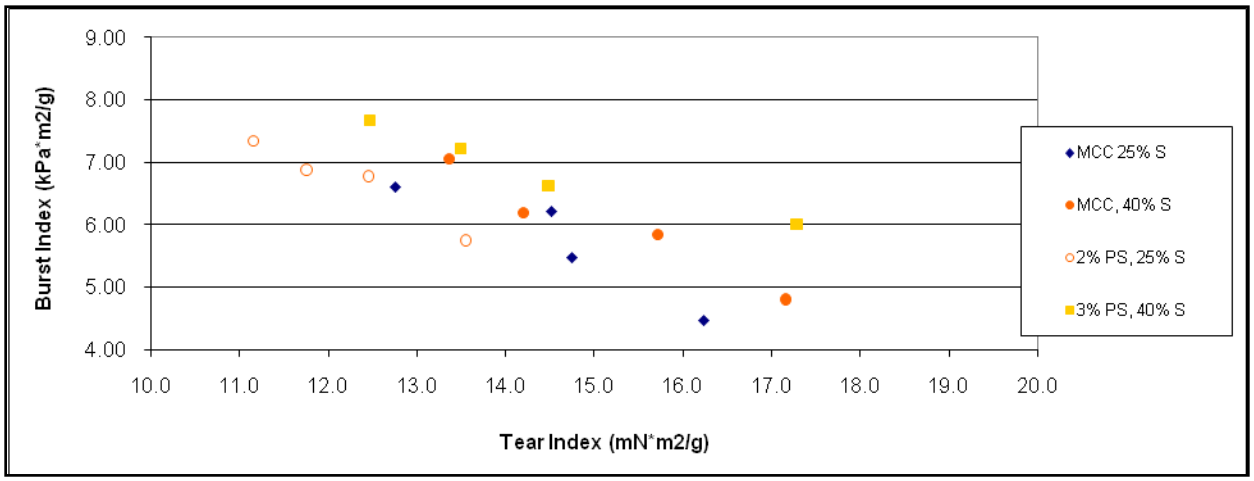

Figure 2.16 Variation of Burst Index with Tear index for the MCC and PSAQ pulps at 25%S and 40%S

2.2.5 Conclusions of laboratory pulping work

Black liquor gasification allows the use of different pulping technologies resulting from the separation of sodium and sulfur in the gasification process. Three different pulping technologies were investigated experimentally relative to conventional Modified Continuous Cooking (MCC); green liquor (GL) pretreatment, split sulfidity (SS) cooking and polysulfide pulping with or without anthraquinone (PS or PSAQ). Mixed southern softwood chips were used in all cases.

The GL pretreatment produced pulps of comparable yield and viscosity as that with the MCC procedure, while the pulp strength was slightly improved. However, the rate of delignification was lower than in the MCC reference procedure, and this could not be overcome by increasing the levels of charged Total Titratable Alkali (TTA). The greatest benefit of GL pretreatment would be a decrease in causticizing load, which decreases the lime kiln fuel demand.

SS pulp yields were 1-2% greater than corresponding MCC pulps at higher delignification rates. Initial high alkali SS cooks generated pulps of lower kappa number and higher yield compared to those of low initial alkali. The SS pulps also had 5 to 10 mPa.s higher viscosity and improved tensile and burst strength. SS pulps were slightly harder to refine relative to MCC pulps.

Compared to MCC cooking, PS pulping at 25% sulfidity and 1-2% sulfur charge produced pulps of 2% greater yield. PS pulping at 40% sulfidity and higher sulfur charge required more alkali charge to maintain the rate of delignification. Also the bleachability of the PS pulps was poorer than that of MCC pulps, with a degree of oxygen delignification of 40% for the PS pulps compared to 60% for MCC pulps.

PSAQ pulping with an optimized alkali distribution procedure resulted in similar rate of delignification compared to the MCC reference. Total pulp yield improvements of approximately 1% per 1% PS charged on OD wood were obtained, in agreement with literature data. PSAQ pulping at a high polysulfide charge of 3% (as PS) requires a high sulfidity (40%) white liquor for its generation. The bleachability of PSAQ pulps is similar to that of control MCC pulps, but the bleached PSAQ pulps have a significant higher pulp viscosity. The PSAQ pulps were easier to refine than corresponding MCC pulps. The tear and bursting strength of PSAQ pulps produced at 25% sulfidity and 2% PS charge is lower than those of 25% sulfidity MCC pulps, while 40% S and 3% PS PSAQ pulps gave slightly higher strength properties than 40% sulfidity MCC pulps.

2.3 Results and discussion of process simulation work

Computer process simulation is frequently utilized to evaluate the feasibility of new technologies or to determine operating parameters for process improvement and optimization. WinGEMS is a software simulation tool designed specifically for applications in the pulp and paper industry. The computer software is built on a modular design, where different unit operations specific to pulp and paper processes can be linked to represent process segments or whole plants. The overall model is then solved in a sequential order through multiple iterations until the specified convergence criteria are met. The software was originally developed at the University of Idaho in the early 1970's and is now marketed and supported by MetsoAutomation ([86],[87]).

Despite continuous evolution, WinGEMS does not have a block model for the BLG process. Initial simulation work around BLG integration into the kraft process was completed using preexisting WinGEMS blocks, achieving estimates of what effects could be expected in process variable operating costs. This work is described by Lindstrom et al. ([88]). In order to better simulate the integration of BLG and BLG enabled modified pulping technologies into kraft mills, it was necessary to develop such a BLG model.

2.3.1 Development of BLG model for WinGEMS

The model developed for this application bases the material and energy balances around the steam reformer on empirical relationships rather than first principles. This approach allows for the prediction of model output streams based on BL input stream and process parameters, as well as the back-calculation of the required amounts of bed fluidizing steam and energy supplied through the pulsed heaters to sustain the endothermic steam reforming reactions. An outline of the unit operation input and output streams are shown in Figure 2.17.

To simplify the BLG model and its control a number of parameters were identified and utilized for user input and reaction constraints internal to the model. These parameters were based on process data provided by MTCI. As a result, the range of operating conditions that can be used with the model in process simulations is limited by the original data. The development and validation of the WinGEMS BLG block model has been described in ([88]).

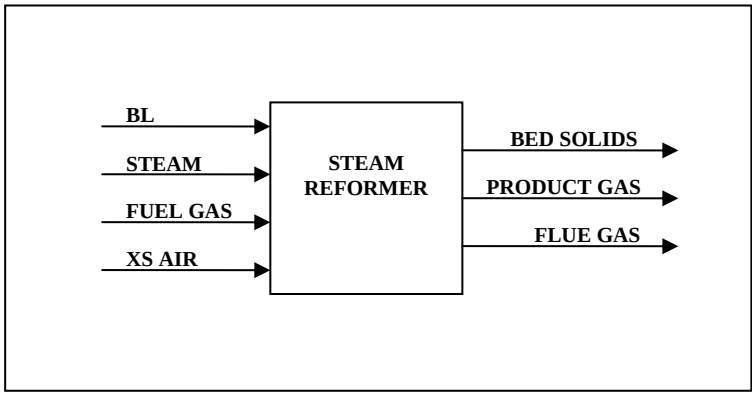

Figure 2.17 Input and output stream structure for BLG model

2.3.2 Simulation of effects of BLG integration on kraft mill operations

Case studies were performed in WinGEMS comparing full mill simulations of a kraft process using modified continuous cooking to BLG processes with split sulfidity and polysulfide-anthraquinone pulping. A detailed discussion of the findings has been described by Lindstrom et al. ([89]). Input assumptions for the different simulations were based on available literature, industry contacts and laboratory results generated by Lindstrom[90]. Process unit operations were comparatively analyzed among the different cases. Important consequences of the introduction of BLG is the increased load on the lime kiln cycle due largely to the much greater generation of carbonate salts in BLG as compared to conventional recovery boiler smelt production. Combined with this fact is the amount of carbonate created from carbon dioxide which is co-absorbed with H_2S during syngas scrubbing with amine systems and green liquor. In addition, the BLG cases also generated less steam from the processed black liquor than conventional recovery boiler operations. To make up the steam demand difference additional hog fuel was combusted in a power boiler, resulting in increased costs. The unit operation variables predicted through the simulation were used to calculate cost factors for variable process cost items. The net variable operating costs for each case were determined from these cost factors.

Initial simulation work around the integration of BLG into the kraft process combined with the modified pulping technologies showed that the net variable process operating cost would increase due to increased processing load of the lime kiln. This cost could be offset through implementation of modified pulping technologies that allowed for greater pulp yield and lower the overall process demand for wood, chemicals and fuel. The work also indicated the desirability of having a BLG WinGEMS module available for further simulation. Further simulation work has resulted in the generation of such a WinGEMS module for the MTCI low temperature steam reformer, or black liquor gasifier. The module has been utilized in simulation case studies exploring SS and PSAQ pulping using BLG as the central unit operation in chemical recovery. The obtained results indicated that the net process variable operating cost was driven by two major factors, lime kiln fuel and power sales price. Under the initial assumptions, where lime kiln fuel was set to $50/barrel and power sales price at $0.35/kWhr, the net variable operating costs for the BLG cases showed a cost increase of about 3% compared to the MCC reference case. The overall conclusion from this simulation case study is that BLG integration into the kraft process is highly dependent on the price of lime kiln fuel and the price and amount of power produced from BLGCC conversion of syngas. Under the initial assumptions made in

this case study, the significantly increased load on the lime kiln is not overcome by the benefits realized in pulping operations through the introduction of modified pulping technologies, nor by the additional revenue generated from the generation and sale of green power. However, if modifications could be made to the causticizing unit operations, such as high sulfidity green liquor pretreatment, offloading the slaker and resulting load on the lime cycle, this would change. Another such approach would be direct causticization of the black liquor stream which is investigated in the second part of this project.

The effect of variable lime kiln fuel (oil) price while keeping all other cost factors constant on the Net variable Operating cost per OD ton pulp produced is shown in Figure 2.18. As seen in the figure, the relative effect of increasing fuel price on the process net variable operating cost is greater in the BLG cases compared to the MCC reference. This is an expected outcome, as the BLG cases require a greater volume of kiln fuel. More importantly, the graph clearly shows that the net variable operating cost for the BLG processes are lower than that of the MCC at lower fuel costs. The break even points for the SS and PS2% processes compared to the MCC process is at a fuel price of about $47/barrel. The corresponding value for the PS3% process is about $38/barrel. These results suggest that the negative effects on variable operating costs for BLG processes, stemming from an increased lime kiln load, could be overcome if a less expensive fuel alternative was available.

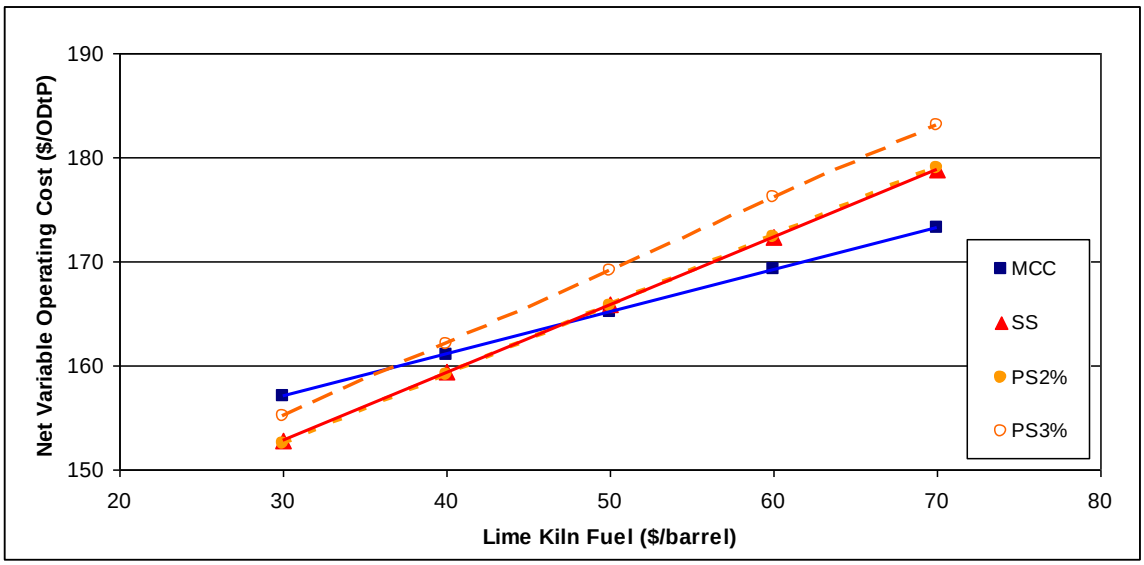

Figure 2.18 The effect of lime kiln fuel price on net variable operating cost, keeping all other cost factors constant (assuming green power sales price at ¢3.5/KWh)

A similar analysis was performed to explore the effect of sales price of power generated in combined cycle operations and sold to the grid. The net variable operating costs were calculated by varying the power sales price and keeping all other cost factors constant. The calculated values for each simulated case are shown in Figure 2.19. The basic assumption around power consumption/production for the kraft-MCC process was that the reference mill was a neutral

user/producer of power, and a change in power sales price would have no effect on the net variable operating cost for the MCC case. Thus, the blue line in the figure, representing the MCC case is flat over the explore range of power sales prices, whereas the calculated values for the BLG cases are highly sensitive to changes in the power sales price. The initial assumed price for power sold to the grid (¢3.5/KWh) was based on current market conditions, and at this level, the MCC process has a lower calculated net variable operating cost. However, as the sales price is increased the effect on the BLG cases net variable operating costs is dramatic and positive. In the current model, if the power sales price is increased from 3.5 to 6 ¢/KWh, the net variable operating costs would decrease by about $40/ODTP.

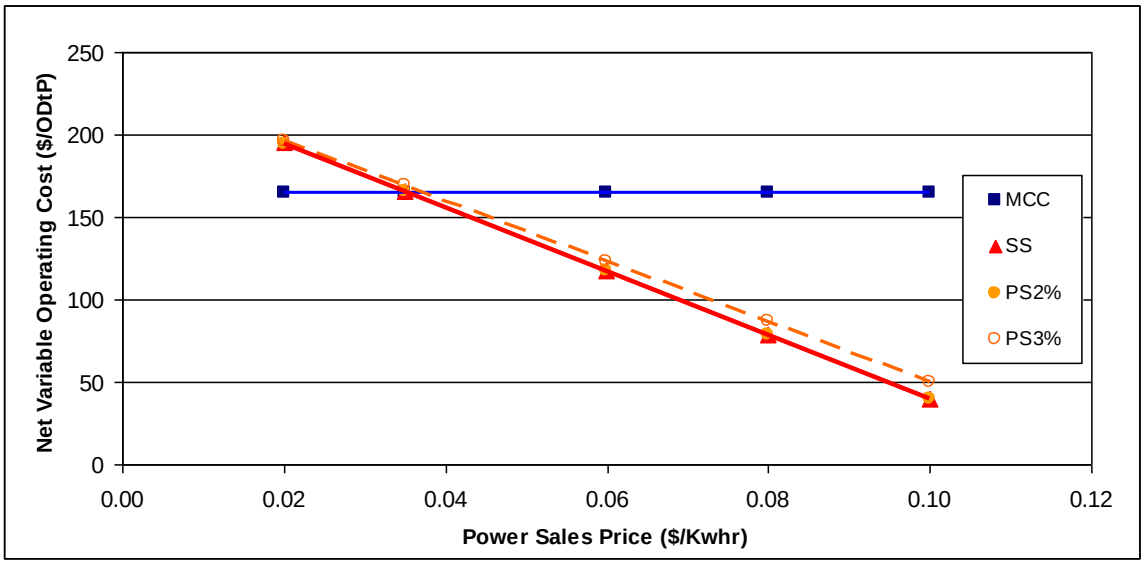

Figure 2.19 The effect of green power sales price on net variable operating cost, keeping all other cost factors constant (assuming lime kiln fuel price at $60/barrel)

2.3.3 Conclusions of simulation work

A WinGEMS module for the MTCI low temperature steam reformer or black liquor gasifier (BLG) was developed. The module has been utilized in simulation case studies exploring SS and PSAQ pulping using BLG for chemical recovery. The results show that the net process variable operating cost was driven by two major factors; lime kiln fuel and power sales price. At an assumed lime kiln fuel cost of $50/barrel and power sales price of $0.35/kWhr, the net variable operating costs for the simulated BLG cases showed a cost increase of about 3% compared to the MCC kraft pulping reference case. The pulp yield benefits of the studied modified pulping technologies plus the additional revenue generated from the generation and sale of green power were insufficient to compensate for this cost increase. However, if the lime kiln fuel cost is decreased or the power sale price increased, the BLGCC kraft process with split sulfidity or PSAQ pulping becomes a more economically favorable than the conventional MCC kraft process, based on variable operating costs. If the sales price for power to the grid is increased from 3.5 to 6 ¢/KWh cost savings of about $40/ODTP could be realized in all BLG processes. Another approach would be to modify the causticizing method such as using direct causticization as will be discussed in the second part of this study.

3. TASK 2 - DIRECT CAUSTICIZATION STUDIES

Gasification of kraft black liquor increases the amount of Na_2CO_3 which needs to be converted into NaOH in the lime cycle because one mole of Na_2CO_3 is created for each mole of gaseous sulfur produced during gasification, while the sulfur ends up as Na_2S in conventional recovery. This disadvantage can be eliminated when kraft black liquor is gasified in the presence of titanates, leading to direct causticization of Na_2CO_3 in the gasification reactor. Steam reforming of black liquor at about 600 °C in an indirectly heated fluidized bed is being developed by MTCI/StoneChem, a technology supported by the US DOE. The purpose of the present direct causticizing studies is to determine whether the sodium in black liquor reacts fast enough and at a sufficient yield with titanate compounds at relatively low temperatures (≤ 750°C) so that the causticizing penalty of kraft black liquor gasification may be eliminated.

3.1 Objectives

3.1.1 Objectives for direct causticization reaction kinetics

To determine the kinetics and mechanism of direct causticization of Na_2CO_3 by titanates at different temperatures over the range of 675 to 800 °C. Important variables to be studied are the effect of CO_2 pressure and the form of titanate supplied such as TiO_2, $Na_2O{\cdot}3TiO_2$ or recycled, hydrolyzed $4Na_2O{\cdot}5TiO_2$. The direct causticization reaction kinetics of mixtures of black liquor and TiO_2, $Na_2O{\cdot}3TiO_2$ or recycled, hydrolyzed $4Na_2O{\cdot}5TiO_2$ will also be determined. Overall and elemental mass balances will be made. Compared to earlier kinetic investigations, the present study uses larger samples so that the yield of sodium hydroxide can be determined by leaching the direct causticization product with water.

3.1.2 Objectives for study of agglomeration of solids during direct causticization of black liquor

During the black liquor gasification and direct causticization trials in the PDU of MTCI operational difficulties were encountered due to bed agglomeration. In order for the technology to be technically viable the bed agglomeration must be eliminated or controlled. To achieve this the mechanism of agglomeration must be understood.

3.2 Results and discussion for direct causticization reaction kinetics

3.2.1 Experimental apparatus and procedures

The kinetics are measured in a tube furnace setup using both on-line analysis of the product gas as well as continuous measurement of the weight loss of the reaction mixture. A schematic diagram of the experimental setup is shown in Figure 3.1.

The reaction mixture is put into trays stacked on top of each other and inserted in a quartz tube which is placed centrally in a vertically oriented tube furnace. High purity, pore-free Al_2O_3 (Aceram-A) trays made by Aceram Technologies (Kingston, ON) fit inside each other, and form a gas conduit through which the product gas is removed. The shape and arrangement of the trays (8mm height, 23 mm od), and their placement inside the tube furnace is shown in Figure 3.2. The assembly inside the tube furnace rests directly on a top weighing balance via three support rods. The bottom part of the outer quartz tube is held firmly in a straight upward position so that the

tube does not touch the inside surface and heating elements of the tube furnace. The sample temperature is recorded by a thermocouple. As shown in Figure 3.2, the design of the assembly allowed the thermocouple to pass through the top first tray and touch the sample bed in the second tray. This temperature is taken as the reaction temperature. Flexible Tygon 1.27 mm ID

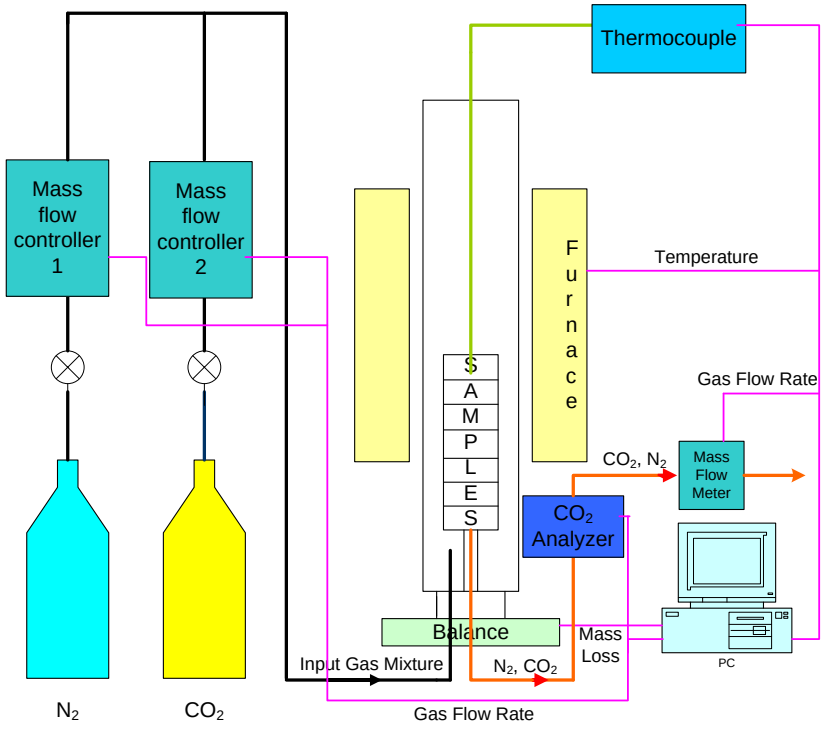

Figure 3.1. Schematic Diagram of the Experimental Setup for Measurement of Direct Causticization Kinetics

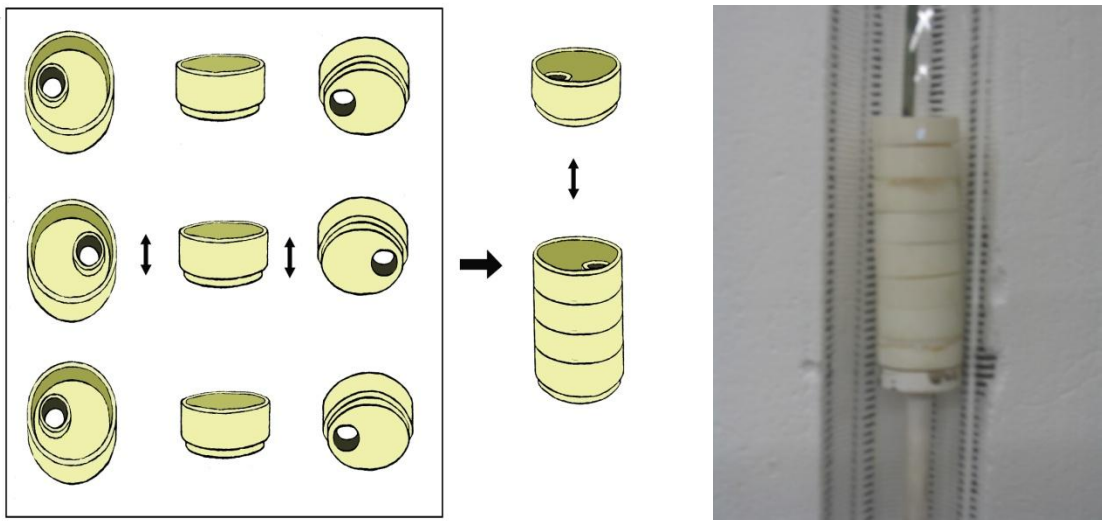

Figure 3.2. Reactor Assembly made from Trays of Aceram-A

tubing forming the gas inlet and outlet at the bottom of the outer quartz tube are attached to fixed points to minimize virtual weight changes due to vertical movement of the reactor resulting from weight change of the reaction mixture. The weight change, flow rates, temperature and exhaust gas composition are recorded by a computer. The reactor system is flushed at a known N_2 flow rate at 500℃ for one hour. Then the furnace temperature is raised in less than 5 minutes to the desired reaction temperature. The CO_2 liberation and weight loss are subsequently recorded. The sample size is varied from 5 grams to 8 grams in the 5 top trays. These top trays are located 15 to 20 cm from top of the furnace where the temperature was found to be uniform within ±3 °C.

3.2.2 Model compound studies

Model mixtures prepared from aqueous solutions of Na_2CO_3 mixed with TiO_2, $Na_2O{\cdot}3TiO_2$ or hydrolyzed $4Na_2O{\cdot}5TiO_2$ were studied.

3.2.2.1 Sample preparation and product analysis

Sodium Carbonate and Sodium Trititanate Mixture

Based on the stoichiometry of the direct causticizing reaction:

$$5\ (Na_2O{\cdot}3TiO_2) + 7Na_2CO_3 \rightarrow 3(4Na_2O{\cdot}5TiO_2) + 7\ CO_2 \qquad (3.1)$$

16.5 g Na_2CO_3 was dissolved in 200 mL deionized water, and then mixed with 33.5 g sodium trititanate in a Teflon beaker. The beaker was heated in a constant temperature bath of 90 °C while mixing its content until all water was evaporated. Then all solids were removed from the bottom and wall of the beaker and put overnight in a muffle furnace at 525 °C to remove all crystal water. The dried sample was then ground and screened to a sieve fraction of 53~125 μm. Finally the sample was stored in a desiccator.

Sodium Carbonate and Titanium Dioxide Mixture

The same procedure as above for sodium trititanate was used except that the mixture ratio was changed according to the stoichiometry of reaction:

$$5\ TiO_2 + 4\ Na_2CO_3 \rightarrow 4Na_2O{\cdot}5TiO_2 + 4\ CO_2 \qquad (3.2)$$

Thus 31.8 g of Na_2CO_3 and 30.0 g of TiO_2 were used for this mixture.

Product Analysis

About 1~2 grams of reacted sample were added to 200 mL deionized water. The suspension was heated to 90 °C and kept at this temperature for 10 minutes while stirring. Then the cooled suspension was filtered using 12μm pore size nylon filter paper. The filtered solution was titrated using two different procedures. (i) To determine the number of moles of NaOH produced, 10 wt% of $BaCl_2$ was added to the solution in order to remove CO_3^{2-} as insoluble $BaCO_3$. The mixture was then filtered and titrated with a 0.1M HCl solution to an end point of pH 7 to determine the number of moles of NaOH. (ii) The number of moles of unreacted Na_2CO_3 was determined by titration directly to pH 4 without the addition of $BaCl_2$ and subtracting the amount of NaOH calculated by procedure (i).

3.2.2.2. Validation of measurement system and techniques

Figure 3.3-a shows the sample temperature and CO_2 concentration in the product gas in a typical kinetic experiment (TiO_2 reaction, N_2 flow rate 100 standard cm^3/minute (sccm), temperature 700 °C, 5 loaded trays). The dynamic weight loss recorded for the same experiment is shown in Figure 3.3-b. The reaction time was extended to 50 hours because this is the approximate solids residence time in the MTCI/StoneChem reactor for black liquor gasification.

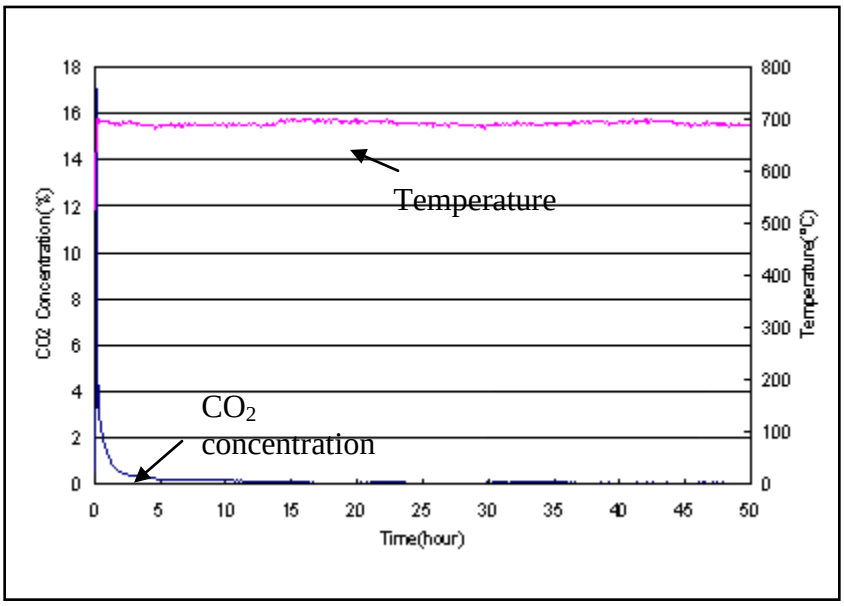

Figure 3.3-a. Typical Raw Data for a Kinetic Experiment

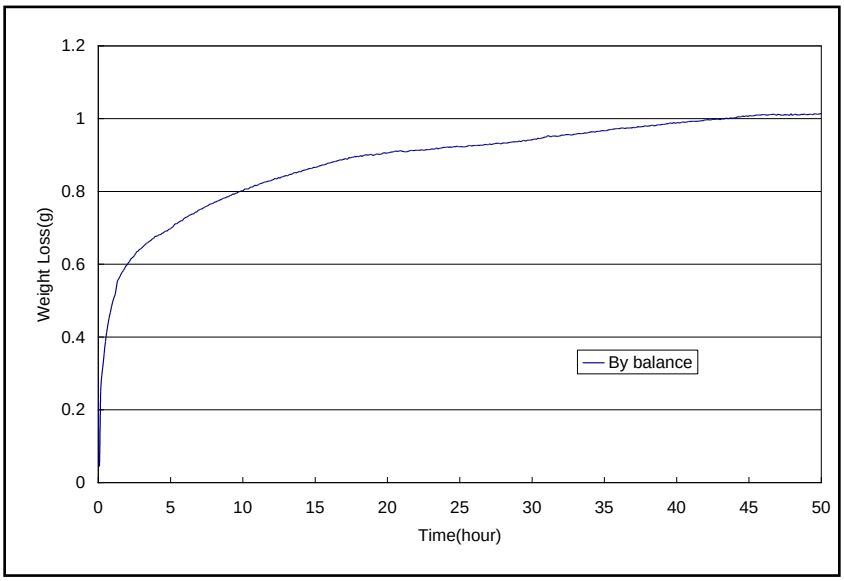

Figure 3.3-b. Typical Raw data for a Kinetic Experiment (Weight Loss Recorded by Balance)

The conversion of Na_2CO_3, *X*, can be calculated either from the concentration of CO_2 released or from the recorded weight loss. The conversion is calculated from the CO_2 release as:

$$X(t) = \frac{\int_0^t \frac{QM}{RT}[Pco_2(t) - Pco_2(o)]dt}{[Wco_2]_i} \qquad (3.3)$$

where Q is the flow rate; M the molecular weight of CO_2; $Pco_2(t)$ the CO_2 partial pressure at time t; $Pco_2(0)$ is the CO_2 partial before reaction and $[Wco_2]_i$ is the theoretical weight of CO_2 which can be released from the initial sample upon complete decomposition of Na_2CO_3.

The conversion of Na_2CO_3 calculated from the weight loss is obtained by the equation below:

$$X(t) = \frac{[W(0) - W(t) - W(Buoyancy)]}{[Wco_2]_i} \qquad (3.4)$$

where W(0) is the original sample weight; W(t) the weight at time t; W(Buoyancy) the weight gain due to buoyancy caused by the high temperature gas in the reactor tube. The W(Buoyancy) data are obtained by another experiment without sample at the same conditions.

Very good agreement between the conversions in figures 3.3a and 3.3b calculated from Equations (3.3) and (3.4) was obtained in Fig. 3.3-c. The slow wavy character of the conversion calculated from the weight loss is due to small and slow temperature changes in the reactor leading to small buoyancy changes which are not fully accounted for. The weight loss of each tray was also measured after the experiment. The weight loss and conversion of each tray are shown in Table 3.1. The total conversion is very close to the final conversion in Figure 3.3-c.

Based on the hydrolysis reaction of $4Na_2O{\cdot}5TiO_2$ as:

$$3(4Na_2O{\bullet}5TiO_2) + 7H_2O \rightarrow 5(Na_2O{\bullet}3TiO_2) + 14NaOH \qquad (3.5)$$

the number of moles of NaOH formed during leaching should be 14/12 times the number of moles of CO_2 released by reaction (3.2). This is more clearly seen in the overall reaction (3.6):

$$15\ TiO_2 + 12\ Na_2CO_3 + 7\ H_2O \rightarrow 5(Na_2O{\bullet}3TiO_2) + 14NaOH + 7\ CO_2 \qquad (3.6)$$

Further validation of the experimental method was obtained by titration of the leachate. The leachate titration results in Table 3.2 show that the amount of Na_2CO_3 reacted (column **(5)**) as determined by gravimetry agrees very well with the titration results for this experiment (column **(3)**). The maximum amount of NaOH formed based on equation (3.6) is shown in column **(6)**, i.e. 23.3 x 14/12 =27.2 mmol. Column **(7)** shows that significantly more NaOH is detected by titration (47 mmol). The explanation for the discrepancy may be that additional NaOH is formed from $Na_2O.3TiO_2$. The data in Table 3.2 suggests that all $Na_2O.3TiO_2$ is also fully hydrolyzed to NaOH and TiO_2, i.e. 2 moles of NaOH are formed per mol of CO_2 released (23.3 x 2 = 46.6 which is close to 47 found experimentally). This is contrary to data reported in literature ([91])

which suggests that the maximum hydrolysis of $Na_2O.3TiO_2$ is 50% to produce $Na_2O.6TiO_2$. Perhaps the absence of CO_2 and very long reaction time (50 hours) leads to sodium being more accessible during product hydrolysis.

Table 3.1. Weight Loss and Conversion for each Tray

Top to Bottom	Weight Before Reaction (g)	Weight After Reaction (g)	Weight Loss (g)	Conversions (%)
Tray 1	1.062	0.881	0.181	79.794
Tray 2	1.351	1.122	0.229	79.359
Tray 3	1.309	1.091	0.218	77.971
Tray 4	1.229	1.021	0.208	79.237
Tray 5	1.154	0.961	0.193	78.301
Total	6.105	5.076	1.029	78.913

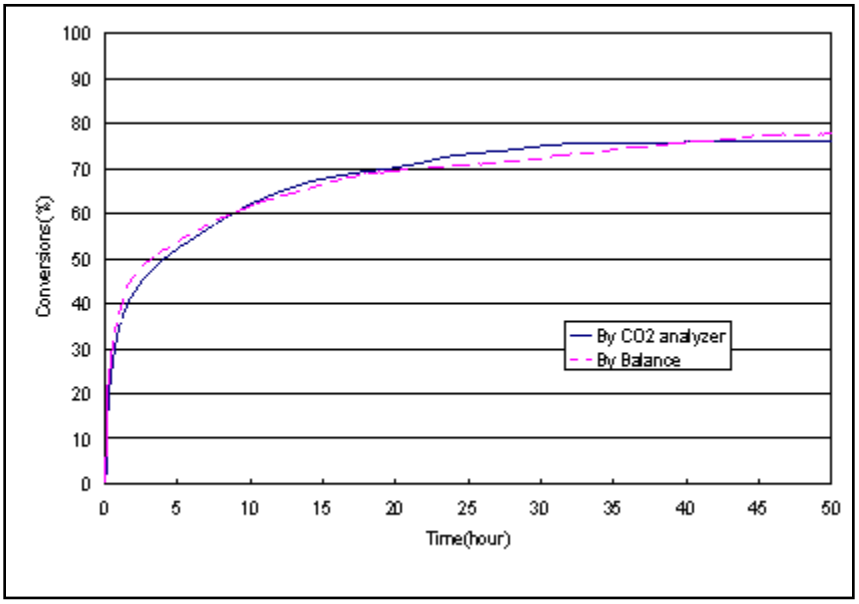

Figure 3.3-c. Comparison of Conversion Data obtained from Eq-3.2 and Eq-3.3

Table 3.2. Na_2CO_3 Reacted and NaOH Formed. Comparison of Titration and Gravimetric Results for Sodium Carbonate and Titanium Dioxide Mixture.

Temperature (°C)	Na_2CO_3 content original sample (mmol) **(1)**	Na_2CO_3 remaining in sample by titration (mmol) **(2)**	Na_2CO_3 reacted (mmol) **(1) - (2) (3)**	Weight loss measured (grams) **(4)**	Weight loss assumed as CO_2 (mmol) **(4)/.044 (5)**	NaOH calculated from weight loss (mmol) **14/12 x(5) (6)**	NaOH by titration (mmol) **(7)**
700	29.6	6.2	23.4	1.029	23.3	27.2	47

Effect of Carrier Gas and Bed Height

Chemical kinetics should not be affected by the type of carrier gas or sample bed height. Experiments at 700 °C were performed with nitrogen or helium as carrier gas at 100 sccm respectively. The development of the conversion calculated from the weight loss for the two experiments (TiO_2 and Na_2CO_3 reaction) in Figure 3.4-a shows excellent agreement. The effect of bed height in the trays is shown in Fig.3.4-b. It shows one experiment with five fully loaded trays and another with half the weight in each of the five trays. Both experiments use pure nitrogen at 100 sccm at 700 °C. The good agreement confirms that the kinetic results are not affected by external or internal mass transfer limitations. The small undulations in the conversion trace are caused by changes in the buoyancy caused by slow temperature variations in the ambient air surrounding the thermo balance set-up.

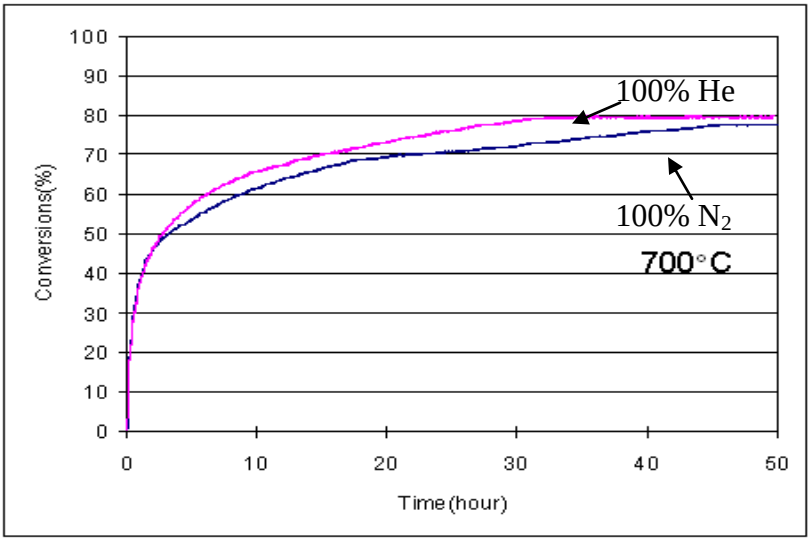

Figure 3.4-a. Effect of Type of Carrier Gas on the Direct Causticization Kinetics

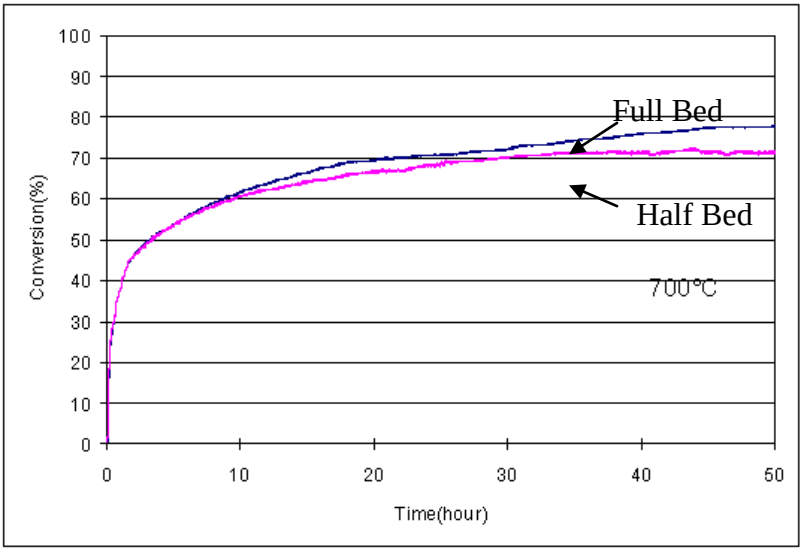

Figure 3.4-b. Effect of Bed Height in the Trays on the Direct Causticization Kinetics

3.2.2.3 Influence of temperature and CO_2 partial pressure on reaction with TiO_2

Figure 3.5 shows the effect of temperature in TiO_2 reactions from 630 to 730 °C in a 100mL/min flow of 100% N_2. It can be seen that the conversion increases from about 60 % after 50 hours at 630 °C to about 90 % after 50 hours at 730 °C. The initial increase to about 20 % is very rapid, followed by a decreasing rate of conversion during the next 10 hours and finally a very slow almost constant rate during the last 40 hours.

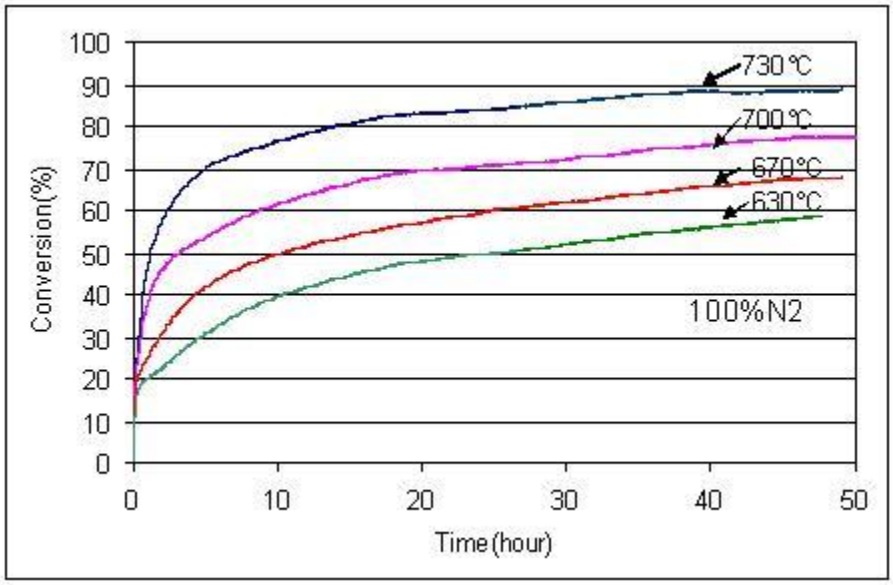

Figure 3.5. Effect of Temperature on the Reaction between Na_2CO_3 and TiO_2 in 100% N_2

The effect of [CO_2] on the conversion of Na_2CO_3 by TiO_2 from 630 to 730 °C can be seen by comparison of Figures 3.5 and 3.6. It can be seen that 10% CO_2 in N_2 suppresses the conversion at all temperatures except at 730 °C. The conversion reaches a plateau at about 40% at 700 °C or lower because the conversion of sodium trititanate, $Na_2O{\cdot}3TiO_2$, to sodium pentatitanate, $4Na_2O{\cdot}5TiO_2$, does not occur at these temperatures in the presence of CO_2 as will be shown below based on the XRD analysis of the final products. Complete conversion of Na_2CO_3 to $Na_2O{\cdot}3TiO_2$ would occur at 41.7% while 100% conversion is defined as a pure $4Na_2O{\cdot}5TiO_2$.

The X-Ray diffraction results of the final sample after reaction of Na_2CO_3 and TiO_2 at 700 °C in 100% N_2 is shown in Figure 3.7. It shows that the sample is mostly sodium penta-titanate and sodium trititanate with a trace amount of sodium hexatitanate, $Na_2O{\cdot}6TiO_2$. The latter is the first product formed when Na_2CO_3 reacts with TiO_2.

The XRD results of the final sample obtained at 700 °C in 10% CO_2 is also shown in Figure 3.7. Here it is clear that sodium pentatitanate is not formed, and that the dominant products are sodium trititanate and some sodium hexatitanate. Since the amount of alkali generated from crystalline sodium trititanate in a single leaching stage is limited to about 50% ([92]), it is clear that the temperature in an industrial gasifier should be raised above 700 °C to obtain sodium pentatitanate which will create NaOH when contacted with water.

The XRD results of the products produced at different conditions are summarized in Table 3.3 Apparently when the temperature is 700 ºC or lower, the presence of 10 % CO_2 prevents the formation of sodium penta-titanate. However above 730 ºC, the products are mostly sodium pentatitanate and sodium trititanate in either pure N_2 or 10% CO_2 in N_2.

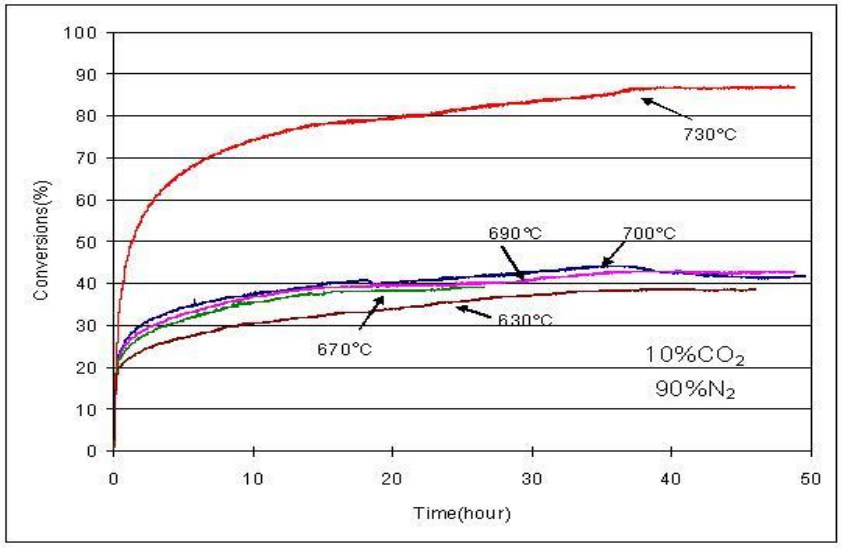

Figure 3.6. Effect of Temperature on the Reaction between Na_2CO_3 and TiO_2 in 10% CO2 and 90% N_2

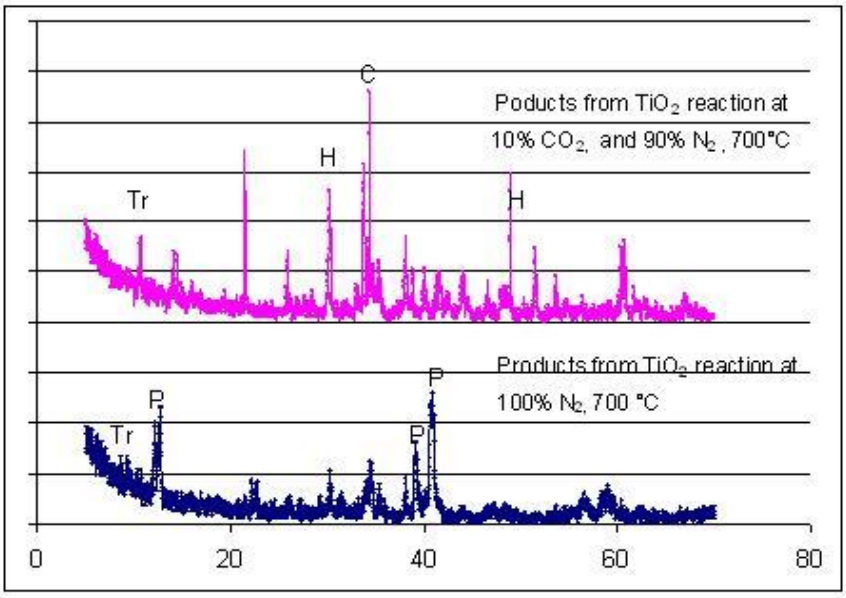

P=Sodium Pentatitanate; Tr= Sodium Trititanate; H= Sodium Hexatitanate; C= Sodium Carbonate

Figure 3.7. Comparison of XRD Results after Reaction of Na_2CO_3 and TiO_2 at 700 °C

Table 3.3 Summary of XRD Results

TiO_2 Reaction Conditions	Sodium Penta-Titanate ($4Na_2O{\cdot}5TiO_2$)	Sodium Tri-Titanate ($Na_2O{\cdot}3TiO_2$)	Sodium Hexa-Titanate ($Na_2O{\cdot}6TiO_2$)
630 C N_2	√	√	√
630 C 10% CO_2	–	–	√
670 C N_2	√	√	√
670 C 10% CO_2	–	–	√
700 C N_2	√	√	–
700 C 10% CO_2	–	√	√
730 C N_2	√	√	–
730 C 10% CO_2	√	√	–

Shown in Table 3.4 are the molar amounts of Na_2CO_3 and NaOH measured by titration. It can be seen that the amount of Na_2CO_3 reacted (fifth column; identified as **(3)**) agrees very well with the weight loss as CO_2 (seventh column; identified as **(5)**).

Based on the overall reaction (3.6), the number of moles of NaOH formed during leaching should be 14/12 times the number of moles of CO_2 released by reaction (3.2). It can be seen in Table 3.4 that the amount of NaOH determined by titration (column (7)) is significantly larger than the calculated amount (column (6)) when pure nitrogen is used as the carrier gas. Again this may be due to sodium being more accessible due to the absence of CO_2 and very long reaction time (50 hours). However, only very small amounts of NaOH are formed from the final samples obtained in 10% CO_2 at 700 and 670 °C. This confirms that the formation of sodium pentatitanate is strongly inhibited by the presence of 10% CO_2 at 700 °C or lower, while at 730 °C the presence of 10% CO_2 has only a minor inhibiting effect.

Table 3.4. Summary of Titration results of the Reaction between Na_2CO_3 and TiO_2

Temp. (°C)	Type of Carrier gas	Na_2CO_3 content original sample (mmol) **(1)**	Na_2CO_3 remaining in sample by titration (mmol) **(2)**	Na_2CO_3 reacted (mmol) **(1) - (2) (3)**	Weight loss measured (grams) **(4)**	Weight loss assumed as CO_2 (mmol) **(4)/.044 (5)**	NaOH calculated from weightloss (mmol) **(14/12)x(5) (6)**	NaOH by titration (mmol) **(7)**
670ºC	Pure N_2	30.7	16.2	14.5	0.648	14.7	17.2	28.7
	10% CO_2	33.0	20.5	12.5	0.574	13.0	15.2	2.1
700ºC	Pure N_2	29.6	6.2	23.4	1.029	23.3	27.2	47
	10% CO_2	29.2	17.0	12.2	0.544	12.4	14.5	1.9
730ºC	Pure N_2	32.2	3.6	28.6	1.271	28.8	33.6	57.3
	10% CO_2	30.4	4.1	26.3	1.162	26.4	30.8	52.3

3.2.2.4 Influence of temperature and CO_2 partial pressure on reaction with $Na_2O{\cdot}3TiO_2$

The effect of temperature on the direct causticization reaction of Na_2CO_3 by $Na_2O{\cdot}3TiO_2$ in 100 mL/min of pure N_2 is shown in Figure 3.8. It shows that the reaction of Na_2CO_3 with $Na_2O{\cdot}3TiO_2$ is somewhat faster than with TiO_2 (Figure 3.5). Complete conversion to sodium pentatitanate is also obtained at 740 °C after 30 hours. As with TiO_2 the initial rate of reaction is fast, although now there is a clear effect of temperature on the initial rate. When 10% CO_2 is introduced in the carrier gas the retarding effect of CO_2 is even more severe than obtained with TiO_2. It can be seen in Figure 3.9 that full conversion is still approached at 740 °C, but that the conversion is limited to about 60 % at 700 °C, while there is essentially no reaction at 670 °C. The latter is expected based on the earlier results obtained with TiO_2 in the presence with 10% CO_2. The XRD result of the product formed at 700 °C is shown in Figure 3.10. Weak peaks around 40 degree shows that penta-titanate is formed in the presence of CO_2. Figure.3.11 shows almost complete conversion of $Na_2O{\cdot}3TiO_2$ and Na_2CO_3 to $4Na_2O{\cdot}5TiO_2$ when the reaction is performed in 10%CO_2 at 740°C. The amount of NaOH generated when leaching the final samples is listed in Table 3.5. The theoretical maximum amount of NaOH which may be obtained from Na2CO3 is given by the overall reaction (3.7) which is the sum of reactions (3.1) and (3.5):

$$Na_2CO_3 + H_2O \rightarrow 2\ NaOH + CO_2 \qquad (3.7)$$

It can be seen in Table 3.5 that the amount of NaOH measured by titration (column 7) is slightly smaller than that calculated using equation (3.7) from the measured weight loss (column 6). The data in the table also shows that at 730 °C the presence of 10% CO_2 has no significant inhibiting effect on the ultimate generation of NaOH.

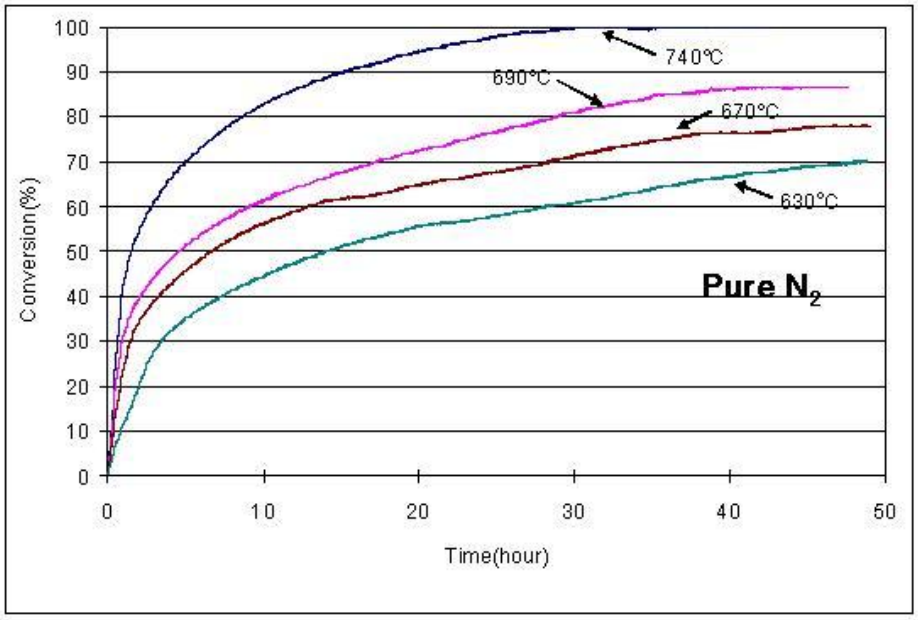

Figure 3.8. Effect of Temperature on Reaction between Na_2CO_3 and $Na_2O{\cdot}3TiO_2$ in 100% N_2

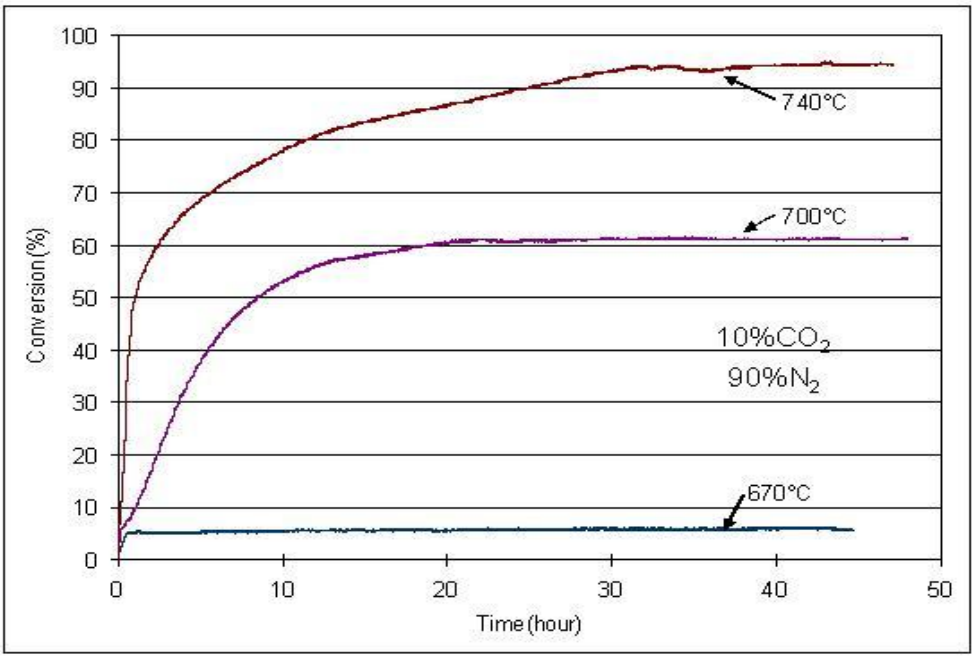

Figure 3.9. Effect of Temperature on Reaction between Na_2CO_3 and $Na_2O{\cdot}3TiO_2$ in 10 % CO_2 and 90% N_2

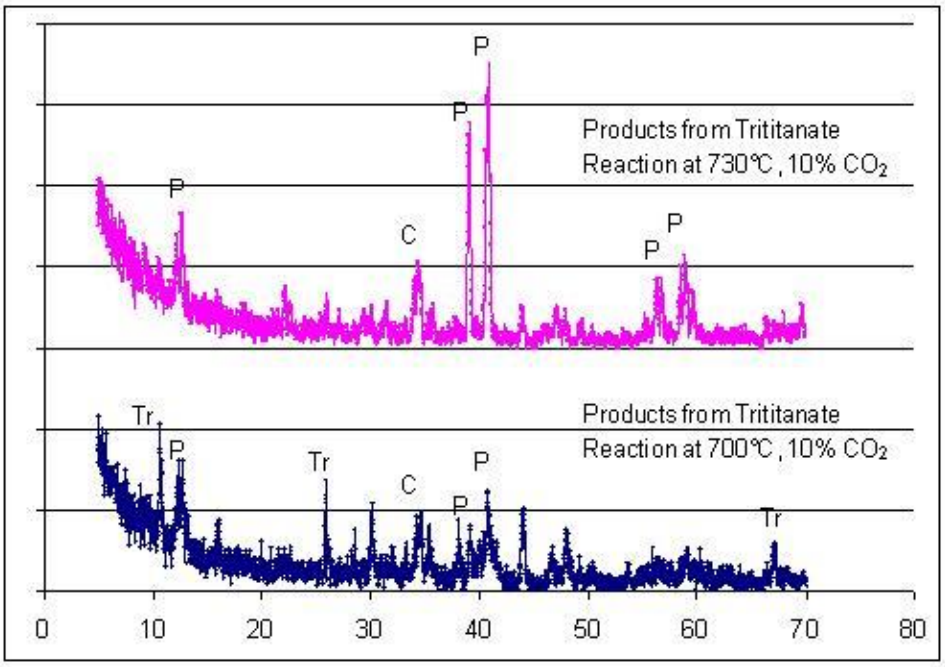

P=Sodium Pentatitanate; Tr= Sodium Trititanate; H= Sodium Hexatitanate; C= Sodium Carbonate

Figure 3.10. Comparison of XRD Results after Reaction of Na_2CO_3 and $Na_2O{\cdot}3TiO_2$ in 10 % CO_2 and 90% N_2

Table 3.5. Summary of Titration results

Temp. (°C)	Type of Carrier gas	Na_2CO_3 content original sample (mmol) **(1)**	Na_2CO_3 remaining in sample by titration (mmol) **(2)**	Na_2CO_3 reacted (mmol) **(1) - (2) (3)**	Weight loss measured (grams) **(4)**	Weight loss assumed as CO_2 (mmol) **(4)/.044 (5)**	NaOH calculated from weight loss (mmol) **2x(5) (6)**	NaOH by titration (mmol) **(7)**
670 ºC	100% N_2	24.1	8.5	15.6	0.878	19.9	39.8	33.4
	10% CO_2	23.0	21.4	1.6	0.077	1.7	3.5	3.2
700 ºC	10% CO_2	23.6	9.8	13.8	0.642	14.2	28.4	24.1
730 ºC	100% N_2	22.8	3.75	19.05	0.994	22.6	45.2	38.4
	10% CO_2	23.2	2.4	20.8	0.941	21.4	42.8	41.5

3.2.3 Soda black liquor and sodium trititanate mixture

Soda black liquor (58.4% dry solids) was obtained from Georgia Pacific, Big Island, VA. The composition in terms of the relevant species and components is given in Table 3.6. Soda rather than kraft black liquor was used to avoid problems with the present measurement technique when the sulfur in kraft black liquor is released as H_2S during direct causticization (see 3.2.3.2).

Table 3.6. Black Liquor Solids Composition (% on dry solids)

Sodium	Potassium	Carbonate, CO_3^{2-}	Org. Carbon	Chloride
21.61	1.59	30.0	18.5	0.0038

3.2.3.1 Sample preparation

100 gram of thick black liquor was mixed with 76.62 gram of $Na_2O.3TiO_2$ and 400 ml distilled water. Then most of the water was removed at 90 °C in the same manner as was done for the model mixture. The sample was dried overnight at 110°C. The final weight is 133.81 gram, close to the expected value based on the black liquor dry solids content of 58.4%. With an effective total sodium content (each mole of potassium is counted as a mole of sodium) of the black liquor solids of 23.2 %, the charge of $Na_2O.3TiO_2$ is 1.2 times the stoichiometric amount needed for complete causticization of all effective sodium according to reaction (3.1).

3.2.3.2 Validation of measurement techniques for black liquor

Similar to the model compound studies, validation experiments were performed for the present black liquor direct causticization (D.C.) experiments. The present system is more complex because organic carbon in black liquor is also consumed by CO_2, the product of D.C., by following reaction:

$$C + CO_2 \rightarrow CO \qquad (3.8)$$

Therefore the weight loss during D.C. will come from two different sources, CO released from reaction (3.8) and CO_2 released by direct causticization of Na_2CO_3. In order to measure the D.C.

kinetics separately, the following pretreatment and calculation method was adopted as described below for a typical experiment:

7.399 gram sample of the black liquor-trititanate mixture was distributed over 5 trays and then combusted in the thermo balance setup at 500°C in a gas mixture of 7.5% oxygen in nitrogen for 5 hours. No direct causticization takes place at this low temperature, but most of the black liquor is combusted and only a small amount of organic carbon is left in the mixture. This procedure led to the release of 0.394 grams of carbon as CO_2. Then the gas was changed to pure nitrogen at a flow rate of 200 scc/min, and the temperature increased to 680 °C. The CO_2 released was measured both by an Agilent microGC and by an online IR detector. CO was also detected by the microGC. The results are shown in Figure 3.11.

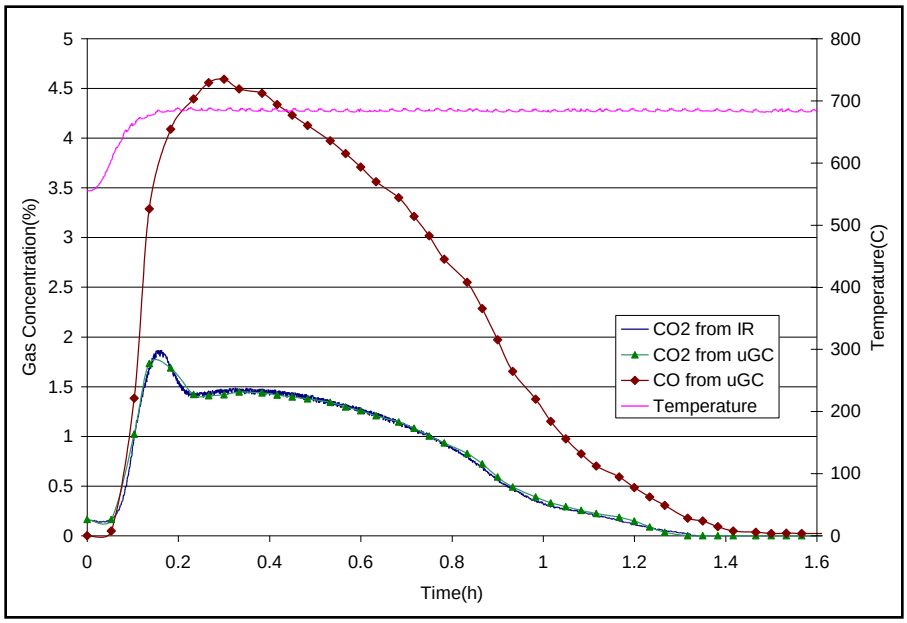

Figure 3.11 [CO], [CO_2] and Temperature versus Time during D.C. of Black Liquor Char by $Na_2O.3TiO_2$

The results in Figure 3.11 show good agreement between the two methods of CO_2 analysis. The CO in the off-gas is due to gasification of the residual amount of organic carbon in the combusted sample by CO_2 generated by the direct causticization reaction. The amount of carbon gasified by CO_2 is calculated as 0.11 gram based on the total amount of CO released of 0.51 gram. Thus the total amount of organic carbon lost by the original mixture is 0.394 + 0.11 = 0.504 gram. The total amount of CO_2 released is 0.28gram. Thus, the weight loss due to CO_2 release is 0.28 + 0.51 – 0.11 = 0.68 gram. This weight loss compares well with the weight loss of the final samples of 1.189 gram minus the carbon weight loss of 0.504 gram or of 0.685 gram.

The weight loss due to the release of CO_2 and CO is compared with the on-line weight loss measurement in Figure 3.12. It shows excellent agreement between the two independent measurement methods. A weight loss of 0.68 gram due to release of CO_2 is equivalent to causticization of 0.01545 moles Na_2CO_3. This means that the conversion of reaction (3.1) is

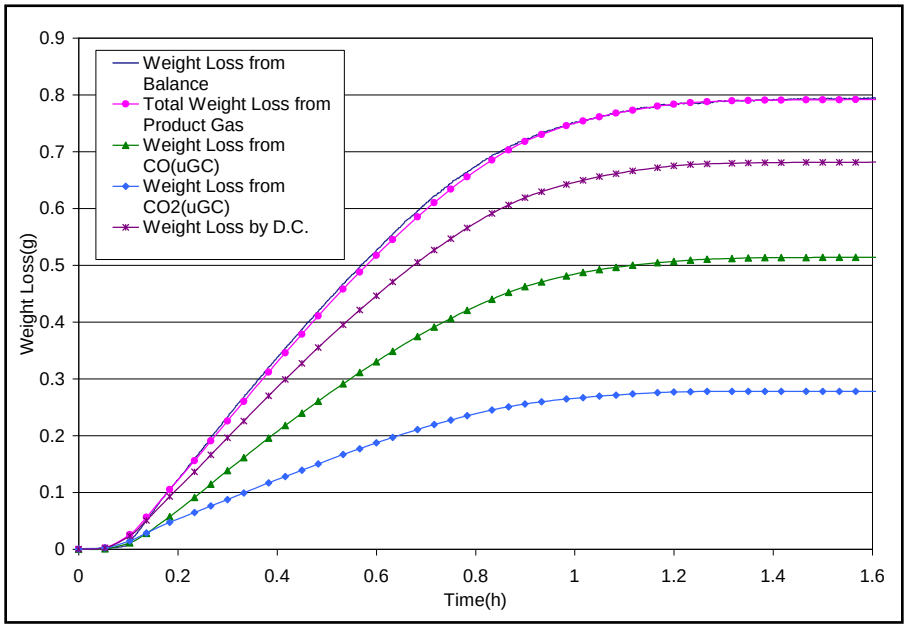

Figure 3.12. Weight Loss during Direct Causticization of Black Liquor with $Na_2O.3TiO_2$

81.9% based on Na_2CO_3. Titration of the final direct causticization product shown in Table 3.7 gives values of 0.027 moles NaOH (or 0.0135 moles Na_2CO_3 converted) and 0.0022 moles unconverted Na_2CO_3 produced from the original 7.399 grams of black liquor/$Na_2O.3TiO_2$ sample. This represents a conversion of Na_2CO_3 to penta titanate of 86%, in good agreement with the conversion based on the final weight loss due to CO_2.

Table 3.7. Na_2CO_3 Reacted and NaOH Formed. Comparison of Titration and Gravimetric Results

Temp. (°C)	Na_2CO_3 content in original sample (mmol)	Na_2CO_3 remaining in sample by titration (mmol)	Na_2CO_3 reacted (mmol)	Weight loss due to release of CO_2 in D.C. reaction (gram)	Weight loss assumed as CO_2 (mmol)	NaOH calculated from weight loss (mmol)	NaOH by titration (mmol)
680	18.9	2.2	16.7	0.68	15.5	31	27

3.2.3.3 Kinetic behavior of D.C. reactions between $Na_2O•3TiO_2$ and black liquor solids

The effect of temperature on the direct causticization of black liquor in a feed stream of pure nitrogen is shown in Figure 3.13. It can be seen that the conversion of Na_2CO_3 reaches high conversions at all temperatures ranging from 630 to 730 °C. The striking difference with the kinetic results reported earlier for the model mixture of Na_2CO_3 and sodium trititanate is that the rate between $Na_2O•3TiO_2$ and black liquor solids is at least an order of magnitude faster at all temperatures studied.

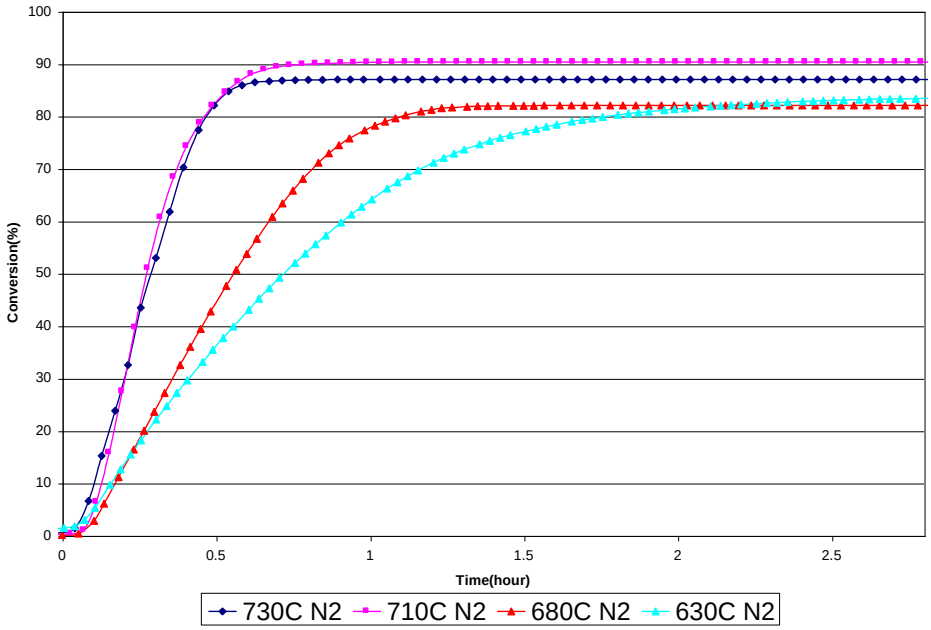

Figure 3.13. Effect of Temperature on Na_2CO_3 conversion in $Na_2O\bullet 3TiO_2$-Black liquor Mixture in 100% N_2

The effect of temperature on the direct causticization of black liquor in a feed gas stream containing 10 % CO_2 is shown in Figure 3.14. Comparison of these results with those in Figure 3.13 shows that except for the reaction at 620°C the final conversion of Na_2CO_3 is about 10 % lower when 10 % CO_2 is added to the carrier gas. The reaction at 620°C has a much lower conversion compared to the other reactions. This behavior is similar to that of the model mixture. It also shows that the direct causticization of Na_2CO_3 in black liquor by Na_2O3TiO_2 in 10% CO_2 does proceed when the temperature is 680°C or higher. The limiting temperature of 680°C is lower than 730°C found in the model compound study.

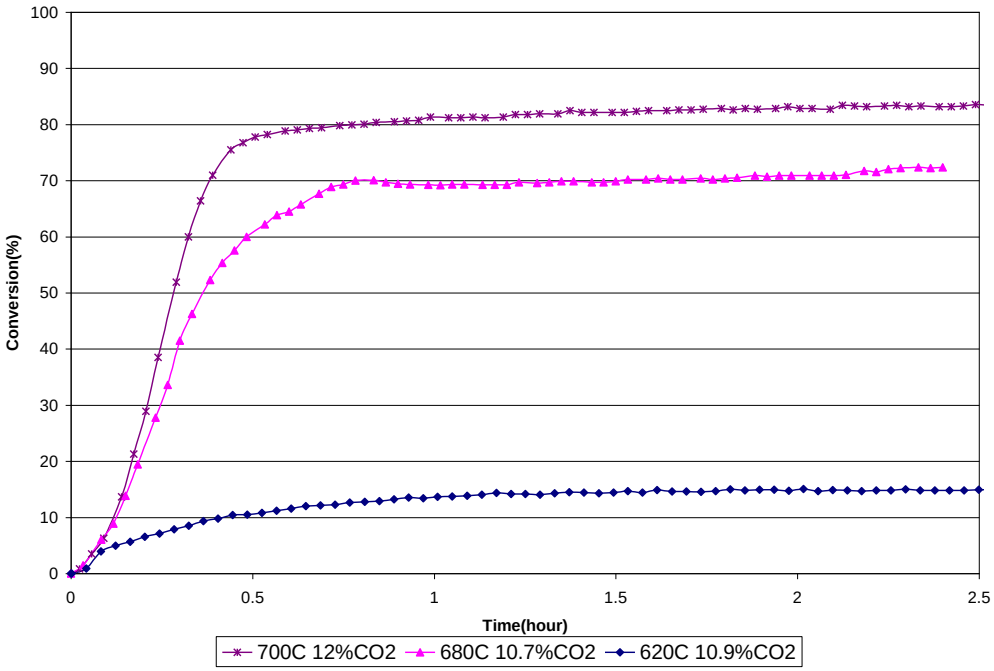

Figure 3.14. Effect of Temperature on Na_2CO_3 conversion in Na_2O• $3TiO_2$-Black liquor Mixture in 10% CO_2

Because the kinetics are so fast it was checked whether they were affected by mass transfer limitations. This was done by using pure helium as the carrier gas rather than nitrogen at otherwise the same experimental conditions. The results in Figure 3.15 for direct causticization at 700 - 710 °C show that the kinetics are indeed faster in helium than in nitrogen, but that the final conversion is not affected. This implies that the intrinsic chemical kinetics for direct causticization of black liquor are even faster than those shown in Figures 3.13 and 3.14.

The conversion of Na_2CO_3 calculated from the weight loss is compared with the conversion based on titration of the final samples in Table 3.8. It can be seen that there is generally a good agreement between the two results except for the first sample (730 °C in pure N_2). It should be noted that this sample was oxidized at 360 °C for 20 hrs, rather than 5hrs at 500 °C as for all other tests.

Table 3.8. Comparison of Conversion Determined from Weight Loss and from Titration

Sample	Conversion from weight loss	Conversion from Titration
730C Pure N_2	86.8%	68.7%
710C Pure N_2	90.7%	99.2%
680C Pure N_2	81.9%	86.0%
700C 10%CO_2	82.1%	76.5%
680C 10%CO_2	70.2%	80.1%
700C He	87.7%	86.1%

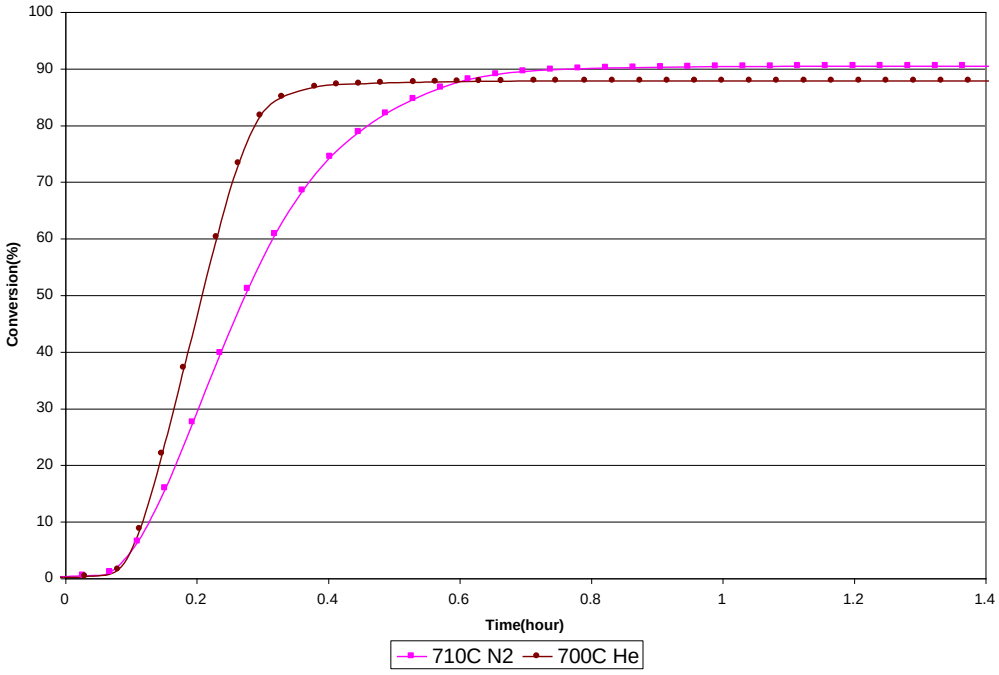

Figure 3.15. Effect of carrier gas type on Na_2CO_3 conversion in Na_2O• $3TiO_2$-Black liquor Mixture

3.2.4 Kinetic modeling

3.2.4.1 Kinetics of model compound mixtures

The experimental data in Figure 3.8 were first fitted following the Valensi-Carter model and modified shrinking core model. As mentioned in the literature review (see section 1.4.3), the SCM (shrinking core model) is only good for describing reactions which proceed to complete conversion. Therefore only the data for the Na_2CO_3-Na_2O•$3TiO_2$ mixture at 740°C in pure nitrogen can be used for SCM analysis. However, as shown in Figure 3.16 both models do not fit the experimental data well. Consequently we used the model by Lee ([84]) represented by equation (1.19) to fit both the fast and slow reaction region at respectively relatively low and high conversions. Figure 3.17 shows an excellent linear fit of Eq. (1.19) with the experimental data at lower conversion levels. From the slopes and intercepts of the straight lines of Figure 3.17 the values of k and b in the chemical reaction controlled regime are calculated and summarized in Table 3.9. Also listed in Table 3.9 are the values of k and b in the chemical reaction controlled regime for the reaction between Na_2CO_3 and TiO_2 in N_2 (original data shown in Figure 3.5) The same good fit is also achieved in the diffusion controlled regime for the Na_2CO_3-Na_2O•$3TiO_2$ mixture as shown in Figure 3.18. The values of k and b are also calculated and summarized in Table 3.9 for both model mixtures.

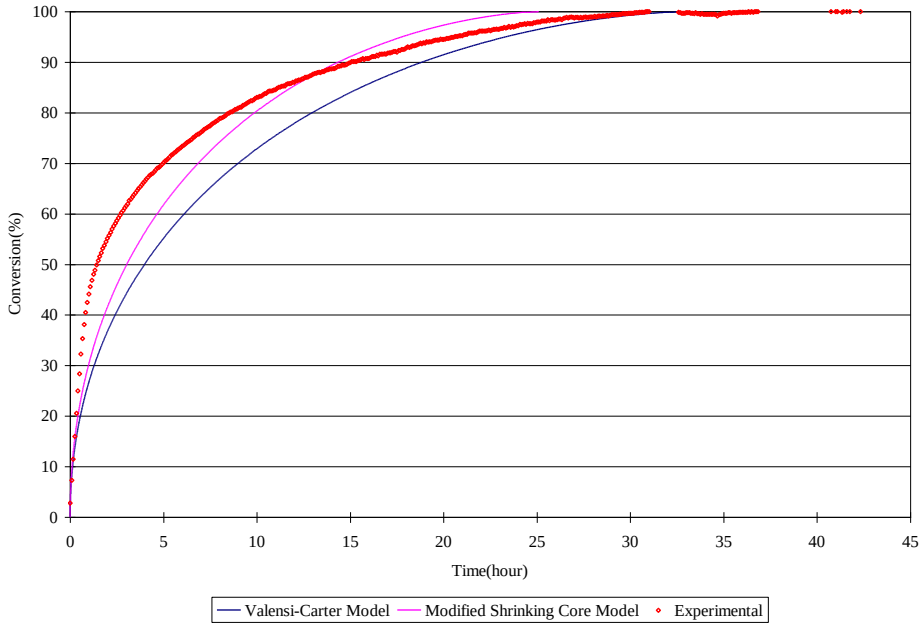

Figure 3.16. Comparison between SCM Model and Experimental Data for Na_2CO_3-$Na_2O•3TiO_2$ mixture at 740°C in pure nitrogen

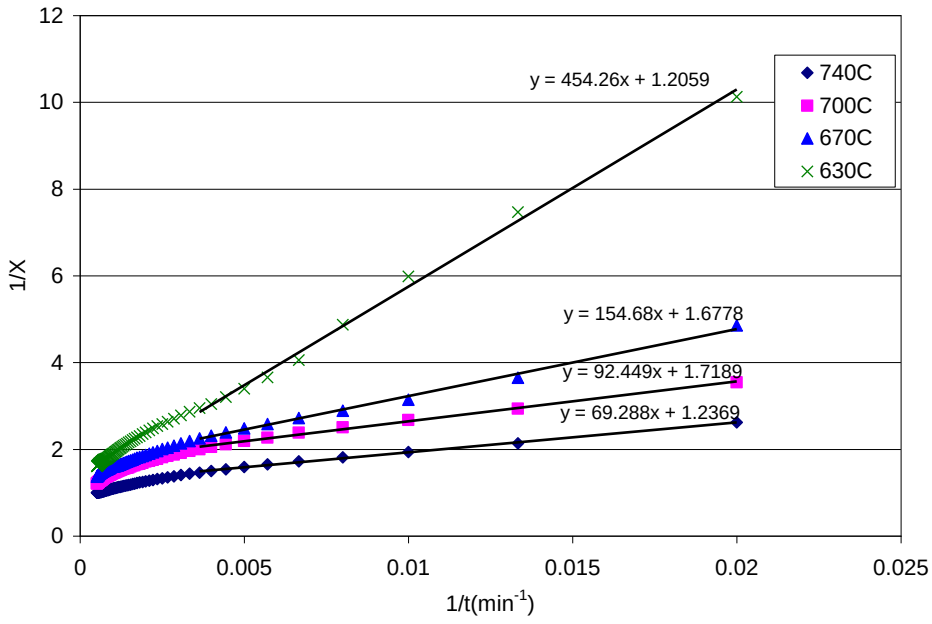

Figure 3.17. 1/X vs. 1/t for Na_2CO_3-$Na_2O•3TiO_2$ in pure Nitrogen in the Chemical Reaction Controlled Regime

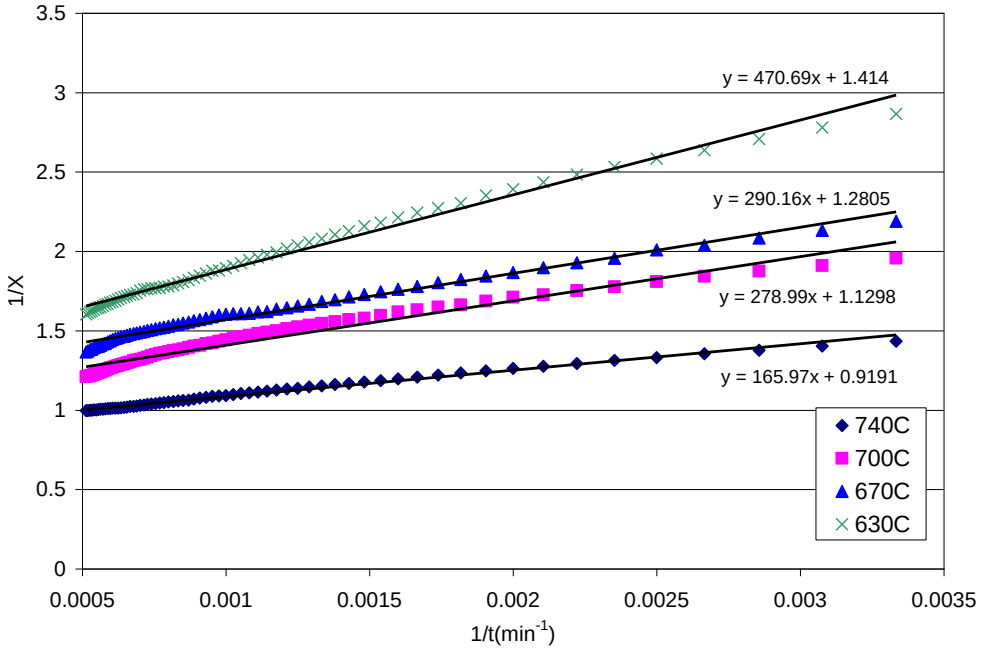

Figure 3.18. 1/X versus 1/t for Na_2CO_3-Na_2O•$3TiO_2$ in the Diffusion Controlled Regime

Table 3.9. Kinetic Parameters for Model Equation (1.19) applied to Model Compound Mixtures

	Temperature (°C)	Chemical Reaction Controlled Regime			Diffusion Controlled Regime		
		k(min^{-1})	b(min)	Xu	k(min^{-1})	b(min)	Xu
Na_2CO_3-TiO_2 in pure N_2	630	0.0131	20.2	0.26	0.0020	295	0.60
	670	0.0151	23.5	0.36	0.0034	194	0.67
	700	0.0186	31.2	0.58	0.0053	145	0.77
	730	0.0199	38.6	0.77	0.0097	92	0.89
Na_2CO_3-Na_2O•$3TiO_2$ in pure N_2	630	0.0022	377	0.83	0.0021	333	0.71
	670	0.0065	92	0.60	0.0034	227	0.78
	700	0.0108	54	0.58	0.0036	247	0.89
	730	0.0144	56	0.81	0.0060	181	1.09

From the values of the second order rate constants, k, obtained in the chemical reaction controlled regime, the activation energy for the titanate surface chemical reaction with sodium carbonate may be determined. Similarly, one may calculate the temperature dependency of the parameter b which represents the time to achieve half of the ultimate conversion Figure 3.19 shows the Arrhenius relationship of the logarithm of k and b against the inverse of the temperature for the reaction with Na_2O•$3TiO_2$. From the slope the activation energies are calculated, and they are summarized in Table 3.10.

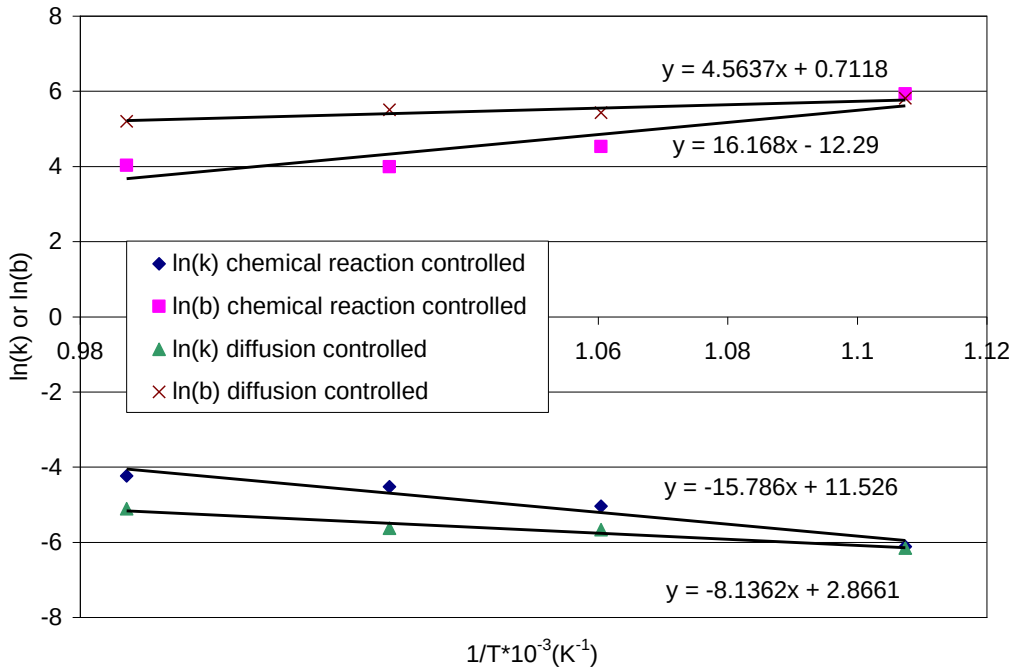

Figure 3.19. Ln(k) and ln(b) vs. 1/T in the Chemical Reaction and Diffusion Controlled Regimes for the Na_2CO_3-Na_2O•3TiO_2 Reaction in pure Nitrogen

Table 3.10. Activation Energy for D.C. Rate Constant k in pure Nitrogen

Activation Energy (kJ/mol)	Chemical Reaction Controlled Regime	Diffusion Controlled Regime
Na_2CO_3 by TiO_2	34	116
Na_2CO_3 by Na_2O•3TiO_2	131	68

The results show that the activation energy in the chemical controlled regime of the reaction of Na_2CO_3 with Na_2O•3TiO_2 is much higher than that with TiO_2. Since Na_2O•3TiO_2 is the intermediate product between TiO_2 to 4Na_2O•5TiO_2, this can be interpreted that the reaction of Na_2CO_3 with TiO_2 (to Na_2O•3TiO_2) is fast at relatively low temperatures while for the reaction with Na_2O•3TiO_2 to 4Na_2O•5TiO_2 a higher temperature is needed. On the other hand the temperature dependency in the diffusion controlled regime of the reaction of Na_2CO_3 with Na_2O•3TiO_2 is lower than that with TiO_2 possibly due to the differences in crystal structure between TiO_2 and Na_2O•3TiO_2. Figure 3.20 shows the excellent prediction of the conversion using the kinetic parameters obtained in the two regimes for the Na_2CO_3-Na_2O•3TiO_2 model system in pure nitrogen at two temperatures, 630 and 740 °C.

.

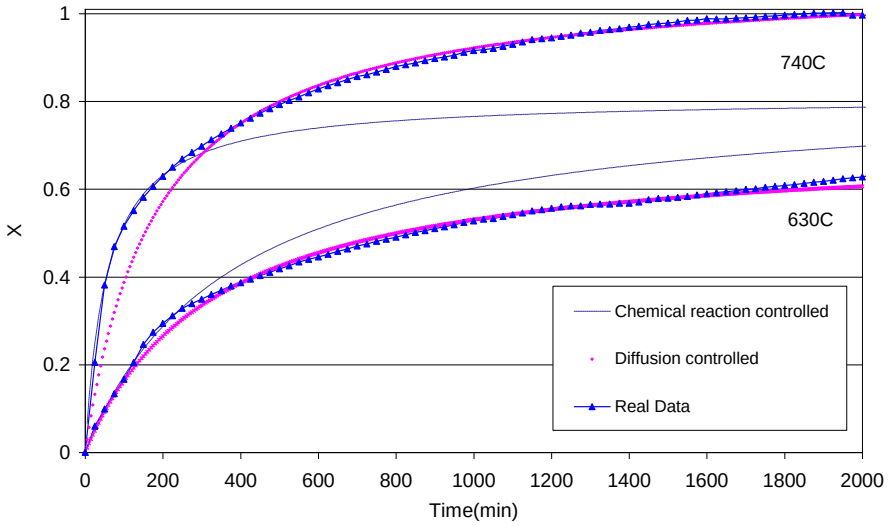

Figure 3.20. Prediction of Conversion using the Kinetic Parameters for the Na_2CO_3-Na_2O•$3TiO_2$ Reaction in pure Nitrogen

3.2.4.2 Modeling the kinetics of direct causticization of black liquor with Na_2O• $3TiO_2$

None of the models described in section 1.4.3 were effective in describing the direct causticizing kinetic data obtained for the black liquor - Na_2O• $3TiO_2$ mixture in pure nitrogen. Therefore a modified phase boundary model was tried which accounted for an ultimate conversion different than 100%, i.e.:

$$k_2 t = 1 - (1 - \frac{X}{Xu})^{\frac{1}{3}} \qquad (3.9)$$

where Xu is defined as the ultimate conversion which can be reached at a certain temperature.

Figure 3.21 shows the predicted curves using the parameter k_2 obtained from the experimental data described in Figure 3.13. It can be seen that the agreement is quite good.

Figure 3.22 shows the Arrhenius relationship of the logarithm of rate constant k_2 against the inverse temperature for the black liquor - Na_2O•$3TiO_2$ mixture in pure nitrogen. The activation energy calculated from the slope is 108 kJ/mol. This value is somewhat smaller than that found for the model compound studies of 131 kJ/mol, presumably caused by the presence of some diffusion limitation in the black liquor - Na_2O•$3TiO_2$ mixture as was shown to be present in Figure 3.15.

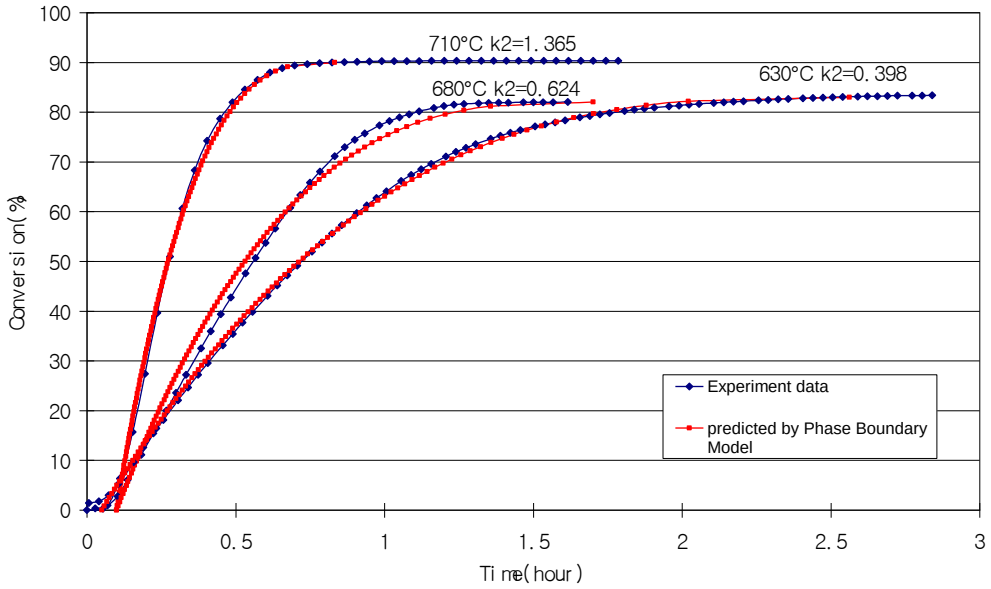

Figure 3.21. Prediction of Conversion using the Kinetic Parameters of Eq. 3.9 for Black Liquor-$Na_2O•3TiO_2$ in pure Nitrogen

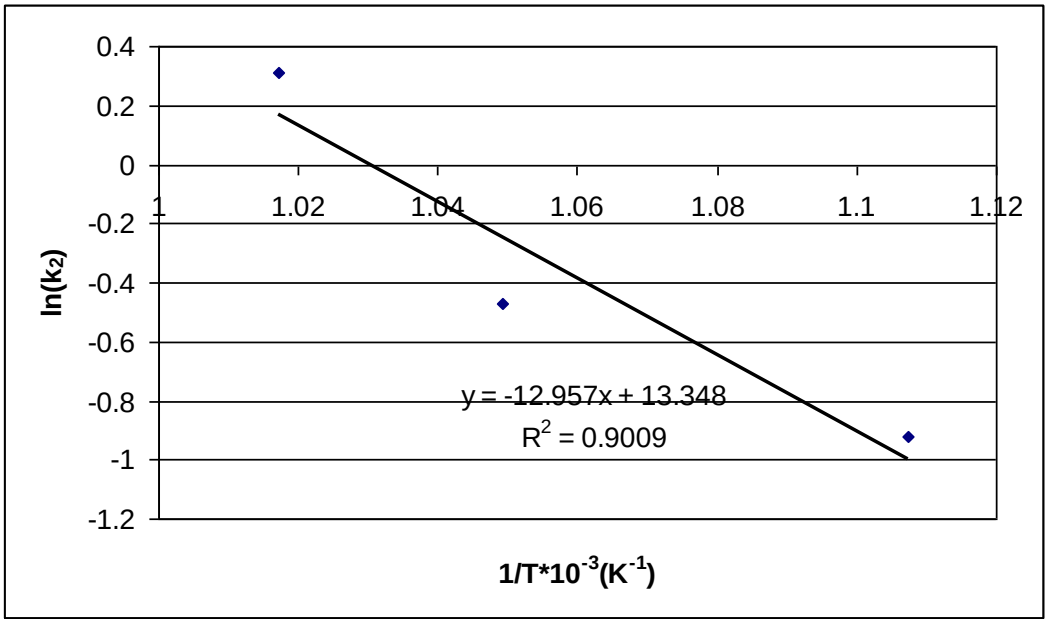

Figure 3.22. Ln(k_2) versus 1/T for Black Liquor-$Na_2O•3TiO_2$ in Pure Nitrogen

3.3 Conclusions for direct causticization reaction kinetics

The direct causticization kinetics of Na_2CO_3 by both TiO_2 and crystalline $Na_2O{\cdot}3TiO_2$ has been determined using stoichiometric mixtures of the reactants. 90% conversion of Na_2CO_3 by TiO_2 into $4Na_2O{\cdot}5TiO_2$ is obtained at 730 °C after 50 hours in an atmosphere of pure nitrogen or a mixture of 10% CO_2 in nitrogen. At 700 °C or lower the presence of 10% CO_2 prevents the formation of $4Na_2O{\cdot}5TiO_2$ and the reaction stops at the formation of the intermediate $Na_2O{\cdot}3TiO_2$. The reaction of Na_2CO_3 with crystalline $Na_2O{\cdot}3TiO_2$ is somewhat faster than that with TiO_2. Complete conversion to sodium pentatitanate is obtained at 740 °C after 30 hours. With 10% CO_2 full conversion is still approached after 50 hours at 740 °C, but the conversion is limited to about 60 % at 700 °C, while there is essentially no reaction at 670 °C. Since sodium pentatitanate creates NaOH when contacted with water, the present results suggest that the temperature should be raised above 700 °C in order to achieve direct causticization of Na_2CO_3 during gasification of black liquor in an industrial gasifier.

Black liquor has an almost two order of magnitude faster D.C reaction rate compared to that of the model mixtures with Na_2CO_3, and the reaction is completed within 30 minutes above 680°C. The fast reaction rate and high final conversion are beneficial when using titanates for direct causticization of black liquor in a gasification process. Also the direct causticization of Na_2CO_3 in black liquor by Na_2O3TiO_2 in 10% CO_2 does proceed when the temperature is 680°C or higher. The limiting temperature of 680°C is lower than 730°C found for the model compound mixtures.

Different solid-solid reaction models were tried to describe the direct causticization of Na_2CO_3 or black liquor by $Na_2O{\bullet}3TiO_2$ or TiO_2 in pure nitrogen. The shrinking core model was not able to model the kinetics for mixtures of Na_2CO_3 and $Na_2O{\bullet}3TiO_2$ or TiO_2. However the experimental data was well represented with the kinetic equation: $X=kbt/(b+t)$, where k is the rate constant and b is the time to attain half the ultimate conversion. These kinetics can be interpreted as a second order chemical reaction during the initial phase of the reaction and a diffusion controlled reaction during the final phase. The activation energy of the reaction of Na_2CO_3 with TiO_2 is estimated as 34 kJ/mol, while the Na_2CO_3 - $Na_2O{\bullet}3TiO_2$ reaction has an activation energy of 131 kJ/mol. This large difference suggests that the reaction of Na_2CO_3 with TiO_2 (to $Na_2O{\bullet}3TiO_2$) is fast at relatively low temperatures while for the reaction with $Na_2O{\bullet}3TiO_2$ to $4Na_2O{\bullet}5TiO_2$ a higher temperature is needed

The kinetic data of black liquor direct causticization by $Na_2O{\bullet}3TiO_2$ in pure nitrogen are well described by a modified phase boundary model. The activation energy for the reaction rate constant is 108 kJ/mol. This value is somewhat smaller than that found for the model compound studies of 131 kJ/mol, presumably because of the presence of some diffusion limitation in the black liquor - $Na_2O{\bullet}3TiO_2$ mixture.

3.4 Leaching of pure titanates

Leaching experiments were done with pure titanates. 1N3T was purchased (Aldrich), while 1N1T, 4N5T and 1N6T were synthesized in the lab. This was done by mixing stoichiometric amounts of Na_2CO_3 and TiO_2 in water, heating the slurry until a paste was formed, drying at 105 °C, grinding and sieving to <180 μm, and finally heating the powder up to 950 °C for 2 hr to

ensure complete conversion. As shown in Table 3.11, conversions of synthesized 1N1T and 4N5T were above 95% as measured by weight loss and total carbon (TC) of the bed residual solids (BRS). However, for 1N6T the conversion by weight loss (as CO_2) was only 76.4%. This sample was then heated again for additional 22 hr at 950 °C to reach a final conversion of 82.5% by weight loss. The reason for the lower conversion with 1N6T is attributed to the formation of a hard shell of 1N6T product around the TiO_2 in the core of the particle that restricts the access of more Na_2CO_3 to reach unconverted TiO_2.

Titanate	Conversion by weight loss (CO_2 emission)	Conversion by TC of BRS
1N1T	97.4%	
4N5T	96.7%	98.3%
1N6T	76.4%	

Table 3.11 Conversion of synthesized titanates.

All titanates were leached with boiling water during 1 hr in a solid to water ratio of 1g per liter. The weight of the remaining solids was measured. Then NaOH and Na_2CO_3 were determined by titration and precipitation with $BaCl_2$ respectively. Figure 3.23 shows that the leaching yield reaches a maximum of 53% for 4N5T. This yield is close to that of 58% if it is assumed that the final residual solids have a 1N3T composition[93]. The leaching yield for 1N3T is 39%, which is smaller than 50% if residual solids had a 1N6T composition. Yield for 1N6T is only about 3% in agreement with findings by other researchers that almost no Na_2O can be leached out from 1N6T[94].

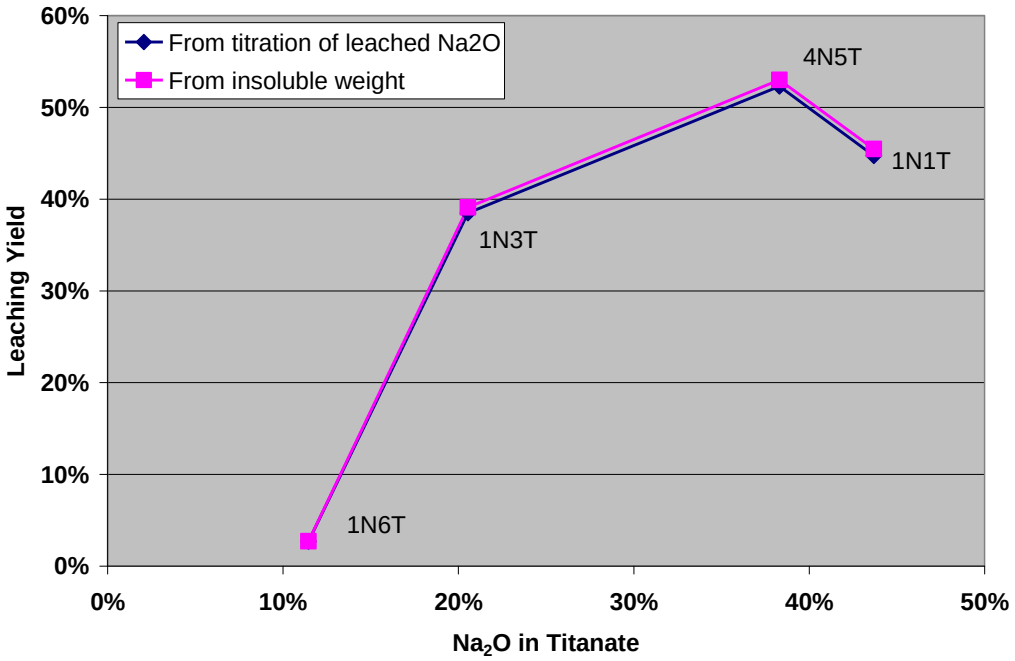

Figure 3.23 Leaching yield vs. Na_2O % of different titanates using two measurement methods.

3.5 Additional experiments of the inhibiting effect of CO_2 on direct causticizing (DC) yield and causticity

In the previous section it was reported that CO_2 inhibits the DC yield. Further experiments were performed to confirm these results, as well as to study other titanate feedstocks were investigated.

The additional thermo balance tests were done on mixtures of KBL (high S) and soda Weak Black Liquor (WBL) (negligible amount of S) with $Na_2O{\cdot}3TiO_2$ (N3T), anatase TiO_2, and Ti-Pure R-103 (DuPont). An elemental analysis of the KBL gave C: 32.3%, H: 3.8%, O: 35.8%, Na: 18.2%, S: 3.0%, Cl: 0.7%, and K: 3.0%. Proximate analysis of the WBL gave combustibles: 56.7%, soluble ash: 42.6%, insoluble ash: 0.7%. Soluble ash had NaOH: 0%, and Na_2CO_3: 41.8% in terms of original (uncombusted) amounts.

The samples were prepared by mixing WBL (or KBL) with titanium containing solids, heating until a paste, drying at 105 °C, and then grinding and sieving to 180-425 μm particle size. The samples were then pyrolyzed under a flow of nitrogen in a separate furnace at 550 °C for 1 hour to eliminate the release of tars in the TG which would contaminate the gas flow meter, micro-GC and CO_2 analyzer. Subsequently the samples were combusted in air in the thermo balance at 550 °C for about 4 hours to minimize the organic carbon (OC) content of the samples which would react with CO_2 added in the DC studies. The final gasified solid samples were leached with water, and then analyzed for total inorganic C (TIC) and total S, and titrated for Na_2CO_3, Na_2S and NaOH. The DC yield was calculated from the weight loss, amount of CO_2 and CO released, and loss of Na_2CO_3 content. The causticity was determined as the ratio of NaOH/(NaOH + Na_2CO_3), all expressed as Na_2O.

Table 3.12 summarizes the experimental conditions, mass balance, leaching and titration data, TIC analysis, and final yield for all lab experiments lasting long enough to reach a stable weight loss or stable gas composition. All weights refer to the original amount before any pretreatment. The line in bold starting at the "Material" column provides the amount of the Ti reactant in the mix ($Na_2O{\cdot}3TiO_2$ or TiO_2), the weight loss during pyrolysis pretreatment, titration data and TIC analysis for the batch of samples that follow in lines below. The amount of Na_2O in the total Na_2O/TiO_2 ratio was obtained by adding the content of Na_2O in Na_2CO_3 and $Na_2O{\cdot}3TiO_2$ for samples starting with $Na_2O{\cdot}3TiO_2$, and from the content of Na_2O in Na_2CO_3 only for samples starting with TiO_2. The original amount of Na_2CO_3 was obtained from the TIC of the starting mix. Notice that the total Na_2O/TiO_2 ratio ranges from 0.63 to 0.75 for mixtures with pure or recycled $Na_2O{\cdot}3TiO_2$, is equal to 0.83 for the WBL-Anatase mix, 1.1 for the KBL-TiPure R103 (from DuPont with >96% TiO_2 rutile and <3.2% Alumina) mix, and 0.32 for the MTCI#8 feedstock. This means that the Na_2O/TiO_2 ratio of the mixtures ranged from a value close to 0.33 for the formation of pure $Na_2O{\cdot}3TiO_2$ to 0.8 for the formation of pure $4Na_2O{\cdot}5TiO_2$ to a value of 1.1 which represents a 10% excess of Na_2O compared to formation of pure $Na_2O{\cdot}TiO_2$.

Ref #	Material	DC Conditins	Pre-treatment	Ti Reactnt	W.Loss Pyrlss.	Weight Loss TOTAL	Weight Loss DC	Weight Loss Other	Leaching/Titration Titratn. Methd.	Leaching/Titration Inslbls.	Leaching/Titration Na_2O	Leaching/Titration Na_2CO_3	Mass Balnce Total	TIC	Na_2O/TiO_2 Total	Na_2O/TiO_2 bound	DC Yield by Weight loss	DC Yield by $CO-CO_2$ count	DC Yield by Na_2CO_3	DC Yield by TIC	Causti-city
	Pyrolyzed WBL-N3T Batch I			**56.9%**	**17.0%**				**II**	**61.0%**	**3.8%**	**21.3%**	**103.1%**	**2.0%**	**0.63**						**23.6%**
DC1		N_2 730°C	Air 570°C			32.0%	7.3%	24.7%	III [1]	58.0%	7.3%	-	-	-		0.63	-	99.7%	-	-	-
DC2		12%CO_2 720°C	-			25.1%	0.9%	24.2%	II	55.4%	4.5%	19.5%	104.6%	1.8%		0.36	14.7%	9.8%	8.3%	9.8%	28.4%
DC3		34%CO_2 700°C	N_2 620°C			25.2%	1.2%	24.0%	II	54.7%	4.3%	19.8%	104.0%	1.8%		0.35	16.6%	13.8%	6.9%	8.3%	27.0%
DC4		100%CO_2 720°C	Air 560°C			25.2%	-	-	III [1]	-	0.2%	18.4%	-	-		0.37	12.9%	-	13.5%	-	-
	Pyrolyzed WBL-N3T Batch II			**56.9%**	**16.7%**				**II**	**59.4%**	**3.9%**	**23.2%**	**103.2%**	**2.3%**	**0.67**						**22.1%**
DC5		N_2 720°C	Air 560°C			32.6%	8.8%	23.8%	IV	60.0%	12.7%	1.7%	107.0%	0.7%		0.57	103.9%	105.6%	92.8%	70.7%	92.9%
DC6		20%CO_2 720°C	Air 560°C			25.8%	3.6%	22.2%	II	53.7%	5.0%	20.3%	104.7%	1.9%		0.39	22.7%	-	12.6%	17.0%	29.5%
DC7		100%H_2O 730°C	Air 560°C			31.0%	-	-	II	61.1%	9.8%	6.8%	108.8%	0.4%		0.61	78.6%	-	70.6%	83.6%	71.1%
DC8		20%CO_2 in H_2O 740°C	Air 560°C			31.7%	-	-	II	56.6%	4.7%	13.0%	105.9%	1.0%		0.52	-	-	34.8%	55.0%	38.1%
DC9		20%CO_2 810°C	Air 560°C			30.3%	5.9%	24.4%	II	59.1%	6.9%	12.2%	108.6%	0.6%		0.58	78.6%	70.9%	38.7%	73.9%	49.3%
	Pyrolyzed WBL-N3T Batch III			**56.9%**	**18.1%**									**2.2%**	**0.65**						
DC10		12%CO_2 730°C	Air 560°C			26.8%	1.4%	25.4%						**1.8%**		0.36	16.2%	18.0%	-	8.8%	
	Pyrolyzed MTCl# 8 Feedstock			**50.0%**	**17.3%**				**II**	**58.6%**	**0.0%**	**22.4%**	**98.3%**	**2.4%**	**0.32**						**0.0%**
DC11		11%CO_2 730°C	Air 560°C			43.1%	7.4%	35.7%	IV	63.0%	0.5%	1.3%	107.8%	0.0%		0.32	-	84.9%	93.1%	99.9%	37.4%
DC12		12%CO_2 730°C	-			43.0%	8.9%	34.1%	-	-	-	-		0.0%		0.32	-	95.9%	-	100.0%	-
DC13		12%CO2 730°C	-			43.2%	7.9%	35.3%	IV	62.0%	1.2%	0.5%	106.9%	-		0.31	-	91.4%	97.6%	-	82.3%
	Pyrolyzed WBL-Anatase (TiO2)			**30.2%**	**23.0%**				**III**	**45.8%**	**0.4%**	**33.6%**	**102.7%**	**3.8%**	**0.83**						**2.0%**
DC14		12%CO_2 730°C	Air 560°C			43.4%	5.6%	37.8%	III	43.3%	2.1%	21.0%	109.8%	2.2%		0.35	53.4%	40.2%	37.5%	42.1%	14.5%
DC15		N_2 730°C	Air 560°C			46.1%	12.2%	33.9%	II	49.3%	10.3%	6.3%	111.9%	0.5%		0.73	87.3%	102.1%	81.3%	87.6%	73.8%
	Pyrolyzed KBL-TiPure R-103			**24.5%**	**20.9%**				**III**	**41.8%**	**0.5%**	**34.7%**	**97.8%**	**3.9%**	**1.10**						**2.4%**
DC16		12%CO_2 730°C	Air 560°C			46.3%	-	-	III	37.2%	6.3%	9.6%	99.4%	-		0.79	64.4%	47.5%	72.4%	-	53.1%
DC17		N_2 730°C	Air 560°C			42.0%	14.4%	27.5%	III	45.8%	13.8%	3.6%	105.1%	0.3%		1.02	106.1%	-	89.5%	92.6%	86.7%
	KBL-Recycled DC17			**47.5%**										**2.1%** [2]	**0.70**						
DC18		12%CO2 730°C	-			44.0%	-	-	III	43.0%	6.7%	7.6%	101.2%	1.7%		0.42	-	-	58.9%	25.1%	60.1%
	KBL-Recycled DC11			**44.1%**										**2.2%** [2]	**0.75**						
DC19		12%CO_2 then 1%CO_2 730°C	-			27.4%	-	-	-	-	-	-	-	0.0%		0.75	-	-	-	98.7%	-
	KBL-Recycled DC13			**44.1%**										**2.2%** [2]	**0.75**						
DC20		9%CO_2, 5% CO, 2%O_2 730°C	-			22.5%	-	-	-	-	-	-	-	1.4%		0.49	-	-	-	36.9%	-

[1] Leaching in hot water at 90 °C for 10 min

[2] Estimated from TIC of KBL

Table 3.12 Experimental conditions, mass balance, leaching and titration data, TIC analysis, and yield for lab experiments.

3.5.1 Mass balance

As can be noticed from Table 3.12, in most cases the mass balance is in excess of 100%. This can be partly explained by the finding of Zhuang et al[95] that leached pentatitanate looses 3.0 to 3.6% weight at around 250 °C because of release of chemically bound water. Consequently, it can be assumed that at least part of the mass excess in Table 3.12 is caused by chemically bound water in the insolubles remaining after leaching. Such behavior has been reported earlier for titanates. Substitution of Na for H was found in hot acid treatment of trititanate.[96] In this case, the formed $H_2Ti_3O_7$ had a strong loss of weight at 250 °C, and this product was shown to be anatase upon further heating to 800 °C and then finally rutile at 1000 °C. Formation of hydrogen alkali tri- and penta-titanate was found during hot alkali treatment of TiO_2.[97] No reference was found on formation of hydrogen alkali titanate for moderate alkaline conditions as in the present study. Further work needs be done to determine the exact stoichiometry of reaction (3.5) where the product is $xNa_2O.yH_2O.3TiO_2$ rather than $Na_2O.3TiO_2$. For a few tests the mass balance was much closer to 100%, such as for pyrolyzed MTCI# 8 feedstock (containing KBL) and pyrolyzed KBL-TiPure R103 batch material. The explanation for this is that the excess chemically bound water is balanced by the release of sulfur from these kraft black liquor tests.

3.5.2 Direct causticizing (DC) conversion

Fig. 3.24 shows the DC conversion vs. time for mixtures of BL with $Na_2O{\cdot}3TiO_2$ or TiO_2 in N_2 at 720-730 °C. As found before, full conversion was reached in all cases, even for test DC17 after 800 min. The present experiments of Fig. 3.23 show that full conversion also occurs for mixtures containing either anatase or rutile TiO_2. Although tests DC1 and DC5 had similar initial compositions (see Table 3.11), conversion of test DC1 was faster probably due to a lower total Na_2O/TiO_2 ratio, which means that more TiO_2 is available for the same amount of Na_2CO_3. Similarly, DC15 was faster than DC17 also because of lower total Na_2O/TiO_2 ratio. The reason why the final conversion of DC17 was lower than the other cases, 90% vs. 100%, may as well be related to its very high Na_2O/TiO_2 ratio (1.1), even above necessary for full conversion to $4Na_2O{\cdot}5TiO_2$.

Fig. 3.25 shows the conversion vs. time for similar mixtures as in Fig. 3.24 but now in about 10% CO_2. Notice that all experiments stopped before reaching 100% indicating an inhibitory effect of CO_2. In experiment DC10 for a mixture of WBL with $Na_2O{\cdot}3TiO_2$ in 10% CO_2 at 730 °C the DC stopped after reaching about 20% conversion, which is considerably lower than the 70-80% shown earlier in Table 3.8. Experiment DC9, also of WBL with $Na_2O{\cdot}3TiO_2$ but now at 810 °C, reached 70% conversion. This means that further raising the temperature reduces the CO_2 inhibiting effect. The final conversion of DC14, WBL-Anatase, and DC16, KBL-TiPure R103, was between 40 and 50%, which is higher than with $Na_2O{\cdot}3TiO_2$. The high conversion for DC12, MTCI#8 FS, is attributed to a lower Na_2O/TiO_2 ratio.

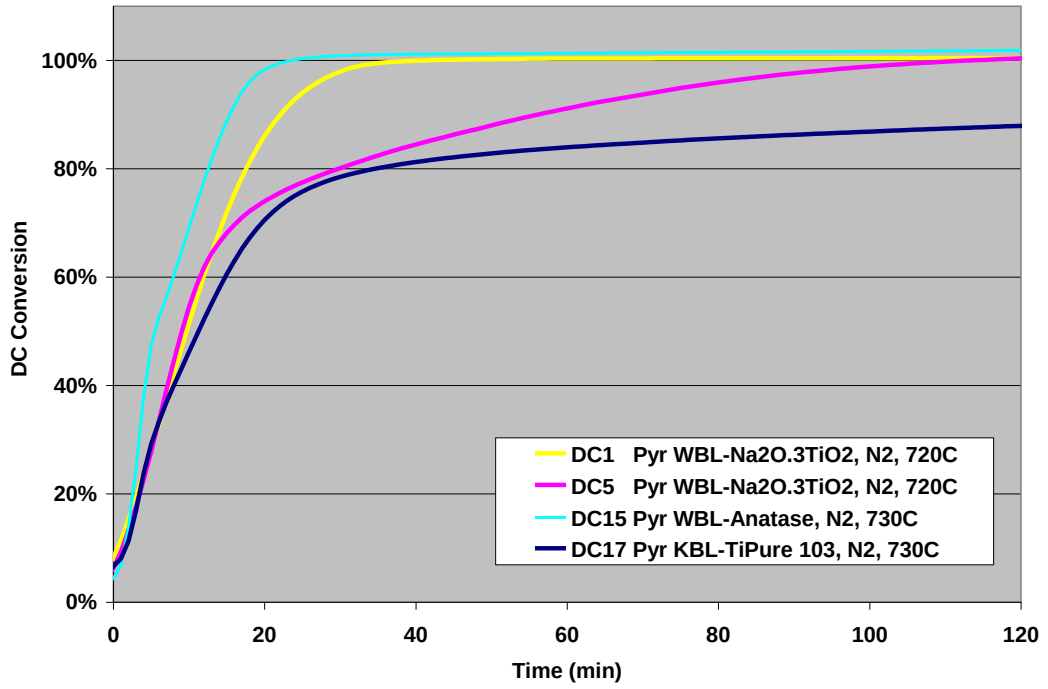

Figure 3.24 DC conversion vs. time for different mixtures in N_2 at 720-730 °C.

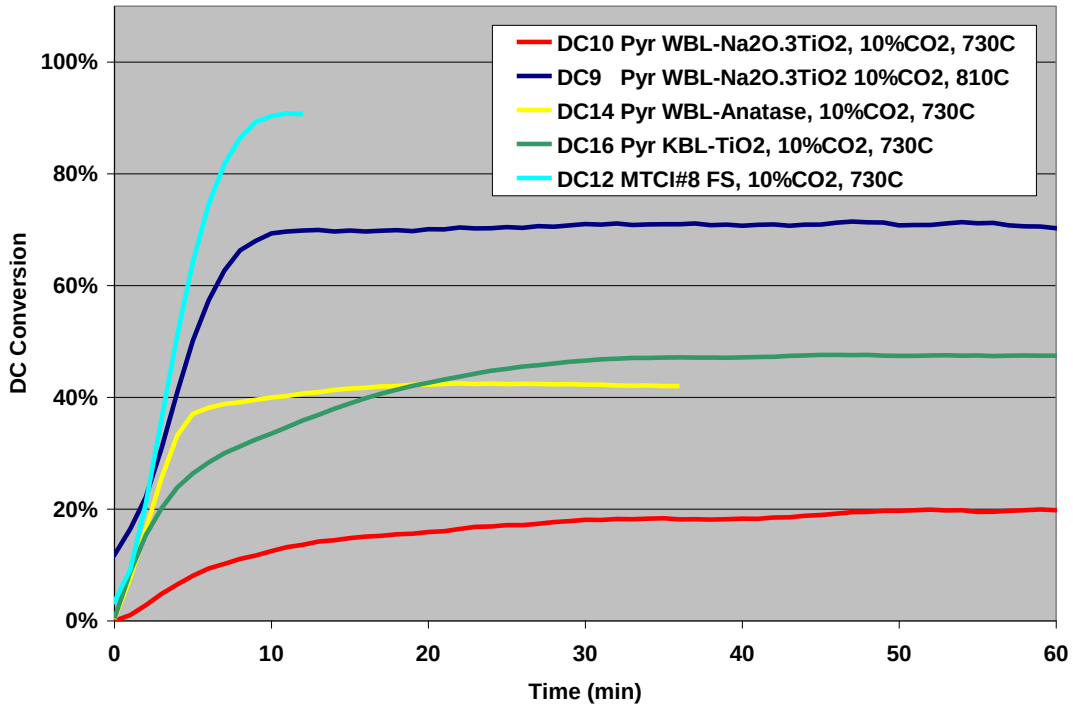

Figure 3.25 DC conversion vs. time in 10% CO_2 and different temperatures.

3.5.3 Causticity of leachate

Tha key measure for direct causticization is the causticity of the leachate, which is the ratio of NaOH/(NaOH + Na_2CO_3), all expressed as Na_2O. In practice this value should be about 80 % or preferably even higher. It can be seen from Table 3.12 that this value is generally achieved in pure nitrogen. However in about 10% CO_2 or higher the causticity varies from about 15 to 60%, with most being about 30 – 40%, values which are too low for practical implementation of the process of combined direct causticization and gasification of black liquor. Since thermodynamic studies predict full conversion even in presence of CO_2 [98], the CO_2 inhibitory effect is caused by a still not understood kinetic problem.

Figure 3.26 displays the influence of CO_2 concentration in N_2 in the inlet gas stream on the DC yield and final bed causticity of BL-$Na_2O{\cdot}3TiO_2$ mixtures at 720 °C. It can be seen that the DC yield determined from either the weight-loss, amount of CO_2 and CO released, or loss of Na_2CO_3 content differ significantly from each other. However in all cases the DC yield drops from a level of about 90 % in pure nitrogen to about 25 % at a [CO_2] of 10% and below 20% at higher [CO_2]. The causticity of the leachate drops to about 30% at the higher [CO_2].

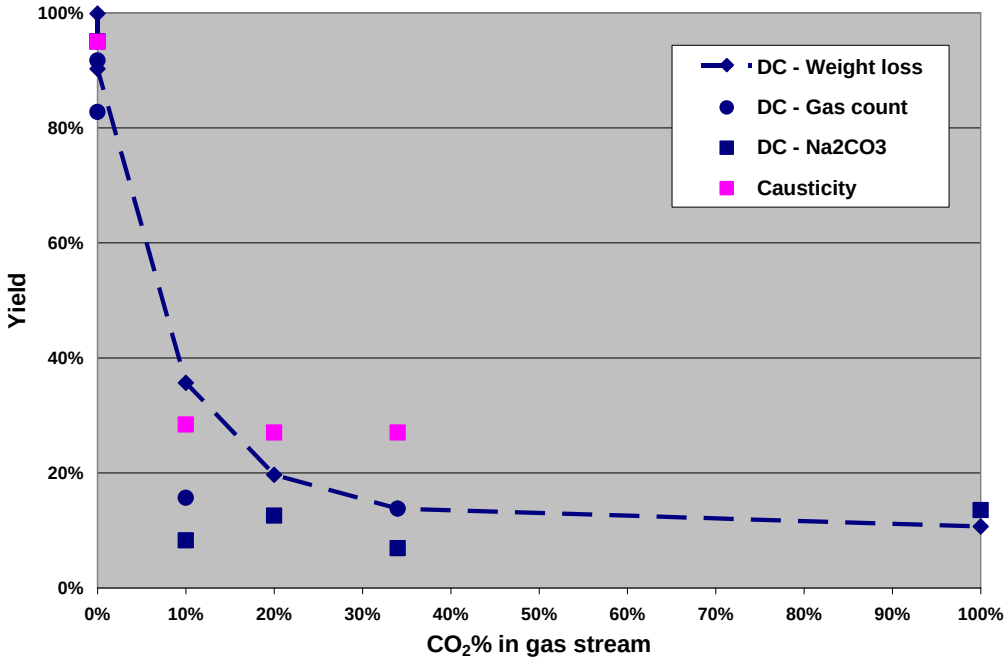

Figure 3.26: Influence of CO_2 in N_2 concentration in the gas stream on the DC yield and causticity of BL- $Na_2O{\cdot}3TiO_2$ mix at 720 °C.

3.5.4 How to achieve high DC conversion and causticity?

Experiment DC18 needs special attention. It was done in two uninterrupted stages while the temperature was kept constant. The first stage was in 12% CO_2 for 1 hr followed by another stage of 1% CO_2 for several hours. After this second stage complete conversion of Na2CO3 was achieved. This leads to the important conclusion that a high DC conversion and causticity can be obtained during steam gasification of BL at 730 °C if the process is divided in two stages; in the first stage most of the carbon is gasified, while in the second stage a low CO_2 atmosphere is

maintained by a purging with steam. Several arrangements are possible, but one process version is where carbon gasification takes place in a fluidized bed while the DC reaction occurs in another reactor which is fed by the solids produced in fluid bed. Steam enters the latter reactor, and the product gas is fed to the fluid bed, thus creating a countercurrent flow of gas and solids.

3.5.5 Carbon gasification rate in 10% CO_2

Fig. 3.27 shows the carbon gasification conversion vs. time of different tests in 10% CO_2. Although DC2 and 9 were both for mixture of WBL-$Na_2O{\cdot}3TiO_2$, carbon conversion in DC2 takes longer because it contains more C since it was not subjected to preburning like most other tests. DC13 with WBL-Anatase displays the same behavior as WBL-$Na_2O{\cdot}3TiO_2$ (i.e. DC9). DC12 and 15 both were done with KBL-Ti-Pure R103 mixtures while DC 17 was done with a recycled mix also originally containing Ti-Pure R103. Since Ti-Pure R103 contains about 3% alumina, it is likely that the reason for DC 15 being slower than DC 13, and DC 17 slower than DC 9 is due to the presence of alumina. Alumina is known to form a thin glassy layer on top of the C structure hindering the gasification process. The low sodium content in DC 12 compared to DC 15 (Na_2O/TiO_2 ratio of 0.32 vs.0.83 resp.) may explain the slow carbon conversion, since alkali catalyzes the carbon gasification rate[99].

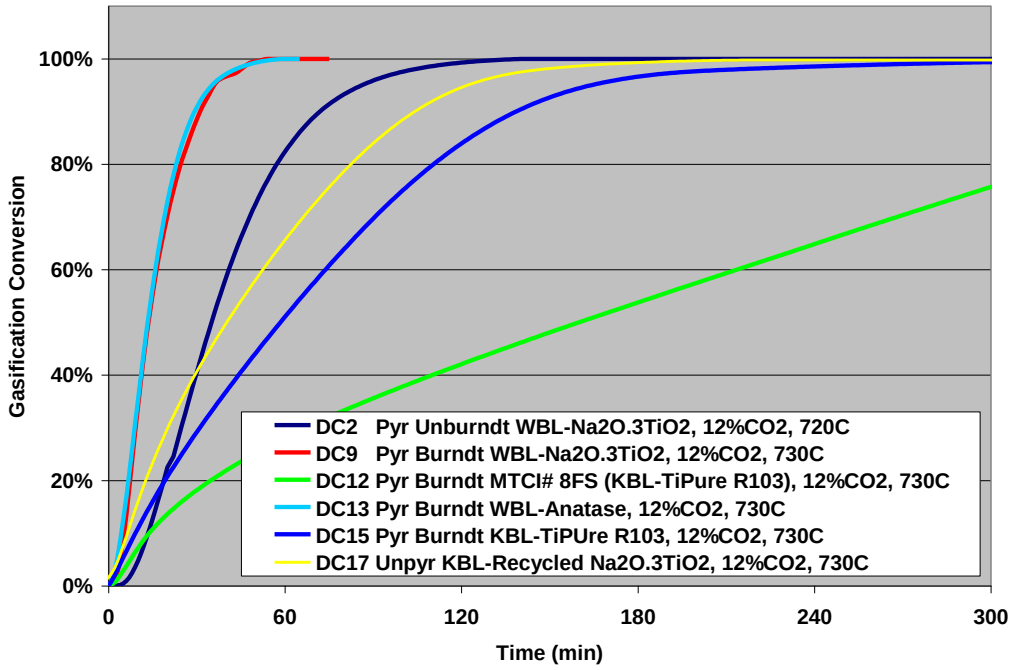

Figure 3.27: Carbon gasification conversion vs. time in 10% CO_2 atmosphere.

3.5.6 Conclusions

- There is a strong decrease in DC final conversion and causticity at a [CO_2] of about 10% or higher during gasification of black liquor – titanate mixtures at about 730 C. This suggest that implementation of the DC-gasification process in a single stage would not be practical.
- However, a two-stage counter current process where carbon gasification takes place in a fluidized bed and the DC reaction in another reactor fed by steam may be a viable option.

3.6 Results and discussion of the study of agglomeration during direct causticization and gasification of black liquor

3.6.1 Introduction

Pilot tests of steam reforming with direct causticization (DC) of black liquor (BL) and titanates mixtures were performed in the MTCI PDU. Several resulted in premature shut down due to bed agglomeration. In order for the technology to be technically viable bed agglomeration must be eliminated or controlled. Therefore the mechanism of agglomeration during this process was studied at the University of Maine using mercury porosimetry, BET surface, and compressive strength and SEM/EDS and SEM/XRD of the agglomerates. The work focused on the role of reaction conditions on mixtures of black liquor and titanates, but model mixtures of Na_2CO_3 and titanates were also studied. In addition the solids produced by MTCI were investigated.

Direct causticization (DC) of black liquor (BL) can be divided in two stages: a) pyrolysis and b) DC reaction. During pyrolysis volatile matter (tar) is released temperatures above 300 °C, and the organics are broken down leaving behind organic C. The end product is commonly referred to as char. During the DC reaction, the Na_2CO_3 contained in the BL is converted to $4Na_2O.5TiO_2$ at temperatures above 670 °C. Two distinctive types of agglomerations take place: a) softening/liquefaction of black liquor solids (BLS) during pyrolysis of the organics starting around 300 °C followed by solidification to a char at higher temperature, and b) shrinking sintering of inorganic solids containing Na_2CO_3 at temperatures above 650 °C when the DC reaction takes place. Experiments were carried out to analyze both types of agglomeration.

3.6.2 Agglomeration during pyrolysis

A stoichiometric mixture (based on $4Na_2O.5TiO_2$ product) of BL and $Na_2O{\cdot}3\ TiO_2$ was dried at 105 °C, ground and sieved to 425-710 μm particle size, and then treated at different temperatures in a N_2 atmosphere for 1-1.5 hr. After treatment at 640 °C the agglomerated particles firmly adhered to the ceramic container and had to be removed with a scraper. Figure 3,28 shows microscopy pictures of the original mix and of the end product for different temperatures. From direct observations and from these pictures it was found that: a) no agglomeration occurs at temperatures up to 200 °C with particles remaining brown; b) partial agglomeration at around 300 °C with particles turning black in some areas; and c) complete agglomeration at temperatures above 400 °C with particles becoming completely black. There was no noticeable difference in bulk density of the particles. The pictures suggest that agglomeration occurred because molten char had accumulated at contact points allowing particles to stick together. Similar observations were mentioned by Gea et al. who analyzed agglomeration of straw black liquor during pyrolysis at 600 °C.[100] Figure 3.29 shows the evolution of the final weight loss vs. temperature for the same samples. Notice that the weight loss increases with temperature and is mostly complete at 300-400 °C.

To better understand the agglomeration during pyrolysis, the well studied process of black liquor swelling will be briefly reviewed. Four stages occur during black liquor pyrolysis and burning: drying, devolatilization, char burning, and smelt reactions[101]as shown in Figure 3.30. During drying, the black liquor droplet volume increases by about 2 without significant loss of combustible gases, and the temperature rises from 150 to 300 °C. During devolatilization above

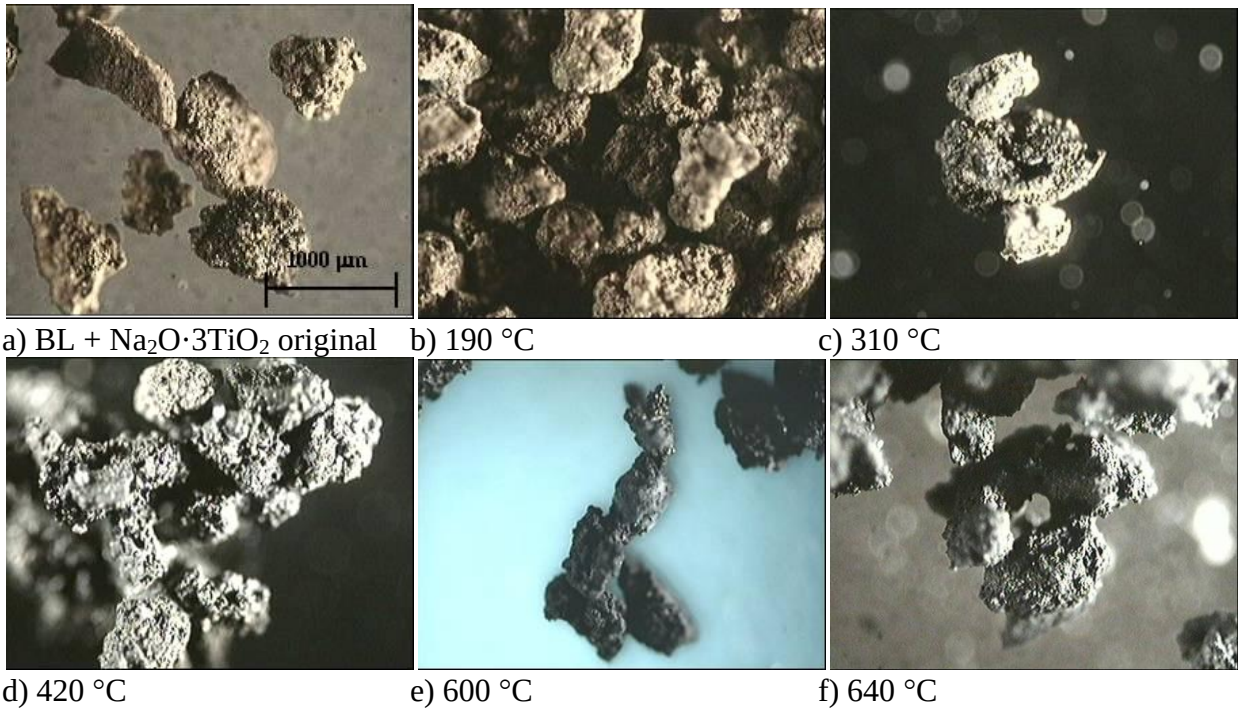

a) BL + $Na_2O{\cdot}3TiO_2$ original b) 190 °C c) 310 °C

d) 420 °C e) 600 °C f) 640 °C

Figure 3.28 Particles of BL and $Na_2O{\cdot}3\ TiO_2$ mixture of 425-710 µm size: a) loose particles before pyrolysis, and b) agglomerated particles after pyrolysis at 640 °C in N_2.

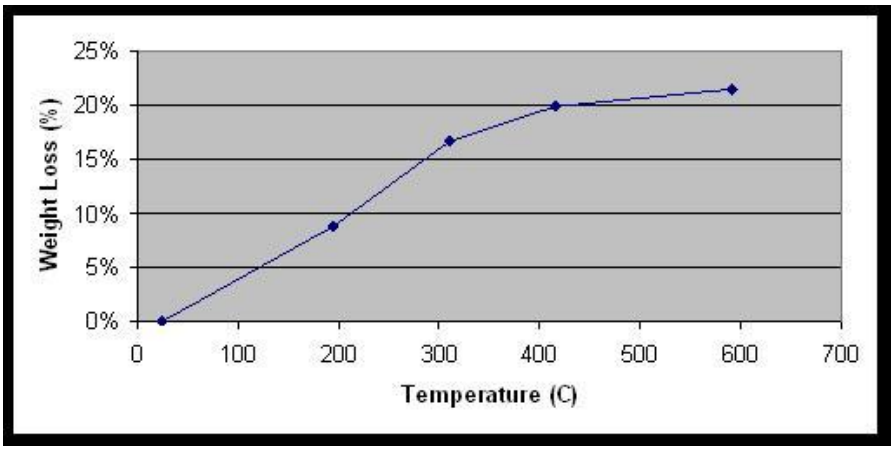

Figure 3.29 Evolution of final weight loss for temperatures up to 600 °C for samples in Figure 3.28.

300 °C, a flame usually appears due to ignition of volatiles, and there is a large increase in volume (up to more than 100 times), and the temperature rises up to that of the surroundings. During char burning, the non-volatile organic C is burned off to inorganic smelt droplet. At 800 °C ambient air, the first three stages take about 5 s.

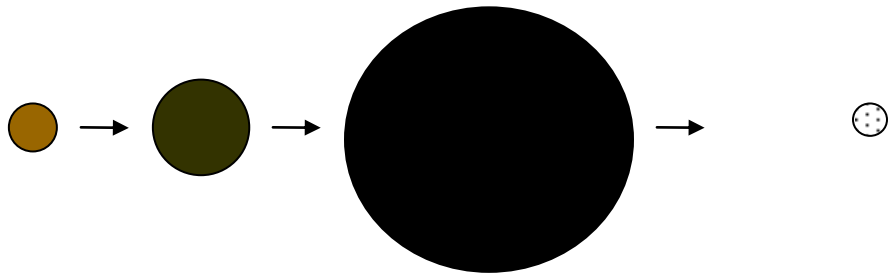

BL particle | Drying | Devolatilization | Char burning and smelt reactions

Figure 3.30: Black Liquor swelling behavior.

The strong swelling of black liquor without titanates was confirmed by an experiment done in the DC furnace (see figure 3.1) by heating up pure BL to 730 °C in N_2. To catch the tar, a cotton trap was placed in the gas line downstream the furnace at a place where the exit gas has already cooled to ambient temperature. At 300 °C, the cotton started to turn brown because of the release of tar (volatiles) indicating the start of the devolatilization stage. After completing the experiment it was found that the BL had over flown the trays, confirming that strong swelling had occurred. The final product consisted of compact agglomerate. To avoid contaminating the DC furnace, additional tests were done with dried BL in ceramic containers placed in a muffle furnace open to air at 480-520 °C. Figure 3.31 illustrates the swelling at different times. Figure 3.31a shows how at 45 s the swelling started at the border of the solid sample where the temperature is assumed to be higher. Figure 3.31 b, at 1 minute 45 s, shows a swollen structure over the entire mass. Figure 3.31 c, at 2 minutes 30 s, shows the swelling at its maximum volume. Figure 3.31 d, after 17 hr, shows solids turned gray because of organic C burned away into inorganic ash. After scraping off the top, agglomerates in Figures 3.31 c and d revealed a hollow structure. In these tests the swelling was considerably slower (min instead of s) than described in the reference as expected because of the lower oven temperature (500 instead of 800 °C).

Similar experiments were done with dry mixtures of BL plus $Na_2O{\cdot}3TiO_2$. Figure 3.32.a shows that after 3 minutes 45 s there was almost no swelling. This can be attributed to the high content of $Na_2O{\cdot}3TiO_2$, inert at temperatures below 650 °C, acting as a dead load that diminishes swelling. This also agrees with the findings of Wintoko and Richards who observed less swelling by adding titanates to BL.[102] Figure 3.32.b shows the product after 17 hr with organic C burned away. The BL plus $Na_2O{\cdot}3\ TiO_2$ mix still shows little swelling but exhibits strong agglomeration. An additional test was done by adding water to the BL + $Na_2O{\cdot}3\ TiO_2$ mixture to form a concentrated slurry. There was some bubbling and foaming attributed to water evaporation but without swelling of the final structure. The final product, as shown in Figure 3.33 at 17 hr, is a dense agglomerate presumably because water allowed the solid to form a compressed packing during evaporation.

a) 45 s b) 1 m 15 s

c) 2 m 30 s d) 17 hr

Figure 3.31 Swelling of pure dried black liquor in air at 500 °C after different times.

a) 3 m 45 s b) 17 hr

Figure 3.32: Agglomeration of dry BL/Na_2O·3 TiO_2 mix in air at 500 °C for different times.

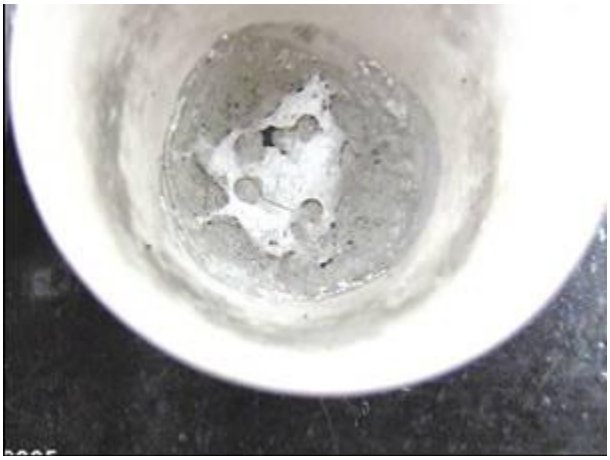

Figure 3.33: Agglomeration of BL plus $Na_2O \cdot 3\ TiO_2$ slurry in air at 500 °C after 17 hr.

From these observations, the mechanism for agglomeration at temperatures below 650 °C is attributed to a softening/liquefaction of the black liquor organics combined with no swelling during pyrolysis of the organics due to the presence of the titanate solids. The relevant steps would be: 1) organic matter melts at ~300 °C; 2) the liquid wets the titanate particles and capillary forces pull the particles together; 3) the liquid tar turns into carbon to solidify the bonding between the titanate particles; 4) strengthening of bond between the titanate particles pyrolysis by neck growth between the particles leading to strong agglomerates over time. The reason that agglomeration is not a major problem in the PDU of MTCI when processing pure black liquor is that the swelling keeps the solid Na_2CO_3 particles separated by fragile char which is easily broken during fluidization of the bed solids.

3.6.3 Sintering with Na_2CO_3

Preliminary experiments with pure or mixtures of model compounds (Na_2CO_3, TiO_2 and $Na_2O.3TiO_2$) showed that some sintering occurs at DC temperatures (above 670 °C). At these temperatures surface diffusion of only Na_2CO_3 occurs because of its lower melting point (858 °C) compared to TiO_2 (1840 °C) and $Na_2O.3TiO_2$ (1130 °C). Thus sintering of Na_2CO_3 may lead to bonding between the particles forming agglomerates.

DC experiments with model compounds were carried out to investigate the influence of particle size and constituents on the strength of agglomerates formed. The qualitative results are summarized in Table 3.13. Three categories were used to qualify the strength of agglomeration: a) strong, when the products in the trays (see Figure 3.1) held together into single mound, b) weak (or none), when the particles were loose and would flow freely under gravity, and c) moderate (or partial), when there was a mix of loose and agglomerated particles.

Type	**Constituents**	**Duration (hr)**	**Particle Size (μm)**	**Agglomeration**
Mix	$Na_2CO_3 + TiO_2$	24 hr	<150	Strong
"	$Na_2CO_3 + TiO_2$	24 hr	200-400	Moderate
"	$Na_2CO_3 + TiO_2$	50 hr	>400	Weak
"	$Na_2CO_3 + Na_2O.3TiO_2$	19 hr	425-710	Weak
Pure	Na_2CO_3	19 hr	90-180	Strong
"	Na_2CO_3	19 hr	425-710	Moderate
"	Na_2CO_3	1 hr	90-180	Strong
"	Na_2CO_3	5 min	90-180	Strong
"	$Na_2O.3TiO_2$	19 hr	90-180	Weak
"	TiO_2	19 hr	90-180	Weak

Table 3.13: Summary of agglomeration strengths for DC mixtures and pure constituents of different particle size after exposure at 730 °C in N_2 for different times.

It can be seen that stoichiometric mixtures of $Na_2CO_3 + TiO_2$ of different particle size at 730 °C in N_2 for 24 hr or more (first three rows in Table 3.13) showed strong agglomeration for particles smaller than 150 μm, moderate agglomeration with particles of 200-400 μm, and no agglomeration with particles larger than 400 μm. Similarly, pure Na_2CO_3 gave strong agglomeration for 90-180 μm and moderate agglomeration for 425-710 μm. Importantly, 90-180 μm particles of Na_2CO_3 revealed no major difference between 19 hr, 1 hr, or 5 minutes exposure on the agglomerate strength. However, 90-180 μm particles of Na_2CO_3 exposed for 5 min at 630 °C showed no evidence of agglomeration. Finally, experiments with pure $Na_2O{\cdot}3TiO_2$ and TiO_2 of 90-180 μm at 730 °C showed no agglomeration. Figure 3.34 shows the Na_2CO_3 particles before and after sintering at 730 °C. The sintered particles have a smoother surface.

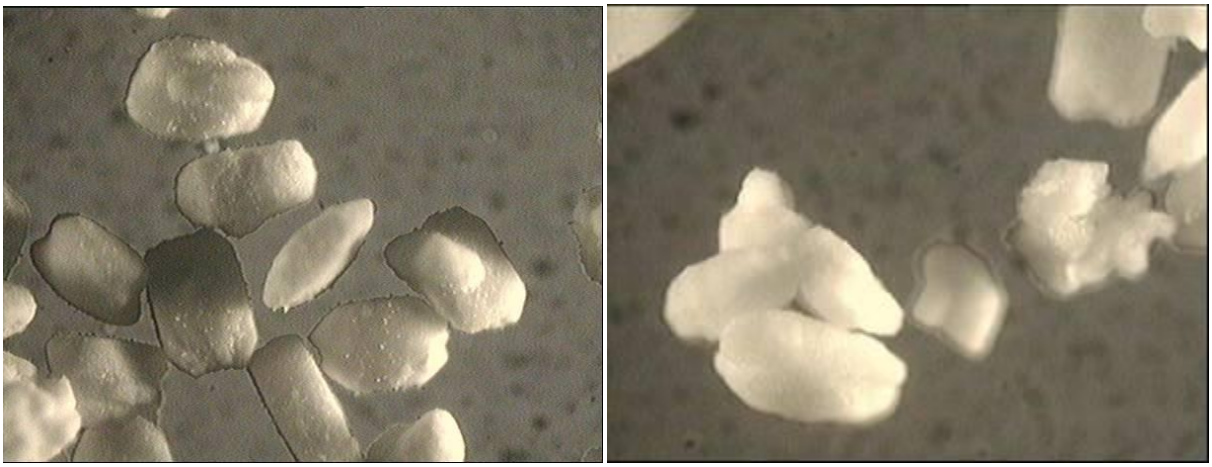

Figure 3.34 425-710 μm Na_2CO_3 particles before (left) and after (right) sintering at 730 °C.

This leads to the conclusions that agglomeration due to sintering of the inorganics in a titanate black liquor mix; a) occurs only in the presence of Na_2CO_3, b) starts at temperatures above 650 °C, c) takes place in the order of minutes or less, d) increases with temperature, and e) diminishes with increasing particle size.

3.6.4 Pore size development during thermal treatment of trititanate/black liquor samples

The pore size distributions of different solid samples were measured using mercury porosimetry. The samples are: a dried mixture of black liquor and trititanate, the same mixture after burning with oxygen at 550 °C, and the same mixture after direct causticization at 700 °C in an atmosphere of 10 % CO_2 in nitrogen or in pure helium. The cumulative and regular pore size distributions are shown in Figures 3.35 and 3.36 respectively.

The results in Figure 3.36 show that the biggest pores in all samples are in the range between 1 and 10 micron. These pores are due to the voids in between the tri-titanate particles, i.e. the external pores. It can be seen from the two figures that these pores become larger in size and volume after direct causticization. The next size smaller pores are only seen for the burned sample, i.e. these pores appear after burning of the organics of the black liquor. So it is likely that that these pores of size slightly smaller than 1 micron are located inside the salt mixture remaining after burning of the organics. During direct causticization these pores increase in size, but become smaller in total volume as indicated by the shoulder in Figure 3.36 for the largest pores at slightly larger than 1 micron. A likely interpretation of this behavior is that the pores inside the black liquor salt mixture become connected and merge with the tri-titanate external pores. This rearrangement is consistent with sintering of the black liquor salts. Finally there are the smallest pores of slightly larger than 0.1 micron in the "black liquor" and "burned" sample. These smallest pores disappear after direct causticization. This behavior may be explained by considering that the trititanate particles are actually agglomerates of smaller solid particles which have a size of about 0.3 micron, and the voids inside these agglomerates are represented by these pores of slightly larger than 0.1 micron. During direct causticization of the trititanate to pentatitanate the molar volume increases significantly and the resulting swelling of the micro particles leads to the disappearance of these smallest pores. Since sintering is mostly associated with shrinkage rather than swelling, the disappearance of these smallest peaks caused by the direct causticization reaction itself, is not responsible for the sintering of the black liquor-trititanate mixture at 700 °C.

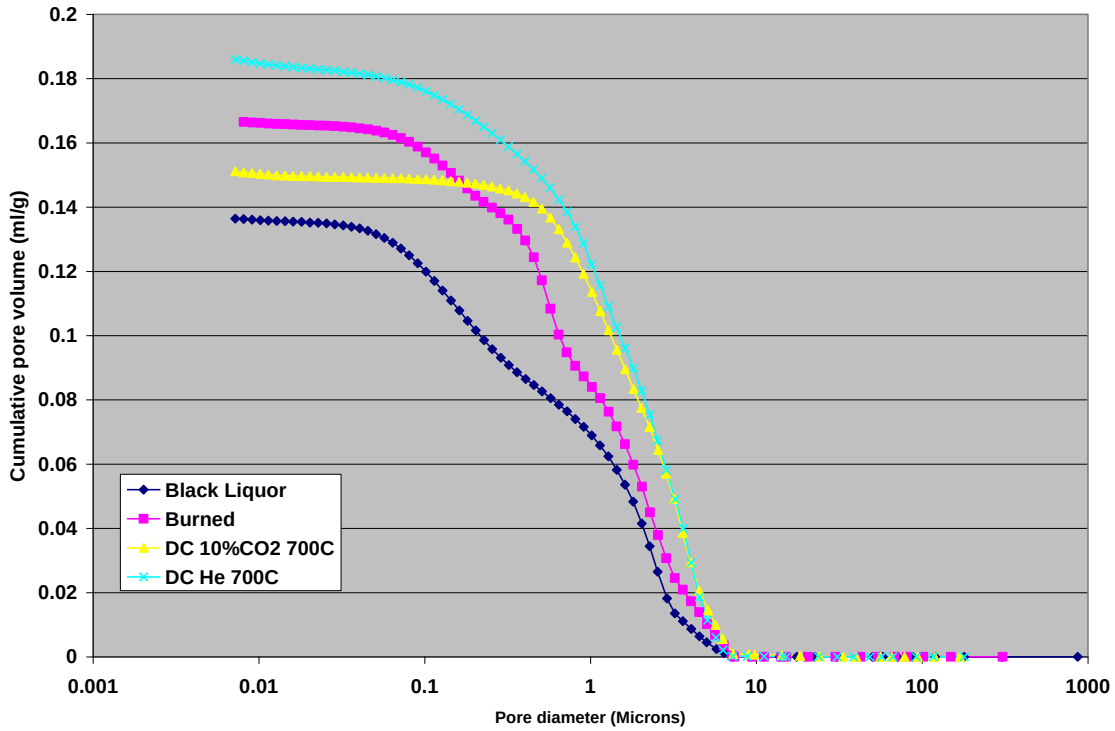

Figure 3.35 Cumulative pore size distribution of trititanate/black liquor samples

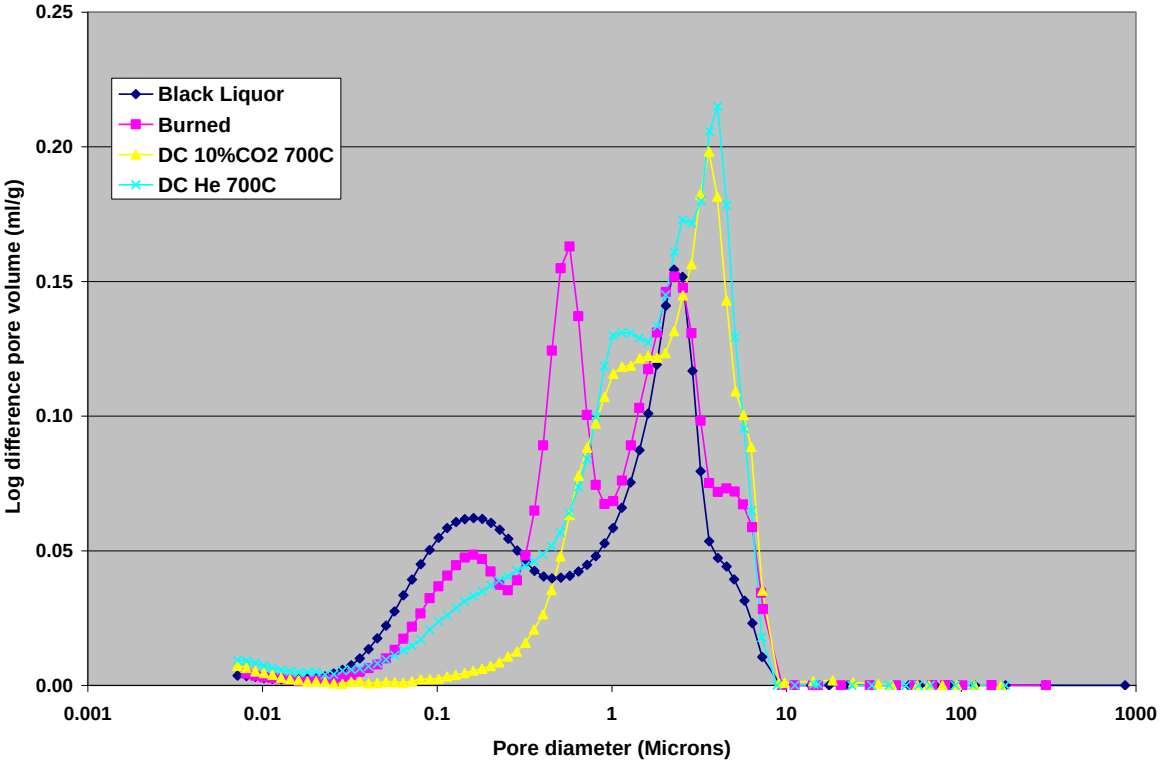

Figure 3.36 Pore size distribution of trititanate/black liquor samples

3.6.5 Quantification of agglomerate strength

The mechanical strength of the free flowing and agglomerated particles were quantified by measuring the load versus displacement of a flat-ended cylindrical probe contacting the samples. The analyzed effects were temperature, pre-pyrolysis, constituent type, and gas type in all cases in conjunction with particle size *d*. The probe has a *D* of 2.92 mm and the height of the sample is 3-5 mm. The test output is the load *P* vs. extension *h* response. Stress *S* is obtained from the ratio of load over area or $P/\pi D^2$. The yield stress (or strength) S_Y is obtained from the end of the linear *S* vs. *h* response. The modulus of elasticity $E = P/Dh$ is obtained from the linear *P* vs. *h* response[103]. The lower limit of S_Y is $2 \cdot 10^4$ Pa (~0.02 atm). Figure 3.37 (taken from many experiments under different conditions) shows that for all analyzed samples there is a strong correlation between both variables with $S_Y \cong 0.3E$.

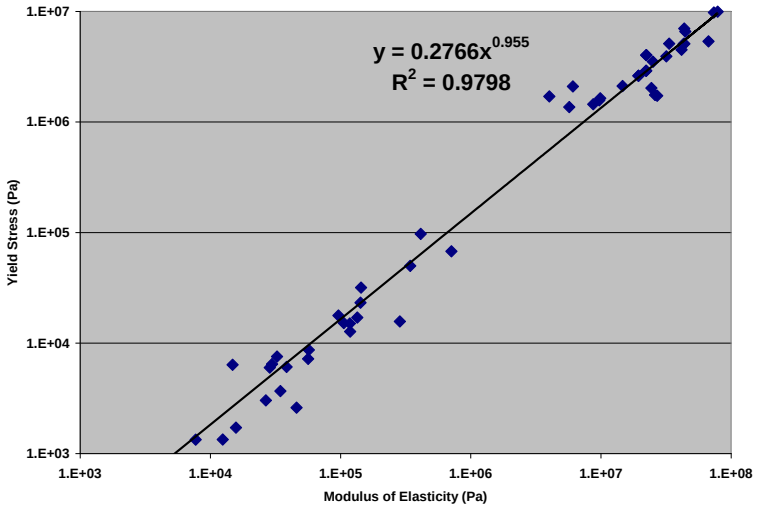

Figure 3.37: Yield Strength vs. Modulus of Elasticity of many experiments under different conditions.

3.6.6 Agglomeration of the BL-$Na_2O \cdot 3TiO_2$ system.

3.6.6.1 Influence of temperature

Experiments with mixtures of BL and $Na_2O \cdot 3\ TiO_2$ with 90-180, 180-425 and 425-710 μm particle size were carried out at different temperatures in a N_2 atmosphere for 1 hr. In these experiments shrinking of the mixtures was noticed for temperatures above 300 °C. Figure 3.38 shows the yield stress vs. temperature of BL-$Na_2O \cdot 3\ TiO_2$ mixture after 1 hr in N_2 for the different particle size ranges. Notice the sharp increase in yield strength (10 logarithmic scale on vertical axis) at around 300 °C. This is attributed to liquefaction/softening of the organic matter without swelling during pyrolysis followed by solidification of the softened organics into a strong char structure, as explained in section 3.6.2. Also notice that, after exposure to higher temperatures, the yield strength increases with decreasing particle size range. The explanation for the latter is that the smaller particles sinter more rapidly, become more densely packed and, ultimately, lead to a stronger structure as compared to powders with larger particles.[104] In contrast, at room temperature the initial mixture of particles exhibit higher yield strength for larger particle sizes, an effect that was always noticed for free flowing powders.

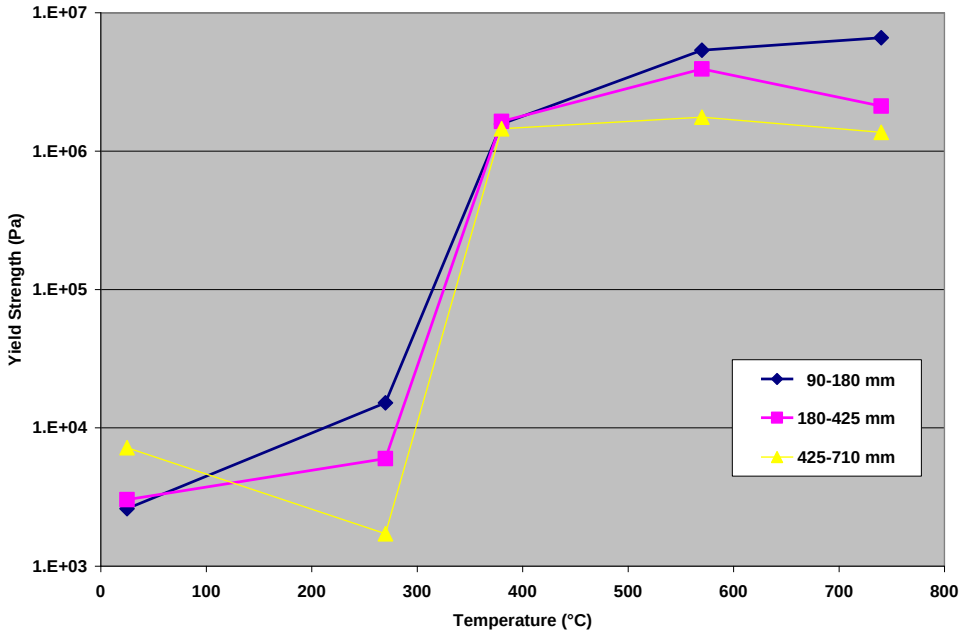

Figure 3.38: Yield Strength vs. Temperature of BL-$Na_2O{\cdot}3TiO_2$ mixture after 1 hr in N_2 for different particle size.

Figure 3.39 shows the stains remaining in the alumina trays after removal of the BL-$Na_2O{\cdot}3TiO_2$ mixtures exposed to 360 and 520 °C in N_2. Notice that the stains are stronger at the higher temperature and particle size range. This effect was always noticed for experiment with solids containing BL. In most of these cases the walls had to be scraped to remove adhered particles and the stains had to be burned off in a muffle furnace at 525 °C since they would not wash off with water. Again, these observations agree with the agglomeration mechanism described above.

Figure 3.39 BL stains on alumina trays from BL-$Na_2O{\cdot}3TiO_2$ mixtures after 1 hr in N_2 at 520 °C and 360 °C for top and bottom row respectively, and from left to right for 90-180, 180-425, and 425-710 μm particle size range respectively.

3.6.6.2 Influence of pyrolysis gas atmosphere

Figure 3.40 shows the yield strength vs. particle size of BL-$Na_2O{\cdot}3\ TiO_2$ (BL+3Tit) after 1 hr at 580 °C under different gas streams with N_2 as carrier gas. The curve noted as "BL+3Tit Premoist 5min" was obtained under an atmosphere of 3% H_2O for 5 min prior to heat up, and under pure N_2 for the rest of the experiment. Notice that the yield strength is higher for cases where the pyrolysis gas is different from pure N_2. This means that, in general, the presence of CO_2 or H_2O (gasification gases) may slightly increase the agglomeration strength during pyrolysis. Notice also that these gases make the slope of S_Y vs. d more negative, an effect attributable to increased sintering.

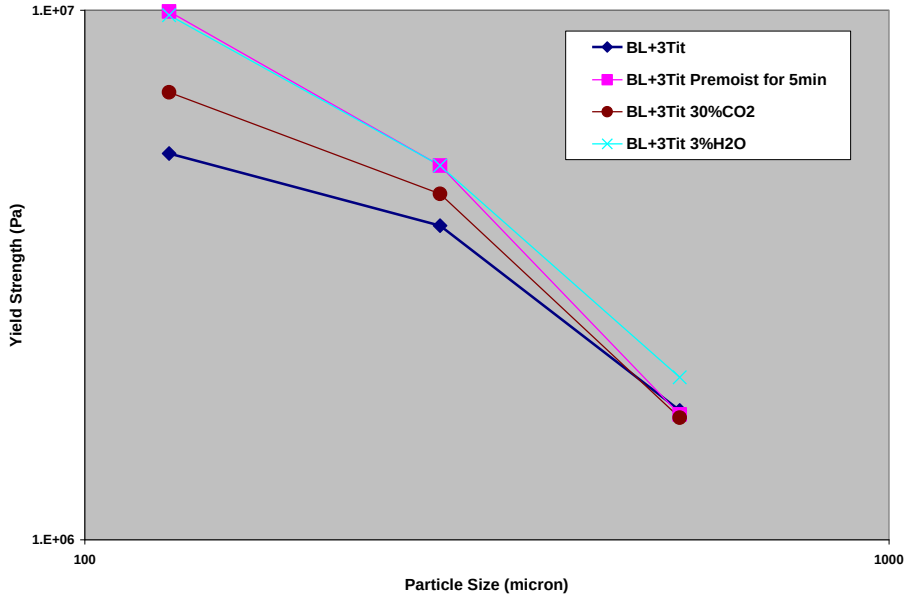

Figure 3.40 Yield Strength vs. Particle Size of BL-$Na_2O{\cdot}3TiO_2$ after 1 hr at 580 °C under different pyrolysis gas streams.

3.6.6.3 Influence of carbon burn-off on agglomeration strength

Figure 3.41 shows the modulus of elasticity vs. particle size for BL-$Na_2O{\cdot}3TiO_2$ in N_2 at 580 °C and in air at 640 °C for 1 hr. The modulus is approximately 1 order of magnitude lower for combustion than for pyrolysis. Although the pyrolysis was done at a lower temperature than the combustion, this should not invalidate the conclusion since the yield strength in Figure 3.38 shows no significant change from 580 to 730 °C. Thus the significant lower agglomerate strength for the case of combustion is due to burn-off of the OC that binds the particles together.

3.6.6.4 Influence of pure components

Figure 3.42 compares the modulus of elasticity of pure components after being exposed to high temperature in N_2 for 1 hr. Indulin C, which is precipitated kraft lignin from Mead-Westvaco, was used to represent the behavior of lignin because it did not exhibit swelling at temperatures above 520 °C. In contrast, Indulin AT, which is Indulin C with sodium removed by leaching, resulted in significant swelling. As can be seen Indulin C (at 580 °C) has the highest strength (3 orders of magnitude above free flowing particles. Next comes Na_2CO_3 (at 740 C) for which the

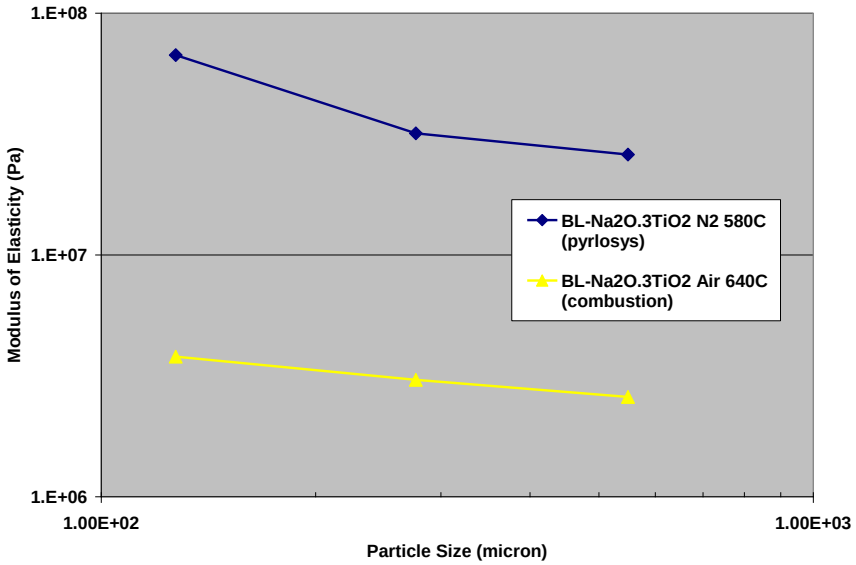

Figure 3.41 Modulus of elasticity vs. particle size for BL-$Na_2O{\cdot}3TiO_2$ in N_2 at 580 °C and in air at 650 °C.

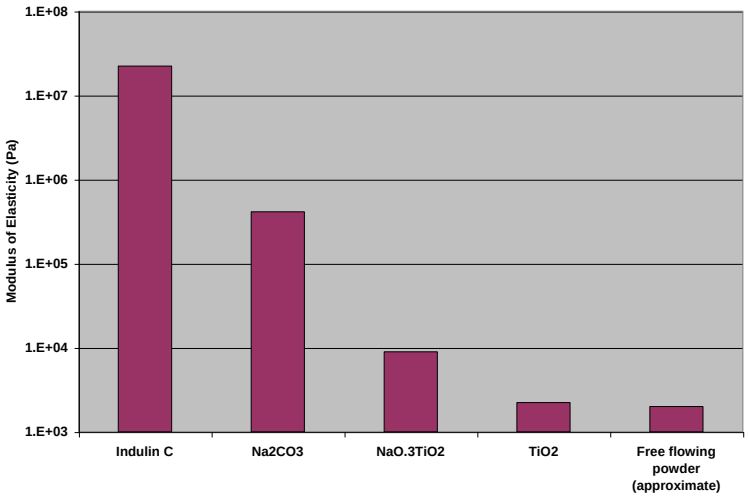

Figure 3.42: Modulus of Elasticity of pure components and of the upper limit of the investigated free flowing powders of 90-180 μm particle size. Indulin C at 580 °C, and Na_2CO_3, $Na_2O{\cdot}3TiO_2$ and TiO_2 at 740 °C. All except free flowing powder after 1 hr in N_2.

agglomeration strength is still 2 orders of magnitude larger than with free flowing powders. Then come $Na_2O{\cdot}3TiO_2$ and TiO_2 (at 740 °C) with TiO2 exhibiting very little increase in strength.

Materials usually start to sinter at temperature ranging between ½ and one times the melting point T_M expressed in K. Either measure is a good rough indicator of sintering tendency. Table 3.14 lists the melting point and ½ melting point for materials of Figure 3.42. The melting point of Indulin C was taken from a reference showing the results of the thermal gravimetric analysis

of a kraft lignin.[105] Notice that the order of decrease in strength in Figure 3.42 corresponds well with an increase in the melting point. Sintering occurs while the inorganic compounds are in the solid phase, while Indulin C proceeds through a liquid phase and then solidifies again.

Constituent	Melting point (°C)	½ Melting point (°C)
Indulin C	440	84
Na_2CO_3	858	293
$Na_2O.3TiO_2$	1130	429
TiO_2	1840	784

Table 3.14: Melting points and ½ melting points of main constituents.

3.6.6.5 Influence of gasification gas atmosphere on sintering of pure components

Figure 3.43 shows the yield strength vs. particle size of several inorganic compounds under N_2 and steam atmospheres for 1 hr at 740 °C and for free flowing particles. The sample of $4Na_2O{\cdot}5TiO_2$ corresponds to a mixture with ~60% purity, where the rest is mostly $Na_2O{\cdot}3TiO_2$ plus impurities. Al_2O_3 was included because it was used by MTCI fluid bed material. Notice that the slope of S_Y vs. d for Al_2O_3 after 740 °C in 3% H_2O remains the same as that of free flowing powders indicating that there is no sintering of Al_2O_3 during this treatment. In contrast, the slope of TiO_2 and that of Na_2CO_3 changes from being positive for free flowing powder to negative after heating treatment, indicating sintering. Thus all constituents in BL + titanates and in particular Na_2CO_3 undergo sintering. However no sintering is observed for Al_2O_3.

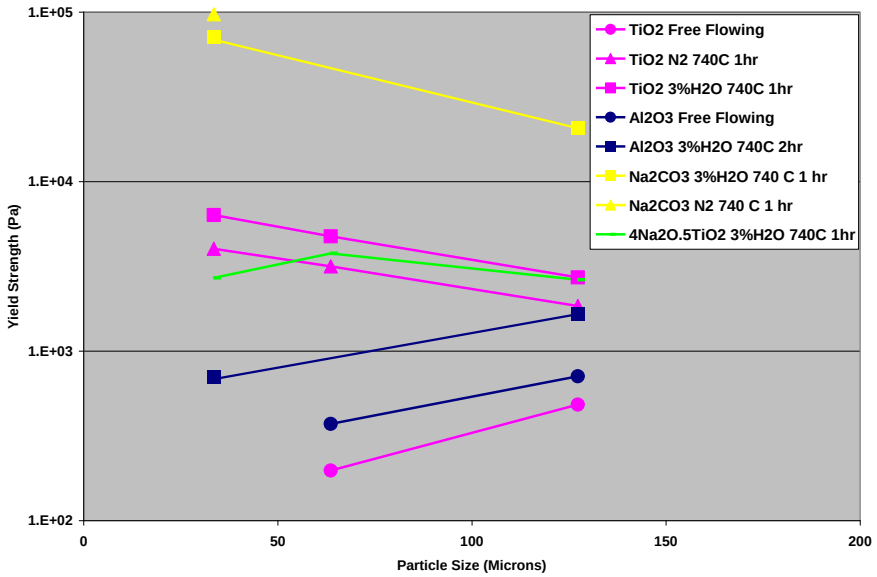

Figure 3.43 Yield Strength vs. Particle Size of pyrolyzed inorganic compounds under different conditions.

3.6.7 Influence of pre-pyrolysis of mixture of BL and $Na_2O{\cdot}3\ TiO_2$

A mixture of BL and $Na_2O{\cdot}3\ TiO_2$ was pyrolyzed at 550 °C for 1 hr. After pyrolysis, the solids were reground and separated into the standard particle size ranges to be subjected to heat treatment in N_2 for 1 hr. Figure 3.44 shows the yield strengths vs. particle size of the BL-$Na_2O{\cdot}3\ TiO_2$ particle mixture before and after 1 hr in N_2 at 580 °C, and the pre-pyrolyzed BL-$Na_2O{\cdot}3\ TiO_2$ particle mixture after 1 hr in N_2 at 580 °C. It can be seen that the pre-pyrolyzed mixture has much lower yield strength than the un-pyrolyzed one. The pre-pyrolyzed heat treated particles showed little agglomeration and microscopy observations revealed that there was almost no neck growth. In contrast, microscopy observations with un-pyrolyzed samples showed neck grew to almost the same size as the parent particles. All observations support that softening of the organics in black liquor is needed to connect the particles and form necks between them. Although the strength of pyrolyzed samples is still about an order of magnitude larger than that of free flowing powders, the increase in strength with increasing particle size suggest that the pre-pyrolyzed mixture still behaves as "free-flowing" after treatment at 580 °C.

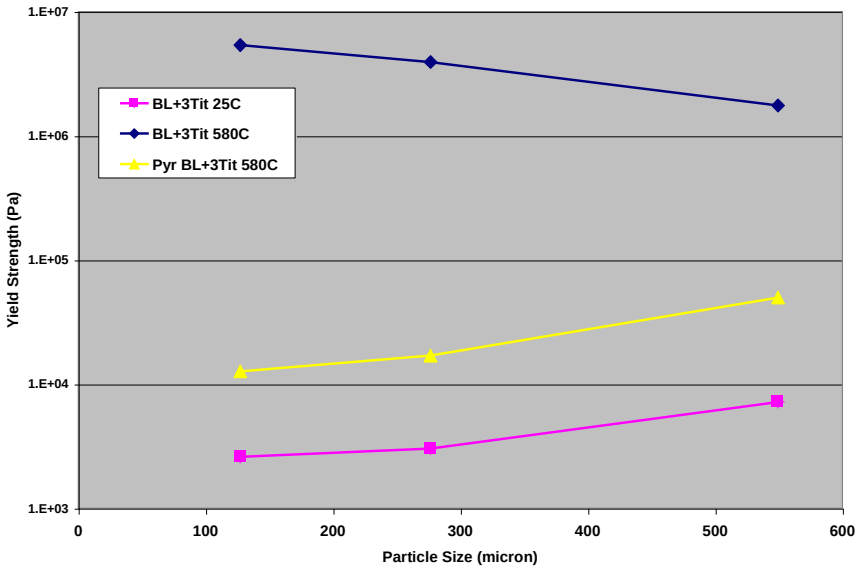

Figure 3.44 Yield Strength vs. Particle Size of free flowing BL-$Na_2O{\cdot}3TiO_2$ and after 1 hr in N_2 at 580 °C, and pre-pyrolyzed BL-$Na_2O{\cdot}3\ TiO_2$ after 1 hr in N_2 at 580 °C.

3.6.8 Effect of mixing of BL with large size (mm) TiO_2 particles

Figure 3.38 shows that the strength of BL-$Na_2O{\cdot}3TiO_2$ agglomerates diminishes with increasing particle size. This suggests that defluidization in a fluidized bed process could be diminished by enlarging the size of the titanate particles injected in the bed. However, the degree of contact between BL penetrates and the titanate particles will decrease with particle size. To test this, TiO_2 of mm size particles were mixed with weak BL in a similar way as was done for the BL - $Na_2O{\cdot}3TiO_2$ mixtures described above. After drying, the particles were cleaved and examined microscopically. Figure 3.45 shows that both phases remain completely separated. Therefore, it is not recommended to use titanate particles of large size.

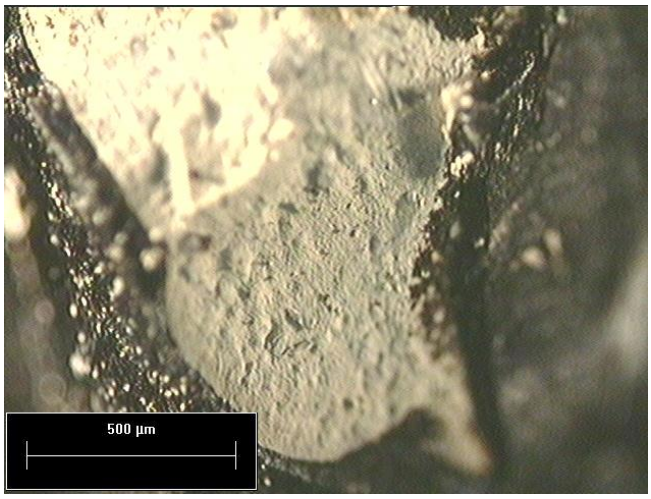

Figure 3.45: Micrograph of a sliced millimeter sized TiO_2 particle coated with BL.

3.6.9 Modulus of elasticity of different samples

Figure 3.46 compares the modulus of elasticity vs. particle size for different powders heated at 550°C and 740°C in N_2 carrier gas for 1 hr. It can be seen that the modulus of elasticity of the BL-$Na_2O{\cdot}3TiO_2$ agglomerates is three or two orders of magnitudes larger than Na_2CO_3 particles or pre-pyrolyzed BL-$Na_2O{\cdot}3TiO_2$ mixtures respectively. The decreasing modulus with increasing particle size indicates modest sintering for Na_2CO_3. Sintering of pure TiO_2, $Na_2O{\cdot}3TiO_2$, $4Na_2O{\cdot}5TiO_2$ and $CaCO_3$ (also used in MTCI tests) is minimal as indicated by the low and increasing modulus of elasticity with increasing particle size. This confirms that softening/liquefaction of black liquor solids (BLS) during pyrolysis of the organics starting at around 300 °C followed by solidification to a char at higher temperature is the major mechanism responsible for agglomeration in the present BL-titanate system. A contributing factor to the strength of the BL-titanate agglomerates is that black liquor does not swell during pyrolysis in admixture with titanates, resulting in strong carbon bridges between the titanate particles. This may also partly explain why low temperature (600 °C) steam reforming of black liquor without titanate does not experience defluidization. In this case the strong swelling of black liquor leads to fragile carbon bridges between Na_2CO_3 particles which can be broken by shear forces in the fluid bed.

3.6.10 Conclusion.

Softening/liquefaction of black liquor solids (BLS) during pyrolysis of the organics starting at around 300 °C followed by solidification to a char without swelling is the major mechanism responsible for agglomeration in the present BL-titanate system. The liquefied black liquor solids pull the titanate particles together by capillary forces, and after resolidification the dense residual char forms strong bridges between the particles. Although most of the carbon is subsequently consumed, solid-phase sintering of Na_2CO_3 in particular at temperatures above 600 °C will retain the strength of the agglomerates. The present results suggest that agglomeration may be prevented or diminished by separately pre-pyrolysing the black liquor or by adding Al_2O_3 particles respectively. It was found that Al_2O_3 particles do not sinter.

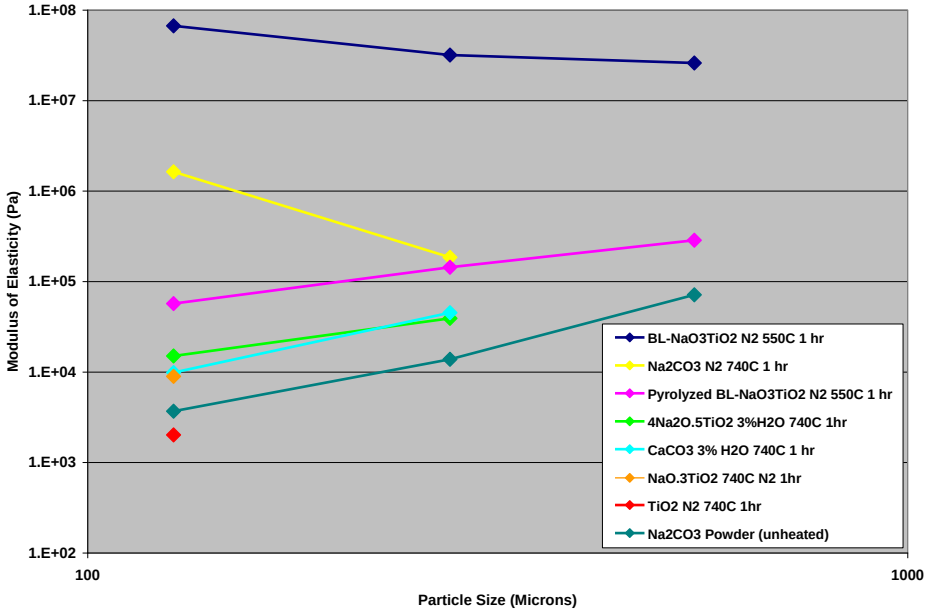

Figure 3.46 Modulus of elasticity versus particle size of different samples.

4. TASK 3 – PDU TESTING

This project comprises tasks pertaining to testing the combined steam reforming and titanate direct causticization process in the Process Development Unit (PDU) of MTCI/ThermoChem. Guided by the bench scale titanate work at the University of Maine (UM), the operating conditions and mill liquor compositions will be defined for several long duration (5 to 10 day) gasification tests.

4.1 Objectives

The objectives of the PDU tests are to verify performance and operability of the combined technology of steam reforming and direct causticization of black liquor, optimize the design and pave the way for mill integration.

4.2. Test Facility modification

A new test unit was fabricated in order to achieve the maximum temperature (1400 F or 760 °C) required for this project. Figure 4.1 shows the new reactor vessel with two liquor injection ports, instrumentation ports and a bottom bed drain.

The modified test facility is shown in Figure 4.2. It consists of the following:

- Steam reformer (electrically heated),
- Steam supply subsystem (water metering pump, evaporator and superheater),
- Sintered metal filter to capture fine particles,
- Impingers immersed in a water bath to drop out condensables from the product gas stream,
- Black liquor/slurry feed subsystem,
- Fluidization gas preheater for optional fluidization gas feed to the reformer, and
- Instrumentation and controls.

Figure 4.3 shows some of the components of the system.

4.3 Feedstock preparation

A kraft black liquor (BL) received from a U.S. pulp mill was employed as feedstock. The as received solids concentration ranged from 48% to 65% by weight depending on the batch. For the test runs, a slurry comprising black liquor and TiO_2 (Dow Chemical Company) was prepared. For the initial test, the mass ratio of TiO_2 to black liquor solids (BLS) was 0.55. For the subsequent tests, a higher mass ratio i.e. 1 was employed. The solids concentration of the as fed slurry ranged between 45 and 50% by weight. The chemical composition of the liquor and black liquor-TiO_2 slurries will be discussed in section 4.5.1.

4.4. Steam reforming and direct causticization testing

4.4.1 Operational procedure

In each case, the bed was warmed up to operating temperature with nitrogen as fluidization medium. Then water flow to the boiler was started and increased gradually with a corresponding decrease in nitrogen flow until the mole fraction of steam in the fluidization medium reached the 85 to 90% level. The liquor injectors were initially supplied with hot water and the bed electrical heater settings were fine tuned to maintain the dense bed at the desired operating temperature.

Figure 4.1. New reactor vessel

Figure 4.2. Modified Test facility

The black liquor / TiO2 slurry was kept warm in a stirred pot and upon achieving stable and uniform bed temperatures, the injectors were switched from water to the slurry. In all cases the slurry feed rate was about 42 cc/min or between 7.5 and 8 lb/h.

4.4.2. Results and discussion

Three shakedown tests were performed and a summary of the test conditions is provided in Table 4.1. In shakedown test # 1, the dense bed temperatures (3 thermocouples at different dense bed elevations above the distributor) started to diverge after about 45 minutes of slurry feed. Attempts were made to increase and/or pulse the fluidization medium flow but the bed temperatures continued to diverge and the fluid bed pressure fluctuations continued to decline. This signaled bed agglomeration and therefore the slurry feed was stopped after a little more than one hour into the test. Samples of the final bed and the filter catch are shown in Figure 4.4. The bed agglomerates ranged in size from corn to a baking potato. It was hypothesized that the simplistic design of the two injectors (each was a ¼-inch tube with connection to slurry and nitrogen purge) may have contributed to the formation of agglomerates due to drip-type flow. A significant transfer of bed material to the filter was noticed and attributed to a relatively large fraction of fines in the initial limestone charge. Carbon fines were also noticed in the filter catch.

Figure 4.3. Selected system components.

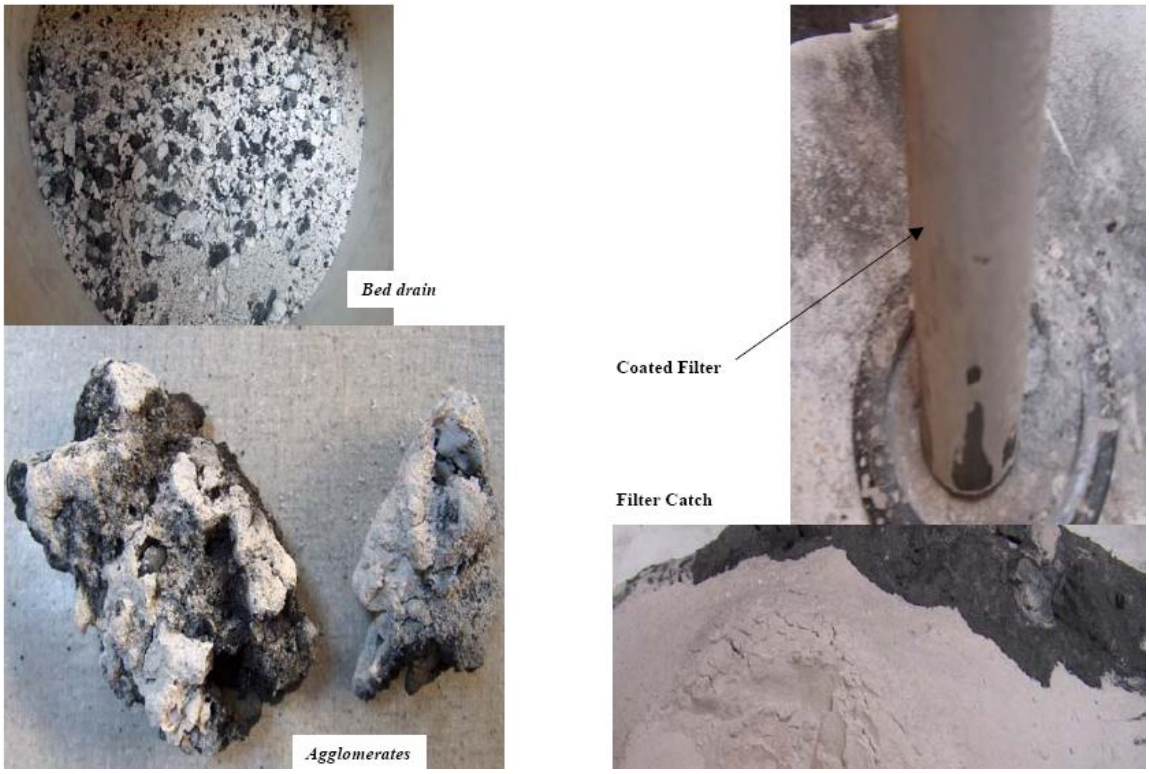

Figure 4.4. Samples from bed and filter in test #1

Table 4.1 Conditions of Test 1, 2 and 3

	Test #		
Parameter	**1**	**2**	**3**
Distributor plenum pressure, psig	5.5	8.8	6.0
Freeboard pressure, in WC	23	36	32
Filter exit pressure, in WC	13	15.5	16
Distributor plenum temperature, F	1,075	1,220	1,171
Fluid bed mean temperature, F	1,348	1,300	1,200
Freeboard temperature, F	1,311	1,249	1,134
Filter exit temperature, F	494	507	501
Fluidization:			
N2 flow rate, lb/h	0.81	0.79	7.17
Steam flow rate, lb/h	2.90	4.76	-
Steam mole fraction in the blend	0.85	0.90	-
Initial bed	Limestone, as received	Limestone, double screened	Final bed from test # 2 and Limestone, double screened
Initial bed charge, lb	15.94	15.40	11.5
bed bulk density, lb/ft^3	101.7	93.6	90.9
surface-mean particle size, microns	239	305	297
Mean superficial fluidization velocity, ft/s	0.67	1.01	0.83
Feedstock	kraft black liquor / TiO2 mixture	kraft black liquor / TiO2 mixture	kraft black liquor / TiO2 mixture
Mass ratio of TiO2 to Black Liquor Solids	0.55	1	1
As fed slurry solids concentration	49.1%	48.6%	46.3%

A modified injector was developed to atomize and inject the slurry into the bed. It was a tube within a tube design and incorporated a flattened injection end to facilitate a spray pattern. Satisfactory atomization without dripping was obtained as shown in Figure 4.5.

A second shakedown test was performed with double screened limestone as starting bed and the modified liquor injectors. The TiO_2 concentration in the slurry was increased to a 1:1 mass ratio with black liquor solids. The bed temperature was decreased to 1300 F. The gas composition is shown in Table 4.2. The product gas composition looks good with a relatively high concentration of hydrogen and a relatively low concentration of hydrocarbon species. The H_2S concentration is low, representing a sulfur release from black liquor of about 20%. This due to capture of H_2S by (calcined) limestone to CaS. This time the test had to be terminated after almost one hour of slurry feed due to both injectors plugging. Samples of the initial bed, final bed and filter catch are shown in Figure 4.6. The final bed sample indicates some growth into particle clusters but no big agglomerates. This validates the importance of slurry atomization. Nevertheless there seems

Figure 4.5. Modified slurry atomizer

Table 4.2. Gas composition during test #2

Component	Vol%
Hydrogen	61.24%
Oxygen	0.00%
Nitrogen	0.00%
Methane	2.55%
Carbon Monoxide	3.53%
Carbon Dioxide	32.16%
Ethylene	0.10%
Ethane	0.10%
Acetylene	0.01%
Hydrogen Sulfide	0.32%
Propylene	0.00%
Propane	0.00%

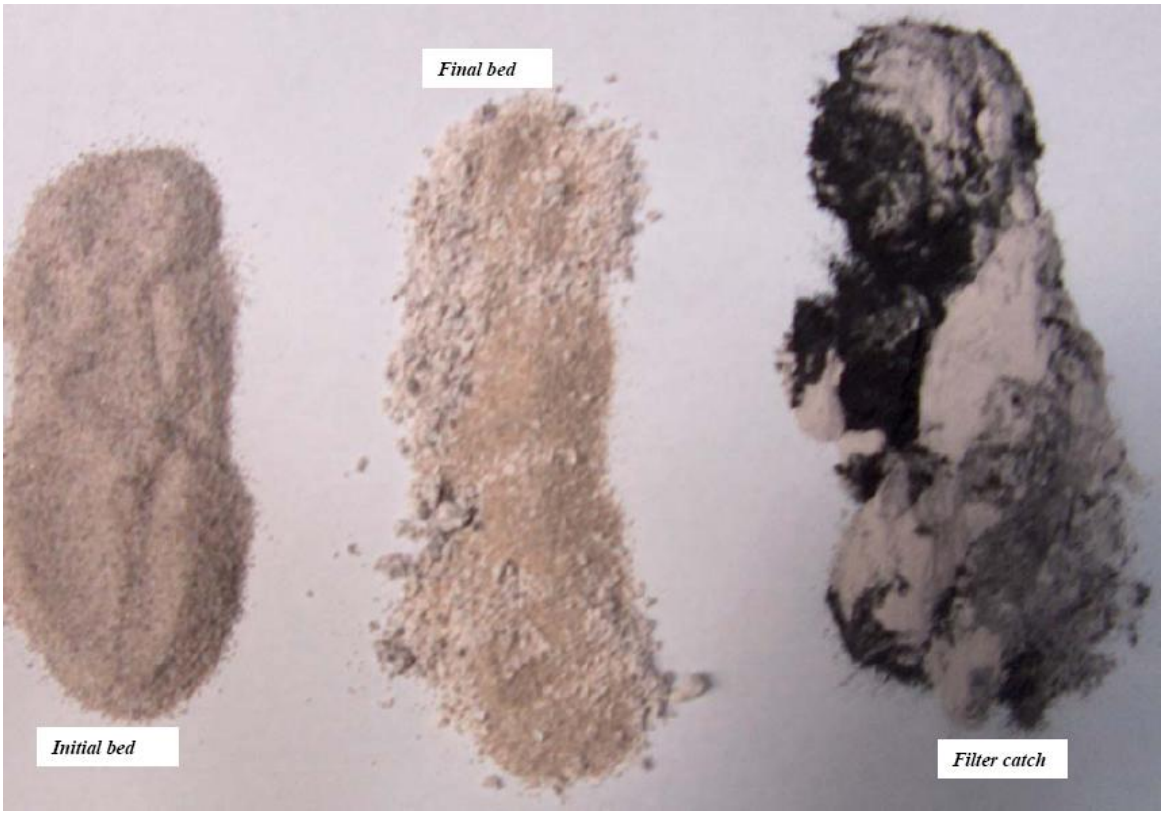

Figure 4.6. Samples from test #2.

to be a tendency for agglomeration albeit at a smaller scale. Again a significant amount of bed material transferred to the filter. This was attributed to a lack of a cyclone separator in the product gas path. Again carbon fines were noticed in the filter catch and attributed to once-through mode of operation (no recycle) and very short residence time in the hot section.

Because of the plugging of the injectors, the design was modified by eliminating the flattened end and by making a provision for steam purge in addition to the N_2 purge. An internal cyclone separator was designed, fabricated and incorporated into the reformer outlet flange. A third shakedown test was run with double screened material (final bed from test # 2 and limestone) and N_2 fluidization. The bed temperature was reduced to 1200 F to promote limited carbon build-up in the bed to deter agglomeration and to hinder limestone calcination and sulfidation. This time the bed thermocouple readings started to diverge rapidly to ~100 F. Water flows to the boiler as well as to the injectors were stopped and the N_2 fluidization flow was increased. The bed temperature differentials decreased and slowly declined to within 15 F. With only N_2 fluidization and the bed temperature averaging ~1200 F, slurry feed was restarted. Within minutes, the bed thermocouple differentials diverged to ~100 F. The bed bottom pressure showed decreasing pulsations and became stationary at a mean value of 50 inch water column. The unit was shut down and material retrieved as in the previous test. Samples of the final bed are shown in Figure 4.7. The final bed included agglomerates ranging in size from a peanut to a lemon. The agglomerates are dark in colour suggesting the presence of unconverted carbon. In this test the lower temperature seems to enhance agglomeration even in the presence of carbon. Once again, a significant transfer of material from the dense bed to the filter was noticed.

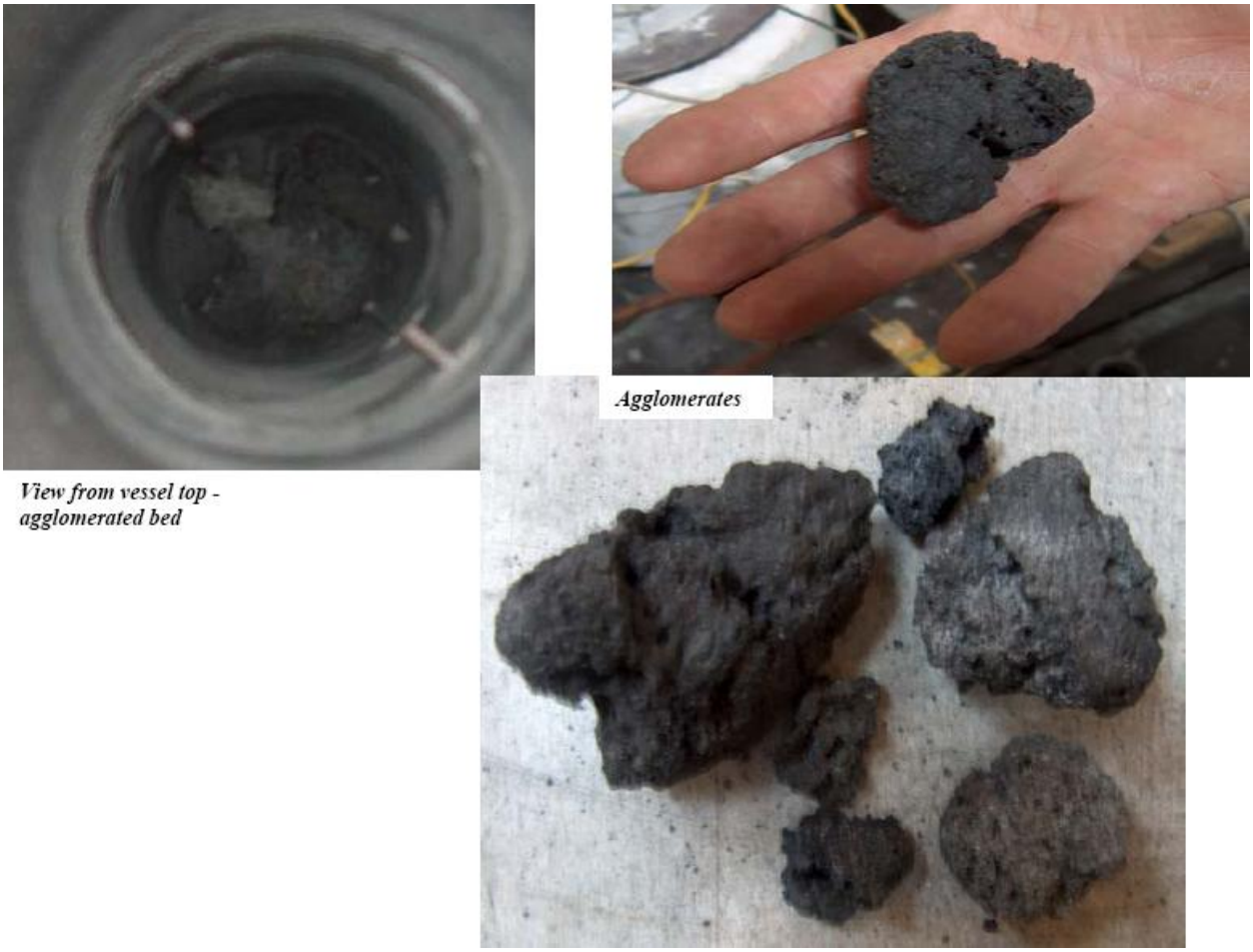

Figure 4.7. Bed samples from test #3

To eliminate the sulfur capture by the initial lime stone bed, the fourth test was performed with TiO_2 granules supplied by Dr. van Heiningen as the starting bed material. The sieve analysis indicated a surface-mean size of the TiO_2 particles of 216 microns. The particles are agglomerates of submicron sized primary particles which attrite with handling. The cyclone was modified by incorporating a trickle-type valve at the dipleg exit to achieve satisfactory cyclone performance. A summary of the test conditions and gas composition is provided in Table 4.3. The TiO_2 concentration in the slurry was 1:1 in mass ratio with black liquor solids. The slurry feed rate was about 25 cc/min or ~5 lb/h. After about 35 minutes of run time with the slurry feed, the bed thermocouple differentials started to diverge. The unit was shut down and the final bed sample indicated some growth into particle clusters but no big agglomerates. The agglomerates are slightly dark in color suggesting the presence of unconverted carbon. The product gas composition in Table 4.3 looks good with a relatively high concentration of hydrogen and a much higher H_2S concentration suggesting a substantial portion of sulfur release from the liquor.

Table 4.3: Test Conditions and gas composition of Test #4

Parameter	**4**
Distributor plenum pressure, psig	5.3
Freeboard pressure, in WC	29
Filter exit pressure, in WC	16
Distributor plenum temperature, F	1,070
Fluid bed mean temperature, F	1,349
Freeboard temperature, F	1,246
Filter exit temperature, F	435
Fluidization:	
N2 flow rate, lb/h	1.50
Steam flow rate, lb/h	3.97
Steam mole fraction in the blend	0.80
Initial bed	TiO2 granules, as received
Initial bed charge, lb	6.80
bed bulk density, lb/ft^3	60.5
surface-mean particle size, microns	216
Mean superficial fluidization velocity, ft/s	0.97
Feedstock	kraft black liquor / TiO2 mixture
Mass ratio of TiO2 to Black Liquor Solids	1
As fed slurry solids concentration	47.9%

Component	**Vol%**
Hydrogen	60.65%
Oxygen	0.00%
Nitrogen	0.00%
Methane	3.30%
Carbon Monoxide	5.63%
Carbon Dioxide	28.41%
Ethylene	0.22%
Ethane	0.22%
Acetylene	0.05%
Hydrogen Sulfide	1.52%
Propylene	0.00%
Propane	0.00%
HHV, Btu/SCF dry basis	267

Two more tests were performed and a summary of the test conditions is provided in Table 4.4. Both tests were performed with the G-P Big Island demonstration unit bed material as the starting bed. The particles appeared relatively round and a sieve analysis indicated the surface-mean size to be 353 microns. The first test was performed with a Na_2CO_3 / TiO_2 slurry (~42% solids, with Na_2CO_3 / TiO_2 mass ratio of 1:0.94:1) to simulate pentatitanate i.e. $4Na_2O.5TiO_2$ behavior in the fluid bed. The objective was to evaluate fluid bed operability, specifically bed agglomeration and fines generation. The slurry feed rate was about 60 g/min or ~8 lb/h. With slurry feed, the reactor backpressure gradually increased from ~1.5 psig to 12.5 psig in about 45 minutes. The bed temperature differentials also started to diverge. The unit was shut down and material retrieved. The cyclone was partly plugged, the filter was mostly plugged with a 20-mm thick dust cake and the filter bypass line was clogged with solids. Samples of the final bed and filter catch were collected. The final bed sample indicated some growth into particle clusters but no big agglomerates. All material appeared gray with many white particles in the bed material.

The second test (test # 6) was run with the same starting bed as in the previous test but with no feed to investigate the origin of the fines. The bed was fluidized with only nitrogen to avoid smelt formation/agglomeration in the absence of causticization reactions. The bed operation was stable and smooth with the bed thermocouples all reading within 1 F. The reactor backpressure also remained low and constant. The filter pressure drop was small as well. After more than 2h of steady operation, the unit was shut down and material retrieved as in the previous test. Samples of the final bed and filter catch were collected. The final bed sample indicated no growth into particle clusters or agglomerates. The filter catch was negligible (2 g) and proved that bed attrition was insignificant. This confirmed that the slurry and in particular TiO_2 is the source of fines.

Table 4.4 Conditions of tests 5 and 6

Parameter	Test # 5	Test # 6
Distributor plenum pressure, psig	5.0 – 15.0	3.5
Freeboard pressure, in WC	27+	12
Filter exit pressure, in WC	12	7.5
Distributor plenum temperature, F	1,335	1,232
Fluid bed mean temperature, F	1,347	1,354
Freeboard temperature, F	1,175	1,039
Filter exit temperature, F	367	350
Fluidization:		
N2 flow rate, lb/h	2.86	12.01
Steam flow rate, lb/h	3.70	-
Steam mole fraction in the blend	0.67	-
Initial bed	GP Big Island bed material	GP Big Island bed material
Initial bed charge, lb	6.50	6.00
Bed bulk density, lb/ft^3	66.0	66.0
Surface-mean particle size, microns	353	353
Mean superficial fluidization velocity, ft/s	1.09	1.67
Feedstock	Na2CO3 solution / TiO2 mixture	-
Mass ratio of TiO2 to Na2CO3	94.3%	-
As fed slurry solids concentration	42.0%	-

Four additional tests (#7 – 10) were performed and a summary of the test conditions and product gas data are provided in Tables 4.5 and 4.6 respectively.

A successful test (#7) in batch mode was performed in the PDU with solids sent by the University of Maine after pyrolysis of a mixture of kraft black liquor and titanium dioxide. The test was run with a Chevron type particle separator in the freeboard. The average bed temperature was 1,350 F, the fluidization medium was steam plus N_2, and the fluidization velocity was approximately 1.3 ft/s. The operation was stable and the bed thermocouples were reading close to each other except in the end when they started to diverge by 6 to 8 F due to carbon depletion. The GC data indicated that the initial product gas corresponded to about 39% H_2, 38% N_2, 8% CO, 14% CO_2, 1% H_2S and trace organics, all on a dry basis. Towards the end, the H_2, CO_2 and CO all approached single digit or near zero. After about 2h45min of steam reforming the test was terminated due to carbon depletion and tapering off of reforming reactions. This successful run with no sign of agglomeration or operational problems confirms that a pre-pyrolysed mixture of kraft black liquor and titanium dioxide eliminates defluidization, and supports the agglomeration mechanism proposed by the University of Maine.

This test (# 8) was performed with GP Big Island bed material as starting bed. The system was heated up on N_2 to about 1,350 F. The previously prepared and warmed feed (kraft BL+TiO_2 slurry) was started and immediately the water feed to the online boiler and superheater were turned on. The water feed was quickly increased to the maximum level that the pump could handle. The N_2 flow rate was slightly reduced to maintain a superficial fluidization velocity of about 2.5 ft/s. A rather high (both in backpressure and flow rate) N_2 purge on the injector was maintained to avoid plugging. The system appeared to perform well with rather uniform bed temperatures (all 3 thermocouple readings within 1 F) and reasonable product gas composition. The system backpressures were higher than normal and were attributed to the rather high operating velocity. It was planned to run a 4h test but after a little over 2h into the test, the slurry feed pump. So the test had to be terminated. When the unit was opened the next day, the bed material had a beautiful burgundy color; while the particle separator (baffles or chevron) in the freeboard was plugged with a disk-type agglomeration was observed about 8 inches below the chevron (see Figure 4.8). This agglomeration was very hard and very difficult to dislodge. Interestingly, the agglomeration occurred in the freeboard and not in the dense bed. Due to the high operating velocity and the attendant attrition the solids carry over was high. The filter had a coating of fines and a significant collection of particles in the housing. The product gas composition suggests incomplete carbon conversion and sulfur release. The short gas and solids residence times and the rapid elutriation are probably the cause. Obviously, this set of operating conditions is unsatisfactory.

Table 4.5 Conditions for tests # 7 - 10

Parameter	Test # 7	Test # 8	Test # 9	Test # 10
Distributor plenum pressure, psig	3.8	8.4	5.4	8.8
Freeboard pressure, in WC	14	75	32	92
Filter exit pressure, in WC	9	21	18	14
Distributor plenum temperature, F	1,109	1,174	1,205	1,248
Fluid bed mean temperature, F	1,353	1,351	1,343	1,352
Freeboard temperature, F	1,200	1,319	1,301	1,241
Filter exit temperature, F	422	520	512	552
Fluidization:				
N2 flow rate, lb/h	2.72	13.40	3.80	7.69
Steam flow rate, lb/h	4.20	4.50	4.50	4.50
Steam mole fraction in the blend	0.71	0.34	0.65	0.48
Initial bed	Pyrolyzed BL + TiO2 solids	G-P Big Island bed material	Alumina Oxide	Alumina Oxide
Initial bed charge, lb	13.45	13.23	17.64	16.53
bed bulk density, lb/ft^3	69.9	66	122.0	122.0
surface-mean particle size, microns	233	353	239	239
Mean superficial fluidization velocity, ft/s	1.28	2.48	1.41	1.71
Feedstock	-	kraft black liquor / TiO2 mixture	kraft black liquor / TiO2 mixture	kraft black liquor / TiO2 mixture
Mass ratio of TiO2 to Black Liquor Solids	-	1	1	1
As fed slurry solids concentration	-	62.6%	45.0%	43.8%
Slurry Feed rate, lb/h		5.00	6.20	6.74

Table 4.6: Product Gas Composition Tests # 7 - 10 (dry basis)

	Test # 7			Test # 8	Test # 9	Test # 10
	From the start of the test					
	26 min	87 min	148 min			
Component	**Vol%**	**Vol%**	**Vol%**	**Vol%**	**Vol%**	**Vol%**
Hydrogen	62.43%	65.48%	75.55%	59.95%	59.24%	58.89%
Oxygen	0.00%	0.00%	0.00%	0.00%	0.00%	0.00%
Nitrogen	0.00%	0.00%	0.00%	0.00%	0.00%	0.00%
Methane	0.34%	0.16%	0.00%	0.87%	4.96%	2.87%
Carbon Monoxide	12.62%	8.22%	0.94%	13.54%	5.16%	5.92%
Carbon Dioxide	22.83%	25.49%	22.60%	25.12%	29.10%	29.15%
Ethylene	0.00%	0.00%	0.00%	0.00%	0.24%	0.34%
Ethane	0.00%	0.00%	0.00%	0.02%	0.18%	0.25%
Acetylene	0.00%	0.00%	0.00%	0.00%	0.00%	0.00%
Hydrogen Sulfide	1.79%	0.65%	0.91%	0.51%	1.11%	2.57%
Propylene	0.00%	0.00%	0.00%	0.00%	0.00%	0.00%
Propane	0.00%	0.00%	0.00%	0.00%	0.00%	0.00%
HHV, Btu/dscf	258	245	254	251	274	266
Relative Gas Make, volumetric basis	100.0%	93.3%	23.8%			

Figure 6: Agglomeration in the freeboard – one view (test #8)

Based on the operating experience with test #8, it was suggested that alumina be used as bed material. It was hypothesized that the absence of sintering with Al_2O_3 (see Figure 3.43) would afford operational stability. It would be preferable to operate in the turbulent fluidization regime to achieve higher shear forces but this small test unit with short freeboard and less than satisfactory particle separator precludes such operation.

Two tests were performed with alumina particles as the starting bed: the first (test #9) was performed with the chevron or baffle type particle separator. The alumina particles used were No.70 grit, irregularly shaped and non-spherical and a sieve analysis indicated the surface-mean size to be 239 microns. The test seemed to proceed smoothly with slurry (~45% solids) feed; the bed temperature readings were stable and close to each other. There was a gradual increase in system backpressure. At 1h45min into the test, the injector plugged. The test was therefore terminated. The product gas composition was similar to those observed in previous tests. Upon dismantling the unit next day, a significant carryover of particles into the filter was observed. However, there was no evidence of agglomeration.

Test #10 was carried out with alumina grit as starting bed material and the original internal cyclone with a modified trickle valve. The injector was redesigned with an inner tube for slurry and atomization N_2 injection and an outer tube with an annulus for N_2 cooling to prevent overheating of the center tube. The fluid bed operation was satisfactory except for the gradual blinding of the particulate filter and a corresponding increase in system backpressure. After 2h43min into the test with feed, the test was terminated due to bed bottom pressure gage needle moving beyond scale i.e. 150 inch H_2O gage. The unit was shut down and material retrieved. The cyclone dipleg was full, the barrel was about half-full and the trickle valve was stuck suggesting cyclone dysfunction and dust re-entrainment. This was corroborated by the significant particulate collection in the filter and filter housing. Samples of the final bed and filter catch were collected. The final bed sample indicated some growth into small particle clusters (~ 1 mm size) but no clinkers or big agglomerates. All the material appeared gray to black in color and many distinct white particles were seen in the bed material. A majority of the sulfur seems to have been released despite the short gas and solids residence time. All the solids samples were tagged and shipped to the U of Maine for analysis.

Tests #7 - 10 show that there are two possibilities to achieve stable bed operation without agglomeration: (1) pre-pyrolyze the black liquor and titanium dioxide (or tri-titanate) slurry in a separate reactor; collect, cool and grind the residual solids, form a slurry and then feed this slurry into a steam reformer for combined steam reforming and direct causticization. (2) employ an alumina bed in the reformer, feed the black liquor and titanium dioxide (or tri-titanate) slurry, operate the reformer preferably in the turbulent fluidization mode. In both cases efficient internal and/or external cyclones are needed to recycle solids and maximize solids retention time in the reaction environment, and employ efficient scrubbers or metal filters to capture the titanate fines.

Three final tests were performed and a summary of the test conditions and product gas data are provided in Table 4.7 Photographs of the test facility are shown in Figures 17 through 21.

Table 4.7: Conditions and gas composition of tests # 11 - 13

arameter	Test # 11	Test # 12	Test # 13
istributor plenum pressure, psig	10.5	12.5	7.3
reeboard pressure, in WC	140	195	74
lter exit pressure, in WC	15	16	16
istributor plenum temperature, F	1,288	1,183	1,308
uid bed mean temperature, F	1,356	1,360	1,359
reeboard temperature, F	1,236	1,298	1,144
lter exit temperature, F	536	534	571
uidization:			
2 flow rate, lb/h	7.48	9.30	9.30
team flow rate, lb/h	4.50	4.50	4.50
team mole fraction in the blend	0.48	0.43	0.43
itial bed	Alumina Oxide+Sodium penta titanate	Alumina Oxide+Sodium penta titanate	Alumina Oxide+Sodium penta titanate
itial bed charge, lb	15.43	15.43	9.92
ed bulk density, lb/ft^3	110	110.0	68.6
urface-mean particle size, microns	450	365	403
ean superficial fluidization velocity, ft/s	1.55	1.60	2.01
eedstock	kraft black liquor / TiO2 mixture	kraft black liquor / TiO2 mixture	kraft black liquor / TiO2 mixture
ass ratio of TiO2 to Black Liquor Solids	1	1	1
s fed slurry solids concentration	42.0%	42.0%	43.4%
lurry Feed rate, lb/h	5.67	5.67	5.67

Component	Test # 11 Vol%	Test # 12 Vol%	Test # 13 Vol%
Hydrogen	58.22%	60.72%	58.09%
Oxygen	0.00%	0.00%	0.00%
Nitrogen	0.00%	0.00%	0.00%
Methane	2.63%	2.68%	2.80%
Carbon Monoxide	5.21%	5.74%	6.32%
Carbon Dioxide	30.79%	28.28%	29.87%
Ethylene	0.32%	0.30%	0.31%
Ethane	0.24%	0.24%	0.23%
Acetylene	0.00%	0.00%	0.00%
Hydrogen Sulfide	2.59%	2.05%	2.37%
Propylene	0.00%	0.00%	0.00%
Propane	0.00%	0.00%	0.00%
HHV, Btu/dscf	259	265	262

Test #11 was performed in the PDU with double screened (2000 by 150 microns) solids (alumina / sodium penta-titanate mixture) from the previous test. The test was run with an internal cyclone comprising a trickle valve and a counterweight and a single sintered metal particulate collection filter. The average bed temperature was 1,356 F (736 °C). The fluidization medium was steam plus N_2, and the fluidization velocity was approximately 1.55 ft/s. The operation was stable and the bed thermocouples were reading close to each other. The filter backpressure increased with time due to filter pluggage. The N_2-cooled liquor injector performed well. The GC data indicated a product gas with significant H_2, CO_2, CO, H_2S and CH_4 content. After about 2h30min of steam reforming the test was terminated due to filter pluggage and high backpressure. It seemed to be a successful run without agglomeration or operational problems. The 21-inch starting bed however had declined to about a 12-inch high final bed, suggesting excessive solids carryover and poor cyclone performance.

Test # 12 was performed with conditions similar to those in the previous test but with the cyclone counterweight trimmed to achieve a balance point wherein the trickle valve will remain

open when the height of solids in the dipleg exceeded about 2 inches. This was computed to be equivalent to about 6-inches of height with filter catch. The system was heated up on N_2 to about 1350 F (732 °C), the previously prepared and heated feed (kraft BL+TiO2 slurry) was started and immediately the water feed to the online boiler and superheater were turned on. The water feed was quickly increased to the maximum level that the pump could handle. The N_2 flow rate was reduced to maintain a superficial fluidization velocity of about 1.6 ft/s. The product gas composition and the operating characteristics seemed similar to those in the previous test. Again, the test had to be terminated after about 2 h due to filter pluggage and high backpressure. The solids carryover into the filter was again found to be high. It was concluded that the short freeboard and the slugging bed fluidization operating regime result in excessive solids entrainment, overload the cyclone with solids and result in poor performance.

Test # 13) was performed with an additional particulate filter assembly and other test parameters as in test # 12. First only one filter unit was valved online; the fluid bed operation was satisfactory except for the gradual blinding of the particulate filter and a corresponding increase in system backpressure. After 2h into the test with feed, the second filter was valved online as well. The fluid bed operation was smooth; after about 3.5 h into the test, the liquor feed was first increased to 6.2 lb/h and later to 6.74 lb/h to gauge the effect of increased liquor loading on bed operational stability. The operation was stable but the liquor feed pump suddenly became noisy and the piston jammed. The test was consequently terminated. The product gas composition seemed similar to those in the previous two tests. The unit was shut down and material retrieved. The final bed sample indicated no clinkers or agglomerates. All the material appeared gray to black in color and many distinct white particles were seen in the bed material. A majority of the sulfur seems to have been released despite the short gas and solids residence time. All the solids samples were tagged and shipped to the U of Maine for analysis.

4.4.3 Conclusion

The above tests have established the conditions whereby the fluid bed can be operated without bed agglomeration for the kraft black liquor gasification and titanate direct causticization process. They involve pre-pyrolysing the kraft black liquor – titanate mixture, or using Al_2O_3 as the bed material and operate the reformer preferably in the turbulent fluidization mode. However the process conditions have been found wanting in terms of fines retention. This has restricted the test duration due to filter blinding. Therefore, additional tests in a properly configured larger test unit are suggested to fully verify and characterize the process.

4.5 Analysis of the bed samples of the MTCI PDU tests

All samples solid samples produced in the MTCI PDU tests and the original Kraft Black Liquor used by MTCI were analyzed and the results interpreted by Dr. Edgardo Schwiderke at the University of Maine.

4.5.1. Experimental details

The feedstock for experiments at MTCI (except MTCI #5) consisted of a mix of a Kraft Black Liquor (KBL) from a U.S. paper mill, and Ti-Pure R-103 from DuPont containing >96% TiO_2 rutile and <3.2% alumina. A mixture of Na_2CO_3 and TiO_2 was used for MTCI #5. Starting fluidized beds consisted of limestone, TiO_2, G-P Big Island demonstration unit bed material

(mostly Na_2CO_3), a pyrolyzed mix of KBL with TiO_2, alumina and final beds of previous tests as indicated. Fluidization was done with a mixture of steam and N_2 at superficial velocities ranging from 0.20 to 0.76 m/s. Bed temperatures were 730 °C except for MTCI #2 (704 °C) and MTCI #3 (649 °C). Table 4.8 summarizes the relevant conditions and gas composition. Running times ranged between 0.1 hr (MTCI #3) to 3.8 hr (MTCI #13) using semi batch operation, i.e. continuous addition of feedstock but no removal of bed material. The bed residual solids (BRS) samples from MTCI were analyzed for total inorganic C (TIC) and total S, and titrated for Na_2CO_3, Na_2S and NaOH. The elemental analysis of the KBL is shown in Table 4.9.

Table 4.8: Experimental conditions, agglomeration results, and average gas composition of MTCI tests.

	MTCI Test Number												
Operating Conditions (MTCI)	**1**	**2**	**3**	**4**	**5**	**6**	**7**	**8**	**9**	**10**	**11**	**12**	**13**
Bed Temperature (°C)	732	704	649	732	731	734	734	733	728	733	736	738	737
Running time (hr)	0.8	0.9	0.1	0.6	1.0	2.1	2.8	2.1	1.8	2.7	2.5	2.0	3.8
Shut down reason	Bed Aggltn.	Injectors plugging	Bed Aggltn.	Defl.no large agglom.	Plugging outlet pipes	Progr. stop	Progr. stop	Slurry feed pump failure	Injector plugging	Cyclone plugging	Filter plugging	Filter plugging	Pump jumming
Feedstock	KBL-TiO_2	KBL-TiO_2	KBL-TiO_2	KBL-TiO_2	Na_2CO_3-TiO_2	None	None	KBL-TiO_2	KBL-TiO_2	KBL-TiO_2	KBL-TiO_2	KBL-TiO_2	KBL-TiO_2
Slurry concentration	49.1%	48.6%	46.3%	47.9%	42.0%	-	-	62.6%	45.0%	43.8%	42.0%	42.0%	43.4%
Mass ratio of TiO_2 to Black Liquor Solids	0.55	1	1	1	0.94	-	-	1	1	1	1	1	1
Initial bed	Limestone	Limestone	F.B. #2 + Limestone.	TiO2	GP Big Island bed	GP Big Island bed	Pyrolyzed BL-TiO_2	GP Big Island bed	Aluminum Oxide	Test #9 Final Bed	Test #10 Final Bed	Test #11 Final Bed	Test #12 Final Bed
Initial Bed Mass (kg)	7.24	6.99	5.22	3.09	2.95	2.72	6.11	6.01	8.01	7.50	7.01	7.01	4.50
Steam mole fraction	0.85	0.9	-	0.8	0.67	-	0.71	0.34	0.65	0.48	0.48	0.43	0.43
Mean superficial fluidization velocity (m/s)	0.20	0.31	0.25	0.30	0.33	0.51	0.39	0.76	0.43	0.52	0.47	0.49	0.61
Final bed color	near white	near white	medium gray	-	medium gray	dark gray	light gray	yellowish	medium gray	medium gray	medium gray	medium gray	medium gray
Agglomeration (order of size)	Yes (cm)	Yes (mm)	Yes (cm)	Yes (mm)	Yes (mm)	No	No	Yes (cm)	No	Yes (mm)	No	No	No
Plugging of filter catch and/or cyclone	Significant	Significant	Significant	NA	Significant	None	Significant	Significant	Significant	Full	Full	Full	Significant
H_2 (molar, dry and non N_2 basis)		61.2%		60.7%				59.9%	59.2%	58.9%	58.2%	60.7%	58.1%
CO_2		32.2%		28.4%				25.1%	29.1%	29.2%	30.8%	28.3%	29.9%
CO		3.5%		5.6%				13.5%	5.2%	5.9%	5.2%	5.7%	6.3%
CH_4		2.6%		3.3%				0.9%	5.0%	2.9%	2.6%	2.7%	2.8%
H_2S		0.3%		1.5%				0.5%	1.1%	2.6%	2.6%	2.1%	2.4%
Heating Value (BTU/dscf)				267			258	251	274	266	259	265	262

Table 4.9 Elemental analysis of KBL solids

Black Liquor Solids Composition (KBL) in weight %	
Carbon	32.3
Hydrogen	3.8
Oxygen	35.8
Sodium	18.2
Sulfur	3.0
Potassium	3.0
Chlorine	0.7
Total	**96.8**

4.5.2. Results and discussion

Table 4.10 shows the analysis of bed residual solids (BRS), freeboard and filter catch particles as well as the composition of the initial bed and feedstock of the MTCI fluidized bed tests. The DC yield is defined as the percentage conversion of Na_2CO_3, and the causticity is the traditional ratio of [NaOH] relative to the sum of [NaOH] + [Na_2CO_3] (all expressed as Na_2O) in the leachate of the solids. It can be seen that the DC yield and causticity in the BRS of MTCI# 7 with the prepyrolyzed mix of black liquor and Ti-Pure R103 and for MTCI# 10-12 with alumina in the bed are high. DC yield and causticity could not be reliable obtained for MTCI# 1 and 2 because of interference of the high content of $CaCO_3$ in the Na_2CO_3 determination. Similarly, DC yield was not calculated for MTIC# 5 and 8 because the initial bed consisted of the GP Big Island demonstration bed mostly consisting of Na_2CO_3. However, it is assumed that MTCI# 8 reached a high DC yield because it gave the highest amount of leached NaOH and, at the same time, a relative strong drop in Na_2CO_3 concentration (from 78% to 73%). This is attributed to the high fluidization velocity which leads to a lower CO_2 concentration inside the fluidized bed. For MTCI# 6, the causticity was 0% because there was no titanate and consequently no DC reaction.

The yield of organic carbon (OC) conversion was calculated from combustibles as $1-OC_{BRS}/OC_{InitialBed}$ for samples ran in batch mode. For tests MTCI#5, 8 and 10-12, it was calculated as $1-OC_{BRS}(W_{InitialBed}+0.58\Delta W_{FS}) / (OC_{Feedstock}\Delta W_{FS} + OC_{InitialBed}W_{InitialBed})$ where $W_{InitialBed}$ is the weight of initial bed, $\Delta W_{Feedstock}$ the mass added by the feedstock, and 0.58 a correction factor accounting for mass loss during DC and gasification. The method may give an underestimation of the OC conversion because in MTCI#8 the result was 84% while the almost white color of the final bed (in contrast to a darker gray for other tests) suggested a close to 100% conversion. This suggests that a high fluidization velocity favors the gasification reaction. OC conversion was low for MTCI# 6 because this test was done in an inert atmosphere. The OC conversion is generally lower for the filter catch than for the final bed because of shorter residence time of fine particles in the fluidized bed.

The H_2 concentration (based on dry gas and N_2 free) was in all cases in a narrow range of 58 to 61%. The CO_2 concentration ranged between 25-32% and was slightly higher for MTCI# 2 because of calcination of limestone in the initial bed. Except for MTCI# 8, the CO concentration ranged between 3.5 and 6.3%. MTCI# 8 had the highest CO concentration (13.5%) and lowest CO_2 concentration (25.1%). This indicates that the higher fluidization velocity promoted the carbon gasification reaction. MTCI#7 starting with a pre-pyrolyzed mix (char) and ran in batch mode, also had a H_2 concentration of 61-62% during the first 90 min, then dropping to 0 after 165 min. The initial CO_2 and CO concentration of this test was 23% and 13% respectively, also indicating increased carbon gasification in comparison to most other experiments. The high $[H_2]/([CO_2]+[CO])$ ratio (near 2) suggests that steam gasification and steam shift are the most important reactions with smaller contributions due to pyrolysis and carbon gasification. The heating value was very steady ranging between 250 and 275 BTU/dscf.

Table 4.10 Analysis of MTCI bed residual solids.

	Final Bed Samples									Free-board	Filter Catch						Initial Bed		Feedstock
MTCI test # »	**1**	**2**	**5**	**6**	**7**	**8**	**10**	**11**	**12**	**8**	**1**	**5**	**7**	**8**	**11**	**12**	**5, 6 & 8**	**7**	**2-3,8-13**
Proximate																			
Solubles	7.8%	7.3%	92.5%	84.0%	4.7%	80.3%	2.5%	6.3%	3.0%	38.8%	5.5%	41.8%	17.9%	27.9%	4.2%	8.0%	80.2%	17.7%	15.7%
Combustibles	1.2%	1.2%	1.5%	15.9%	0.8%	1.1%	1.5%	1.7%	0.7%	2.1%	1.2%	14.6%	10.8%	11.3%	1.3%	4.4%	18.6%	11.9%	23.5%
Ash	91.0%	91.5%	6.0%	0.1%	94.5%	18.6%	96.0%	92.0%	96.3%	59.1%	92.0%	43.6%	71.3%	60.9%	94.5%	87.6%	1.7%	70.4%	60.8%
Elemental																			
TIC	5.7%	6.3%	9.7%	8.8%	0.0%	7.7%	0.0%	0.0%	0.0%		9.3%	4.4%	0.9%	1.9%	0.0%	0.0%	8.3%	1.0%	2.4%
Total S								0.0%	0.0%						0.0%	0.0%			2.0%
Leaching																			
Na_2O	0.9%	0.7%	0.2%	0.0%	1.5%	4.8%	0.3%	0.7%	0.7%	10.3%	0.4%		1.6%	1.2%	0.7%	1.1%	0.0%	0.7%	0.0%
Na_2S					0.0%	0.6%				0.9%			0.0%	0.0%			0.0%	1.5%	0.3%
Na_2CO_3	2.7%	2.6%	86.4%	85.0%	0.9%	72.5%	0.1%	0.3%	0.2%	49.4%	2.6%		10.0%	23.2%	0.4%	0.6%	77.9%	13.3%	24.2%
TIC soluble	0.3%	0.3%	6.7%	8.3%	0.2%	7.4%	0.2%	0.2%	0.2%								8.1%	0.9%	2.4%
Yield																			
DC					97.1%		96.5%	93.6%	94.8%				15.5%		93.1%	94.4%			
Causticity				0.0%	74.0%		80.5%	80.0%	85.7%		20.8%		21.1%	8.2%	75.5%	76.7%	0.0%	8.3%	0.0%
OC Conversion			79.4%	14.5%	93.3%	83.6%	78.5%	72.4%	84.2%				8.8%	19.4%	75.8%	40.0%			
S Consumption								100.0%	100.0%						100.0%	100.0%			

The concentration of H_2S ranged between 0.3 to 2.6% and was higher for MTCI# 10-13 containing alumina in the initial bed. MTCI# 7, a test run in batch mode with no feedstock and a prepyrolyzed KBL-Ti Pure R103 bed, had 1.5% Na_2S in the initial bed and no Na_2S in either final bed or filter catch. This indicates that all Na_2S initially present was converted to H_2S according to reaction (5). In agreement, the concentration of H_2S at 165 min dropped to about 1/10 of the starting concentration. It is presumed that pyrolysing the material prior to fluidization helped conversion to H_2S. There was no Na_2S in the initial MTCI# 8 bed consisting of the GP Big Island demonstration plant material. The feedstock was a KBL-Ti Pure R103 mix and the test was run at a fluidization velocity of 0.76 m/s, the highest of all MTCI tests. There was almost no agglomeration in the bed, however very hard agglomerates formed in the freeboard. The amount of Na_2S was 0.6% and 0.9% in the final bed and freeboard agglomerates respectively. This indicates that, even at high fluidization velocities, it is difficult to convert all Na_2S to H_2S. The even higher amount of Na_2S in the freeboard is attributed to a slow rate of reaction (5) in the hard agglomerates, as it is known that the conversion of Na_2S to H_2S is mass transfer controlled. There was no Na_2S in the filter catch, attributed to the small particle size which increases the rate of release of H_2S and to the lower temperature in the filter which shifts the equilibrium reaction (5) towards H_2S. MTCI tests # 11 and 12 had the same feedstock as MTCI# 8. The initial bed of these tests consisted of final beds of former tests containing a high amount of alumina. No S was found in either final bed or filter catch for these tests indicating that all S had been released. This is consistent with gas analysis showing that MTCI# 10-13, all with alumina in bed, had the highest concentration of H_2S in the off gas. Presumably alumina assists the mass transport of H_2S out from the bed particles because the presence of alumina prevents or minimizes particle agglomeration. MTCI# 2 that started with a limestone bed had a significantly lower H_2S concentration than the other tests. This is attributed to the presence of CaO that reacts with H_2S to form CaS.

Of the 13 tests, 3 had to be shut down prematurely because of agglomeration related problems occurring in the bed. Another 3 were halted because of filter or cyclone plugging, 4 because of slurry feed related problems, and one because of plugging of outlet pipe. The first 4 tests with either limestone or TiO_2 particles as the initial bed resulted in agglomeration and thus bed defluidization. No agglomeration was noticed for tests 6 and 7 that started respectively with pyrolyzed BL and pyrolyzed BL-TiO_2 mix as initial bed and had no addition of feedstock. There was also no significant agglomeration for tests 5, with Na_2CO_3-TiO_2 as feed, i.e. without any addition of BL. These results are consistent with lab tests indicating that at 730 °C agglomeration is only important in presence of raw (unpyrolyzed) BL. There was also no significant agglomeration for tests 9 through 13 attributed to the presence of aluminum oxide in the bed. There was some agglomeration for test 8 especially in the freeboard. Because of the high superficial fluidization velocity (0.76 m/s) during this test, small injected BL-TiO_2 particles were quickly blown out of the bed resulting in drying-pyrolysis in the freeboard thus promoting agglomerates to form there.

4.5.3 Conclusions

To overcome limitations due to CO_2 inhibition, high DC conversion in steam gasification with DC of KBL is possible at 730 °C if the process is divided in two stages, first in a normal and then a much lower CO_2 atmosphere. Maximum Na_2CO_3 conversion in presence of 10% CO_2 is limited to a final Na_2O/TiO_2 molar ratio in the titanate product of 0.35 when using pure anatase

or trititanate, to 0.47 with recycled Ti-Pure R103, and of 0.61 with fresh Ti-Pure R103. At 730 °C, the final DC conversion is reached between 10 to 60 min.

A medium BTU gas (on nitrogen and moisture free basis) and a relatively high causticity of about 80% of the leachate of the bed residual solids may be obtained in a steam reformer when a relatively high fluidization velocity and alumina oxide is present in the bed solids. During these tests, the majority of the S ended up in the gas phase. S release to gas phase increased under improved mass transfer conditions, with alumina helping these conditions.

85% of the MTCI tests were shut down prematurely due to plugging of pump or injector, defluidization due to bed agglomeration, and/or plugging of filter or cyclone. Results indicate that bed agglomeration can be controlled by using high fluidization velocity or by adding aluminum oxide to the bed.

The above results were presented at the International Chemical Recovery Conference in Quebec City, Canada held from May 29th to June 1st, 2007.

5. TESTING OF PROCESS IN LARGE PILOT SCALE FLUIDIZED BED SYSTEM

5.1 Background

The MTCI tests showed that the size of the PDU was too small; in particular the fines retention was insufficient so that the duration of a test was restricted to only a few hours. Therefore, additional tests in a properly configured larger test unit were suggested to fully verify and characterize the process. A large pilot scale (10 in diameter) fluidized bed system was available at the gasification facility of the University of Utah in Salt Lake City. Under the direction of Professor Kevin Whitty of UUtah with assistance by Dr. Edgardo Schwiderke of UMaine the steam reforming with titanate causticization of KBL-TiO_2 process was tested during the week of April 30 – May 5th, 2007.

The experimental conditions were: 300 um size alumina as starting bed material, temperature of about 715 °C, TiPure R103 as the titanate causticization agent, and relative amounts of KBL to TiPure R103 to make the molar ratio [Na_2CO_3] / [TiO_2] equal to 0.7. The estimated amount of solids of the feed slurry mix was 61%. These conditions were recommended based on the UMaine and MTCI tests.

5.2 Materials

The initial bed was of Al_2O_3 (alumina) with nominal particle size of 230 μm, range 100 – 500 μm, from AGSCO. 16 barrels of softwood KBL with 52% solids were obtained from the Texarkana mill of International Paper. The elemental composition of the KBL solids is listed in Table 5.1.

KBL solids composition

C	36.82%
H	3.39%
O (by diff.)	36.60%
S	4.51%
N	0.15%
Na	16.80%
K	1.50%
Cl	0.23%
Total	**100.00%**

Table 5.1: Elemental analysis of KBL.

The titanate causticization agent was TiPure R103 from DuPont, with >96% TiO_2 and <3.2% Al_2O_3. The KBL- TiO_2 slurry had a mass ratio of TiO_2 / KBL solids of 0.43 to make the molar ratio $[Na_2CO_3]$ / $[TiO_2]$ equal to 0.7. This mixture is pumpable even at room temperature. However the slurry was be added to the fluid bed reformer at 80-90 °C to minimize heat load

5.3 Test procedures

First the reactor was loaded with 250 lb of Al_2O_3. Then fluidization with N_2 was started at a rate of 2.5 ft/sec followed by the start of the heat up cycle. After four days of heating up, the test was started in semi batch mode, i.e. the KBL- TiO_2 slurry was added without removing products, for a total period of 29 hr with several adjustments in the process parameters as indicated in the event file shown in Table 5.2. The total time of injection of feedstock was 24 hr. After shutting down the feedstock and heaters, fluidization with steam continued during several more hours to cool down the reactor. After cooling down, the final bed was emptied for future use and analysis. Bed samples were titrated for carbonate and hydroxide content and inspected under the microscopy.

5.4 Results and discussion

The most important result from this test is that it demonstrated that the fluidized bed operation could be maintained for the TiO_2-KBL steam gasification process at a high temperature of about 715 °C as long as the fluidization velocity is maintained at about 1m/s.

Solid samples were taken from the bed and leached with deionized water, and the leachate was titrated. The causticity was calculated from the ratio [NaOH] / {[NaOH] + $[Na_2CO_3]$} (all expressed as Na_2O) obtained from the leachate titration.

Table 5.2: Log of events for test at UUtah

Time (hr)	Event
0.0	Thermocouples reading are in the range 705 - 725 °C. Fluidization is switched from N_2 to steam at a velocity of 0.76 m/s. Start feeding BKL-TiO_2 at a rate of 3.63 kg/hr. No smell of H_2S.
9.0	Outlet of condensed water of afterburner had to be cleaned because of plugging with fine Al_2O_3 particles and chunks of large size (order of cm) insulation material.
18.0	Because of poor fluidization quality, overheating problems emerged in the electric heaters. Steam flow at the injector that helps atomize the particles was very low. KBL-TiO_2 feeding is stopped. Fluidization velocity is increased to 1.07 m/sec.
22.0	Fluidization quality improved. Fluidization velocity is adjusted to 0.92 m/sec.
23.0	KBL-TiO_2 feeding is turned on again. Steam flow at the injector was raised to proper amount.
24.0	Micro GC is turned on.
24.5	Micro GC is turned off. Fluidization velocity is adjusted to 1 m/sec.
29.0	The system is shut down because of pressure build up, about 2-3 psi, in the afterburner that would not allow the natural gas to be fed. This is attributed to large amount of carryover accumulating in the afterburner. Although the flame could be turned on again, the pressure build up persisted and could only be diminished by lowering the fluidization velocity to 0.31 ft/sec. Since this velocity is too low for sustaining a good fluidization, feeding and heaters were turned off while steam fluidization continued.

5.4.1 Direct causticization conversion and causticity

The value of causticity was 72%, 83%, 75% and 85% for samples taken at hour 18.5, 22, 24 and after cooling down the system respectively. Former lab tests indicate that, for high values of direct causticization (DC) conversion, causticity calculated from titration is typically about 15% lower than the actual DC conversion. This is attributed to a systematic overestimate of [$CO_3^{=}$] due to limitations of the titration method. It is therefore concluded that the final bed sample of this test reached near complete DC conversion. This means that the [Na_2O] / [TiO_2] molar ratio at the end of the test most likely became very close to initial ratio [Na_2CO_3] / [TiO_2] of 0.7. This is a little higher than the final ratio of 0.61 for thermo balance tests with KBL-Ti Pure under a 12% CO_2 and carbon dioxide (no steam) gasification conditions. This increase in the final [Na_2O]) / [TiO_2] ratio is attributed to a lower CO_2 concentration of the UUtah test, estimated to be around 5%. The causticities of samples taken at hour 18.5 and 24, roughly representative of steady state operation, were 72% and 75% respectively. The causticities of samples taken at hour 22, after momentarily shutting off the injection of feedstock, and of the final bed were 83% and 85% respectively. The about 10% higher causticity of these samples with respect to those near steady state operation is because the material had been more time in the reactor and therefore reached a more complete conversion.

5.4.2 Organic carbon conversion

The color of the outside and inside of the final bed sample particles was of a pale yellow. This indicates that a uniform high gasification conversion has been reached that would otherwise turn particles into a dark gray. Table 5.3 shows the off gas composition on steam and N_2 free basis at hour 24 and compared to the average results of MTCI# 9-13, also with alumina in the bed. Notice that the test at UUtah had a higher H_2 (62% vs. 59%) and a lower CO (2% vs. 6%) concentrations. This is attributed to a more complete water shift reaction due to a larger residence time of the gases in the UUtah as compared to the MTCI reactor. The presence of O_2 in the UUtah test is attributed to a leak in the sampling system. The lower amount of CH_4 of UUtah (1%) compared to the MTCI# 9-13 average (3.2%) is compensated by a considerable amount of iso-butene (0.9%) and n-butene (1.2%). The high $[H_2]/([CO_2]+[CO])$ ratio (near 2), similarly to tests at MTCI, suggests that steam gasification and steam shift are the most important reactions with smaller contributions due to pyrolysis and carbon dioxide gasification.

Gas	UUtah	MTCI #9-13 (average)
H2	61.94%	59.03%
O2	1.16%	-
CH4	1.00%	3.19%
CO	1.94%	5.67%
CO2	30.57%	29.44%
H2S	0.80%	2.14%
Iso-butane	0.92%	-
n-butane	1.16%	-
Total	**99.50%**	**99.47%**

Table 5.3: Off gas composition on steam and N_2 free basis for test at UUtah at hour 24

5.4.3 Sulfur conversion

The concentration of H_2S at UUtah was about 0.8% which is considerably lower than the 2.1% for the average MTCI test # 9-13. This is attributed to the larger size of the UUtah test particles whose diameter was 3-5 mm diameter, as illustrated in Fig. 5.1, imposing additional mass transfer restrictions to convert Na_2S to H_2S.

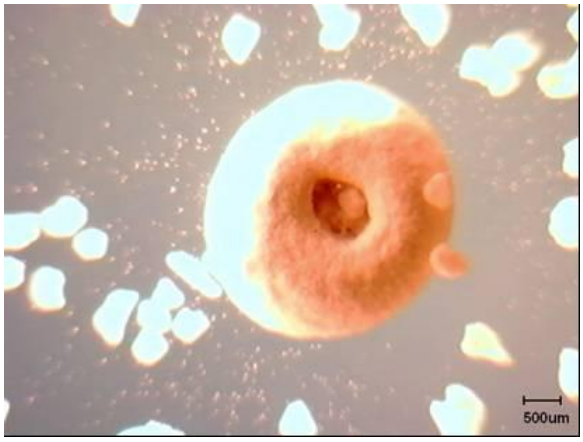

Figure 5.1 Micrograph of final bed particles; large particle: KBL-TiO2 ash; small particles: Al_2O_3.

5.4.4 Carryover

A large amount of material was carried out from the reactor during the test. This caused the plugging of the after-burner system and the eventual shut down of the test. Direct observations and sieve fraction analysis (Fig. 5.2) indicated that most of the carryover material was composed of alumina from the initial bed. The large amount of carryover is attributed to the high fluidization velocity and the flake shape of the Al_2O_3 particles (Fig. 5.1) that facilitates the elutriation from of the bed. It is recommended that future tests start with round shape alumina material. In addition, a reduction of the particle size of the injected material to around 300 um would further allow a reduction of the fluidization velocity that would then be another contributor to diminish the amount of carryover.

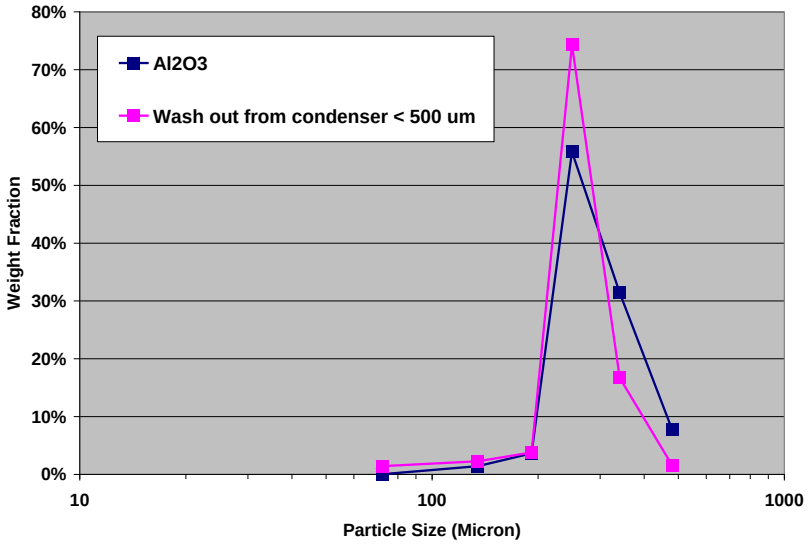

Figure 5.2 Sieve analysis of Al_2O_3 and smaller than 500 um particles from condenser of afterburner.

5.4.5 Plugging of slurry feed system

In contrast to MTCI tests, there was no plugging of the feedstock injection system during the UUtah tests. This is attributed to injectors of UUtah ending in an open tube.

5.5 Conclusions

- Complete DC conversion is possible for an initial $[CO_3Na_2]$ / $[TiO_2]$ molar ratio of 0.7 in the KBL-TiPure R103 mix under steam gasification conditions at 715 C and in the presence of 5% or less CO_2 in the gas phase.
- Complete C conversion is obtained under the present conditions.
- Particle size needs to be reduced to much less than 3 mm to overcome poor S conversion due to mass transfer limitations.
- There are no agglomeration problems at a fluidization velocity of 1 m/s and with alumina in the bed.

- Alumina particles need to be round instead of flock shape to reduce dragging and therefore carryover.
- The open ended tube injectors of UUtah showed no plugging of injector problems.

6. OVERALL CONCLUSION

Three different pulping technologies were investigated using southern softwood chips relative to conventional Modified Continuous Cooking (MCC); green liquor (GL) pretreatment, split sulfidity (SS) cooking and polysulfide pulping with or without anthraquinone (PS or PSAQ).

SS pulp yields were 1-2% greater than corresponding MCC pulps at higher delignification rates. Initial high alkali SS cooks generated pulps of lower kappa number and higher yield compared to those of low initial alkali. The SS pulps also had 5 to 10 mPa.s higher viscosity and improved tensile and burst strength. SS pulps were slightly harder to refine relative to MCC pulps.

Compared to MCC cooking, PS pulping at 25% sulfidity and 1-2% sulfur charge produced pulps of 2% greater yield. PS pulping at 40% sulfidity and higher sulfur charge required more alkali charge to maintain delignification rate. Also the bleachability of the PS pulps was less than that of MCC pulps, with a degree of oxygen delignification of 40% compared to 60% for MCC pulps.

PSAQ pulping with an optimized alkali distribution procedure resulted in similar rate of delignification compared MCC. Total pulp yield improvements of approximately 1% per 1% PS charged on OD wood were obtained, in agreement with literature. PSAQ pulping at a high polysulfide charge of 3% (as PS) requires a high sulfidity (40%) white liquor for its generation. The bleachability of PSAQ pulps is similar to that of control MCC pulps, but the bleached PSAQ pulps have a significant higher pulp viscosity. The PSAQ pulps were easier to refine than corresponding MCC pulps. The tear and bursting strength of PSAQ pulps produced at 25% sulfidity and 2% PS charge is lower than those of 25% sulfidity MCC pulps, while 40% S and 3% PS PSAQ pulps gave slightly higher strength properties than 40% sulfidity MCC pulps.

A WinGEMS module for black liquor gasifier (BLG) was developed. The module was utilized in simulation case studies exploring SS and PSAQ pulping using BLG for chemical recovery. The results show that the net process variable operating cost was driven by two major factors; lime kiln fuel and power sales price. At an assumed lime kiln fuel cost of $50/barrel and power sales price of $0.35/kWhr, the net variable operating costs for the simulated BLG cases showed a cost increase of about 3% compared to MCC kraft pulping. The pulp yield benefits of the studied modified pulping technologies plus the additional revenue generated from the generation and sale of green power (using BLG combined cycle (BLGCC)) were insufficient to compensate for this cost increase. However, if the lime kiln fuel cost is decreased or the power sale price increased, the BLGCC process with split sulfidity or PSAQ pulping becomes more economically favorable than the conventional MCC kraft process. If the sales price for power to the grid is increased from 3.5 to 6 ¢/KWh cost savings of about $40/ODT pulp could be realized.

Direct causticization (DC) of black liquor by TiO_2 or $Na_2O.3TiO_2$ is completed within 1 hour above 680°C in a pure nitrogen atmosphere. These kinetics are reasonably well modeled by the phase-boundary model. However, there is a strong decrease in DC final conversion and

causticity (i.e. yield of NaOH from Na_2CO_3) at a [CO_2] in the gas phase of about 10% or higher during gasification of black liquor – titanate mixtures at about 730 C. This suggest that implementation of the DC-gasification process requires a two-stage counter current process where carbon gasification takes place in a fluidized bed and the DC reaction in another reactor fed by steam to maintain a low [CO_2] in the gas phase.

Softening/liquefaction of black liquor solids (BLS) during pyrolysis of the organics starting at around 300 °C followed by solidification to a char without swelling is the major mechanism responsible for agglomeration in the present BL-titanate system. The liquefied black liquor solids pull the titanate particles together by capillary forces, and after resolidification the dense residual char forms strong bridges between the particles. Although most of the carbon is subsequently consumed, solid-phase sintering of Na_2CO_3 retains the strength of the agglomerates. These results suggest that agglomeration may be prevented or diminished by separately pre-pyrolysing the black liquor or by adding Al_2O_3 particles since Al_2O_3 does not sinter at the temperatures studied.

Initial tests in the fluid bed PDU by MTCI established that particle agglomeration resulted in bed defluidization and premature shut down when processing black liquor with TiO_2. UM determined that the agglomeration was due to sintering of the organic matter in black liquor starting at ~300 °C. A contributing factor to the agglomeration is the absence of black liquor swelling during pyrolysis in the presence of TiO_2. Based on these results it was recommended by UM that the MTCI PDU be operated in the turbulent fluidization mode, preferably with larger particle sizes than 150 µm.

Subsequent PDU tests at 740 °C and a superficial velocity of about 2.0 ft/s (i.e. an increase by a factor of almost 2) with an initial bed of Al_2O_3 particles showed that the reformer could be operated without agglomeration problems for about 4 hours. The water-free product gas was approximately 62% H_2, 13% CO, 23% CO_2, 2 % H_2S and trace organics. Analysis of the bed solids showed a carbon gasification of about 90% and degrees of direct causticization varying from 25 to 80 %. However the test duration was still limited by the formation of a large amount of fine particles, leading to filter blinding. Therefore, additional tests in a properly configured larger test unit were needed to fully verify and characterize the process.

Because the PDU at MTCI was too small to fully verify and characterize the gasification and direct causticization process, the process was also tried in the 10 inch diameter fluidized bed steam reformer at the University of Utah under the direction of Kevin Whitty. The steam reformer was fed with a mixture of TiO_2 and kraft black liquor for 24 hours. The titanate causticization agent was TiPure R103 from DuPont, with >96% TiO_2 and <3.2% Al_2O_3. The KBL- TiO_2 slurry had a mass ratio of TiO_2 / KBL solids of 0.43 to make the molar ratio [Na_2CO_3] / [TiO_2] equal to 0.7. The following conclusions were made based on this test:

1. Fluidized bed operation can be maintained for the TiO_2-KBL steam gasification process at a high temperature of about 715 °C as long as the fluidization velocity is maintained at about 1m/s. There are no agglomeration problems at these conditions with alumina as starting bed.

2. Complete DC conversion is possible under steam gasification conditions at 715 C and in the presence of 5% or less CO_2 in the gas phase.
3. Complete C conversion is obtained under the present conditions.
4. Bed particle size needs to be much less than 3 mm to avoid poor sulfur release as H_2S due to mass transfer limitations.

7. REFERENCES

[1]) Larson, E.D., Consonni, S. and Katofsky. R.E., "*A Cost Benefit Assessment of Biomass Gasification Power Generation in the Pulp and Paper Industry*", Final Report, October 8 (2003)

[2]) Nohlgren, Ingrid, "*Recovery of Kraft Black Liquor with Direct Causticization using Titanates*", Doctoral Thesis, Department of Chemical and Metallurgical Engineering, Luleå University of Technology, Luleå, Sweden (2002)

[3]) Nilsson, L.J.; Larson, E.D.; Gilbreath, K.R.; Gupta, A. *Energy Efficiency and the Pulp and Paper Industry;* ACEEE: Washington D.C./Berkeley, CA, 1995.

[4]) Jahne, F. *"Commercial Success of Gasification Technology",* Tappi J. **1999**, *82(10):* 49.

[5]) Whitty, K.; Verrill, C.L. *"A Historical Look at The Development of Alternative Black Liquor Recovery Technologies and The Evolution of Black Liquor Gasifier Designs",* Proc. *2004 TAPPI Int. Chem. Rec. Conf.;* TAPPI Press: Atlanta, GA, 2004; p 13-33.

[6]) Stigsson, L., *"ChemrecTM [Kvaerner Chemrec AB's] Black-Liquor Gasification",* Proc. *1998 TAPPI Int. Chem. Rec. Conf.;* TAPPI Press: Atlanta, GA, 1998; p 663-674.

[7]) Grace, T.M.; Timmer, W.M. *"A Comparison of Alternative Black Liquor Recovery Technologies",* Proc. *1995 TAPPI Int. Chem. Rec. Conf.;* TAPPI Press: Atlanta, GA, 1995.

[8]) Dahlquist, E.; Jones, A., "*Presentation of a Dry Black Liquor Gasification Process with Direct Causticization*", Tappi Journal (2005), 4(6), 15-19.

[9]) Rowbottom, B.; Newport, D.; Connor, E. *"Black Liquor Gasification at Norampac",* Proc. *2005 TAPPI Engineering Pulping & Environmental Conference;* TAPPI Press: Atlanta, GA, 2005.

[10]) Chemrec ; URL http://www.chemrec.se; 2005.

[11]) Whitty, K.; Ekbom, T.; Stigsson, L. *"Chemrec Gasification of Black Liquor";* published on website URL http://www.chemrec.se/forsta.htm; 2000.

[12]) Lindblom, M. *"An Overview of Chemrec Process Concepts";* Presentation at the Colloquium on Black Liquor Combustion and Gasification; Park City, Utah, May, 2003.

[13]) Erickson, D.; Brown, C. *"Operating Experience with Gasification Pilot Project";* Tappi J. **1999,** *82(9).*

[14]) Kleppe, P.J., TAPPI 53:1 35-47 (1970)

[15]) McDonough, T.J., "*Kraft Pulp Yield Basics",* Proc. *Breaking the Yield Barrier Symposium*; TAPPI Press: Atlanta, GA, 1998, Vol. 1, p1.

[16]) Sixta, H. ed., "*Handbook of Pulp and Paper",* Vol. 1, Wiley-VCH Verlag GmbH & Co. KGaA, Weinheim, Germany, **2006,** Ch. 4

[17]) Aurell, R., Hartler, N., "*Kraft Pulping of Pine. I. Changes in the Composition of the Wood Residue during the Cooking Process*", Svensk Papperstidning 68(4):59-68 (1965)

[18]) Kondo, R., Sarkanen, K.,V., "*Kinetics of Lignin and Hemicellulose Dissolution during the Initial Stage of Alkaline Pulping*", Holzforschung, 38(1), 31-36 (1984)

[19]) Gellerstedt, G., " *Pulping Chemistry*", in Wood and Cellulosic Chemistry, 2nd ed., Hon, D.N.S., Shiraishi, N., Eds., M. Dekker, New York, Basel, **2001** p.859

[20]) Johansson, B.; Mjoberg, J.; Sandstrom, P.; Teder, A. *"Modified Continuous Kraft Pulping - Now a Reality"*; Svensk Papperstidning--Nordisk Cellulosa. **1984,** *87(10):* 30-35

[21]) Andrews, E.K., Ph.D. thesis, North Carolina State University, Raleigh, NC, 1982.

[22]) Andrews, E.K.; Chang, H-m.; Kirkman, A.G.; Eckert, R.C. *"Extending Delignification in Kraft and Kraft/Oxygen Pulping of Softwood by Treatment with Sodium Sulfur Liquors";* Proc. *Japan Tappi Symposium on Wood Pulp Chemistry;* TAPPI Press: Atlanta, GA, 1982.

[23]) Lopez, I.; Chang, H-m.; Jameel H.; Wizani, W. *"Effect of Sodium Sulfide Pretreatment on Kraft Pulping";* Proc. *1999 TAPPI Pulping Conference;* TAPPI Press: Atlanta, GA, 1999; pp135.

[24]) Herschmiller, D.W. *"Kraft Cooking with Split Sufidity- A Way to Break the Yield Barrier";* Proc. *Breaking the Yield Barrier Symposium;* TAPPI Press: Atlanta, GA, 1998; Vol. 1 pp 59.

[25]) Olm, L.; Tisdat, G. *"Kinetics of the Initial Stage of Kraft Pulping";* Svensk Papperstidning--Nordisk Cellulosa. **1979,** *82(15):* 458-464.

[26] LeMon, S.; Teder, A. *"Kinetics of Delignification in Kraft Pulping (1). Bulk Delignification of Pine";* Svensk Papperstidning--Nordisk Cellulosa, **1973,** *76(11):* 407.

[27]) Olm, L.; Tormund, D.; Jensen, A. *"Kraft Pulping with Sulfide Pretreatment-Part-1 Delignification and Carbohydrate Degradation";* Nord. Pulp Pap. Res. J. **2000,** *15*, 62.

[28]) Jiang, J.E; Herschmiller, D.W. *"Sulfide Profiling for Increased Kraft Pulping Selectivity";* Proc. *1996 TAPPI Pulping Conference*; TAPPI Press: Atlanta, GA, 1996, p. 311-318.

[29]) Lownertz, P.P.H.; Herschmiller, D.W., *"Kraft Cooking with Split White Liquors and High Initial Sulfide Concentration: Impact on Pulping and Recovery";* Proc. *1994 TAPPI Pulping Conference;* TAPPI Press: Atlanta, GA, 1994, p. 1217-1224.

[30]) Mao, B.; Hartler, N. *"Improved Modified Kraft Cooking. (1). Pretreatment with a Sodium Sulfide Solution";* Paperi ja Puu. **1992,** *74(6):* 491-494.

[31]) Mao, B.; Hartler, N. *"Improved Modified Kraft Cooking. (2). Modified Cooking Using High Initial Sulfide Concentration";* Nordic Pulp and Paper Research J., **1992,** *7(4):* 168-173.

[32]) Mao, B.; Hartler, N. *"Improved Modified Kraft Cooking,4: Modified Cooking with Improved Sulfide and Lignin Profiles";* Paperi ja Puu. **1995,** *77(6/7):* 419-422.

[33]) Olm, L.; Backstrom, M.; Tormund, D. *"Pretreatment of Softwood with Sulfide Containing Liquor Prior to Kraft Cook";* Proc. *1994 TAPPI Pulping Conference;* TAPPI Press: Atlanta, GA, 1994; 29.

[34]) Jiang, J.E.; Greenwood, B.F.; Phillips, J.R.; Stromberg, C.B. *"Improved Kraft Pulping by Controlled Sulfide Additions";* Proc. *7th ISWPC Conference;* CICCST: Beijing, China, 1993.

[35]) Lindstrom, M.; Naithani, V.; Kirkman, A.; Jameel, H.; *"Effects on Pulp Yield and Properties Using Modified Pulping Procedures Involving Sulfur Profiling and Green Liquor Pretreatment";* Presented at 2004 Tappi Fall Technical Conference, Atlanta, GA, 2004.

[36]) Van Heiningen, A.; Schwiderke, E.; Chen, X. *"Kinetics of the Direct Causticizing Reaction Between Black Liquor and Titanates During Low Temperature Gasification";* Proc. *2005 TAPPI Engineering, Pulping & Environmental Conference;* TAPPI Press: Atlanta, GA, 2005.

[37]) Li, Z.; Li, J.; Kubes, G.J. *"Kinetics of Delignification and Cellulose Degradation During Kraft Pulping with Polysulphide and Anthraquinone";* JPPS. **2002,** *28(7):* 234-239.

[38]) Griffin, C.W.; Kumar, K.R.; Gratzl, J.; Jameel, H. *"Effects of Adding Anthraquinone and Polysulfide to the Modified Continuous Cooking (MCC) Process";* Proc. *1995 TAPPI Pulping Conference*; TAPPI Press: Atlanta, GA, 1995; 19-30.

[39]) Jiang, J.E. *"Extended Delignification of Southern Pine [Pinus spp.] with Anthraquinone and Polysulfide";* TAPPI J. **1995,** *78(2):* 126-132.

[40]) Jiang, J.E. *"Extended Modified Cooking of Southern Pine [Pinus] with Polysulfide: Effects on Pulp Yield and Physical Properties";* TAPPI J. **1994,** *77(2):* 120-124.

[41]) Landmark, P.A.; Kleppe, P.J.; Johnsen, K. *"Pulp Yield Increasing Process in Polysulfide Kraft Cooks";* Tappi J. **1965,** *58(8):* 56.

[42]) Vennemark, E. *"Some Ideas on Polysulfide Cooking";* Svensk Papperstidning. **1964,** *67(5):* 157.

[43]) Kleppe, P.J.; Minja, R.J.A. *"The Possibilities to Apply Polysulfide-AQ in Kraft Mills";* Proc. *Breaking the yield barrier symposium*; TAPPI Press: Atlanta, GA, 1998, Vol. 1, pp 113.

[44]) Sanyer, N.; Laundrie, J.F. *"Factor Affecting Yield Increase and Fiber Quality in Polysulfide Pulping of Loblolly Pine, Other Softwoods, and Red Oak";* Tappi J. **1964,** *47(10):* 640.

[45]) Luthe, C.; Berry, R. *"Polysulphide Pulping of Western Softwoods: Yield Benefits and Effects on Pulp Properties";* Pulp. Pap. Can. **2005,** *106(3):* 27-33.

[46]) Munro, F.; Uloth, V.; Tench, L.; MacLeod, M.; Dorris, G. *"Mill-Scale Implementation of Paprican's Process for Polysulphide Liquor Production in Kraft Mill Causticizers - Part 2: Results of Pulp Mill Production Trials"*; Pulp. Pap. Can. **2002,** *103(1):* 57-61.

[47]) Tench, L.; Uloth, V.; Dorris, G.; Hornsey, D.; Munro, F. *"Mill Scale Implementation of Paprican's Process for Polysulfide Liquor Production in Kraft Mill Causticizers. Part-1 Batch Trials and Optimization";* TAPPI J. **1999,** *82(10):* 120.

[48]) Yamaguchi, A. *"Operating Experiences with the MOXY Process and Quinoid Compounds";* In Anthraquinone Pulping: Anthology of Published Papers 1977-1996; Goyal, G.C., Ed.; TAPPI Press: Atlanta, GA, 1997; pp 287-291.

[49]) Nishijima, H.; et al., *"Review of PS/AQ Pulping to Date in Japanese Kraft Mills and the Impact on Productivity";* Proc. *1995 TAPPI Pulping Conference;* TAPPI Press: Atlanta, GA, 1995; 31-40.

[50]) MacLeod, M.; Radiotis, T.; Uloth, V.; Munro, F.; Tench, L. *"Basket Cases IV: Higher Yield with Paprilox™ Polysulfide-AQ Pulping of Hardwoods";* TAPPI J. **2002,** *1(10):* 3-8.

[51]) Olm, L.; Tormund, D.; Bernor Gidert E. *"Possibilities to Increase the Pulp Yield in a Kraft Cook of [the] ITC-Type";* Proc. *Breaking the Yield Barrier Symposium;* TAPPI Press: Atlanta, GA, 1998; Vol. 1, 69-78.

[52]) Hakanen, A.; Teder, A. *"Modified Kraft Cooking with Polysulfide: Yield, Viscosity, and Physical Properties";* TAPPI J. **1997,** *80(7):* pp 86,93,100, 189-196.

[53]) Jiang, J.E.; Crofut, K.R.; Jones, D.B. "*Polysulfide Pulping of Southern Hardwood Employing the MOXYRG and Green-Liquor Crystallization Processes";* Proc. *1994 TAPPI Pulping Conference;* TAPPI Press: Atlanta, GA, 1994; pp 799-806.

[54]) Gustafsson, R.; Ek, M.; Teder, A. *"Polysulphide Pretreatment of Softwood for Increased Delignification and Higher Pulp Viscosity";* JPPS. **2004,** 30(5): 129-135.

[55]) Mao, B. F.; Hartler, N.; *"Improved Modified Kraft Cooking,3: Modified Vapor-Phase Polysulfide Cooking";* TAPPI J. **1994,** *77(11):* 149-153.

[56]) Lindstrom, M.; Teder, A. *"Effect of Polysulfide Pretreatment When Kraft Pulping to Very Low Kappa Number";* Nordic Pulp Paper Res. J. **1995,** *10(1):* 8-11.

[57]) Olm, L.; Tormund, D. *"ZAP Cooking- Increase Yield in PS and PS-AQ Cooking with Zero Effective Alkali in the Pretreatment Stage"*; Nordic Pulp Paper Res. J. **2004,** *19(1):* 6.

[58]) Brannvall, E.; Gustafsson, R.; Teder, A.; *"Properties of Hyperalkaline Polysulphide Pulps";* Nordic Pulp Paper Res. J. **2003,** *18(4):* 436-440.

[59]) Kiiskilä, E. and Virkola, N.-E., "*Recovery of Sodium Hydroxide from Alkaline Pulping Liquors by Autocausticizing. Part 1. General Aspects*", Paperi Puu 60(3), p. 129-132 (1978)

[60]) Budney, J., "*Method of Recovering Caustic Soda from Spent Pulping Liquors*", Canadian patent 1,283,256 (1991)

[61]) Kiiskilä, E., "*Recovery of Sodium Hydroxide from Alkaline Pulping Liquors by Smelt Causticizing, Part II, Reactions between Sodium Carbonate and Titanium Dioxide*", Paperi Puu 61(5), p.394-401 (1979)

[62]) Kiiskilä, E., "*Recovery of Sodium Hydroxide from Alkaline Pulping Liquors by Smelt Causticizing, Part III, Alkali Distribution in Titanium Dioxide Causticizing*", Paperi Puu 61(6), p.453-464 (1979)

[63]) Zou X. , "*Recovery of Kraft Black Liquor Including Direct Causticization*", Ph.D Thesis, Dep of Chem Eng, McGill University, Montreal, Quebec, Canada.(1991)

[64]) Zeng, L., "*Kraft Black Liquor Gasification and Direct Causticization in a Fluidized Bed*", Ph.D. Thesis, University of New Brunswick, Fredericton, N.B., Canada. (1997)

[65]) Richards, T. , "*Recovery of Kraft Black Liquor – Alternative Processes and System Analysis*", Ph.D. Thesis, Chalmers University of Technology, Gothenburg, Sweden (2001)

[66]) Nohlgren, Ingrid, "*Recovery of Kraft Black Liquor with Direct Causticization using Titanates*", Doctoral Thesis, Department of Chemical and Metallurgical Engineering, Luleå University of Technology, Luleå, Sweden (2002)

[67]) Eriksson, G. and Pelton, A.D, "*Critical Evaluation and Optimization of the Thermodynamic properties and Phase Diagrams of the MnO-TiO_2, MgO-TiO_2, FeO-TiO_2, Ti_2O_3-TiO_2, Na_2O-TiO_2, and K_2O-TiO_2 Systems*", Metall. Trans. B Vol. 24B, p. 795-805 (1993)

[68]) Nohlgren, I., Edin, M. and Theliander, H., "*Influence of Carbon Dioxide on the Kinetics of the Reaction between Sodium Carbonate and Sodium Tri-Titanate*", Pulp Paper Can. 104(1), p. T4-T8 (2003)

[69]) Nohlgren, I., Zhuang, Q., Theliander, H. and van Heiningen, A.R.P., "*Direct Causticization Using Titanates in a Fluidized Bed Reactor*", Nordic Pulp Paper Res. J. 17(3), p. 246-253 (2002)

[70]) Nohlgren, I., Theliander, H., Zhuang, Q. and van Heiningen, A.R.P.,"*Model Study of the Direct Causticization Reaction Between Sodium Trititanate and Sodium Carbonate*", Can. J. Chem. Eng. 78 (3), p. 529-539 (2000)

[71]) Richards, T. and Theliander, H., "*The leaching of NaOH from 4:5 Sodium-titanate Produced in an Autocausticization Process: Kinetics and Equilibrium*", Nordic Pulp Paper Res. J. 14 (3), p. 184-192 (1999)

[72]) Backman, R. and Salmenoja, K., "*Equilibrium Behaviour of Sodium, Sulfur and Chlorine in Pressurized Black Liquor Gasification with Addition of Titanium Dioxide*", Paperi Puu 76(5), p.320-325 (1994)

[73]) Zeng, L. and A.R.P. van Heiningen, "*Sulfur Distribution during Air Gasification of Kraft Black Liquor Solids in a Fluidized Bed of TiO_2 Particles*", Pulp and Paper Canada, **100**(6): 58-63 (1999)

[74]) Nohlgren, I. and Sinquefield, S., "*Black Liquor Gasification with Direct Causticization Using Titanates: Equilibrium Calculations*", Ind. Eng. Chem. Res. 43(19), p.5996-6000 (2004)

[75]) Bouaziz, R. and M. Mayer, "*Sodium Oxide-Titanium Dioxide Binary System*", C. R. Acad. Sci., Ser. C, 272(23), 1874-1877(1971)

[76]) Zeng, L. and A.R.P. van Heiningen, "*Sulfur Distribution during Air Gasification of Kraft Black Liquor Solids in a Fluidized Bed of TiO_2 Particles*", Pulp and Paper Canada, 100(6), 58-63 (1999)

[77]) Nagano, R., Miyao, S. and Niimi, N., "*Method of Recovering Sodium Hydroxide from Sulfur-Free Pulping or Bleaching Liquor by Mixing Ferric Oxide with Condensed Waste Liquor Prior to Burning*", U.S. Pat. 4000264 (1976)

[78]) Kiiskilä, E. and Valkonen., N., "*Recovery of Sodium Hydroxide from Alkaline Pulping Liquors by Smelt Causticizing, Part IV, Causticizing of Sodium Carbonate with Ferric Oxide*", Paperi Puu 61(8), p. 505-510 (1979)

[79]) Scott-Young, R.E. and Cukier, M., "*Commercial Development of the DARS Process*", 1995 International Chemical Recovery Conference, Toronto, ON, Canada, April 24-27, p. B263-B267 (1995)

[80]) Nohlgren, I., Theliander, H., Zhuang, Q. and van Heiningen, A .R.P, "*Model Study of the Direct Causticization Reaction between Sodium Trititanate and Sodium Carbonate*", CJChE, 78(3), 529-539(2000)

[81]) Jander, W., "*Reactions in Solid State at High Temperatures"*: I", Z.Anorg. Allgem. Chem. 163, p.1 (1927)

[82]) Carter, R.E., "*Kinetic Model for Solid-Solid Reactions*", J. Chem. Pys., 34(6), p. 2010-2015 (1961)

[83]) Tamhankar, S.S. and Doraiswamy, L.K., "*Analysis of Solid-Solid Reactions: A Review*", AIChE J., 25(4),P. 561-582 (1979)

[84]) Deuk Ki Lee, "*An Apparent Kinetic Model for the Carbonation of Calcium Oxide by Carbon Dioxide*", Chemical Engineering Journal 100, 71-77(2004)

[85]) Dorris, G. M. and Uloth, V. C., "Analysis of Oxidized White Liquors. Part II. Potentiometric Titrations for the Determination of Polysulfides and Sulfoxy Anions", Journal of Pulp and Paper Science (1994), 20(9), 242-248

[86]) Edwards, L.L., et al., *GEMS User's Manual*", University of Idaho, Moscow, ID, 1972, 1977, 1983, 1989

[87]) Metsoautomation website: http://www.metsoautomation.com/automation/index.nsf/FR?ReadForm&ATL=/Automation/pp_prod.nsf/WebWID/WTB-061205-2256F-8ECE6

[88]) Lindstrom, M., Naithani, V., Kirkman, A., Jameel, H., "*The Development and Validation of a Low-Temperature Black Liquor Gasifier Model for Use in WinGEMS*© ",TAPPI J. Vol. 5 No. 2 (2006) p.24.

[89]) Lindstrom, M., Naithani, V., Kirkman, A., Jameel, H., "*The Effect of Integrating Polysulfide Pulping and Black Liquor gasification on Pulp Yield and Properties*", TAPPI Engineering, Pulping and Environmental Conference, Philadelphia, PA, August 28-31, 2005

[90]) Lindstrom, Matthias, "*Integrating Black Liquor Gasification with Pulping? Process Simulation, Economics and Potential Benefits*", North Carolina State University, Rayleigh, NC, PhD thesis, March 2007

[91]) Nohlgren, I., "*Non-conventional Causticization Technology: A Review*", Nordic Pulp and Paper Research Journal, (2004), 19(4), 470-480

[92]) Nohlgren, I., and Bladlund, H., "*Black Liquor Gasification with Direct Causticization Using Titanates-Leaching of Sodium Trititanate*", 2004 Int. Chemical Recovery Conf., Charleston, SC, USA, 6-10 June, 2004

[93]) Pels, J.R., Zeng, L., and van Heiningen, A.R.P., „*Direct Causticization of Kraft Black Liquor with Titanium Dioxide in a Fluidized Bed – Identification and Analysis of Titanates*", *J. Pulp and Paper Sci*, 23(12), 549-554 (1997)

[94]) Papp, S., Koroesi, L., Meynen, V., Cool, P., Vansant, E.F. and Dekany, I., "*The Influence of Temperature on the Structural Behavior of Sodium Tri- and Hexa-Titanates and their Protonated Forms*", *J. Solid St. Chem*. Vol. 178, 2005, p. 1614

[95]) Zhuang, Q et al., "*Direct Causticization of Kraft Black Liquor with Recycled Sodium Titanate*", *International Chemical Recovery Conference*, v. 2, 1998, p. 831

[96]) Papp, S., Koroesi, L., Meynen, V., Cool, P., Vansant, E.F. and Dekany, I., "*The Influence of Temperature on the Structural Behavior of Sodium Tri- and Hexa-Titanates and their Protonated Forms*", *J. Solid St. Chem*. Vol. 178, 2005, p. 1614

[97]) Menzel. R, Peiro, A, Durrant, J., and Shaffer, M., "*Impact of Hydrothermal Processing Conditions on High Aspect Ratio Titanate Nanostructures*", *Chem. Mater*, Vol. 18, 2006, p. 6059

[98]) Nohlgren, I. and Sinquefield, S., "*Black Liquor Gasification with Direct Caustization Using Titanates: Equilibrium Calculations*", *Ind. Eng. Chem. Res*., vol. 43, p. 5996, 2004

[99]) Li, J. and van Heiningen, A.R.P., "*Sodium Emission during Pyrolysis and Gasification of Black Liquor Char*", *Tappi Journal*, Vol. 73, No. 12 (1990), p. 213

[100]) Gea, G, Murillo, M.B., Sanchez, J.L., Bilbao, R. and Arauzo, J., "*Straw Black Liquor Gasification Studies at the University of Zaragoza*", Pulp and Paper Canada, Vol. 104, No. 3 (2003), p. 44

[101]) Hupa, M. and Frederick, W.J., "*Black Liquor Combustion Properties*", Proceedings of International Conference of Baltic Sea: 30 Years Recovery Boiler Co-Operation in Finland, 24-26 May 1994. p. 37

[102]) Wintoko, J. and Richards, T., "*Swelling Behavior of Black Liquor Droplet with Addition of Sodium Borates or Sodium Titanates during Drying and Devolatilization*", 2004 International Chemical Recovery Conference, v2, 2004, p 757-761

[103]) Sakai, M., Zhang, J., and Matsuda, A., "*Elastic Deformation of Coating/Substrate Composites in Axisymmetric Indentation*", J. Mater. Res., Vol. 20, No. 8 (2005), p. 2173

[104]) German, R., "*Sintering Theory and Practice*",John Wiley & Sons, New York, 1996

[105]) Ružinská, E., "*The Study of Thermal Characteristics of Modified Products Isolated from Kraft Black Liquor for Formulation of New Type of Adhesive Mixtures*", Wood Research, Vol. 48, No. ½ (2003), p. 22.